HUMAN KERATINOCYTES UTILIZE THE INTEGRATED STRESS RESPONSE TO ADAPT TO ENVIRONMENTAL STRESS

Ann E. Collier

Submitted to the faculty of the University graduate school
in partial fulfillment of the requirements
for the degree
Doctor of Philosophy
in the Department of Biochemistry & Molecular Biology,
Indiana University

June 2017

Accepted by the Graduate Faculty of Indiana University, in partial fulfillment of the requirements for the degree of Doctor of Philosophy.

Doctoral Committee

_____

Dan F Spandau, Ph.D., Co-Chair

_____

Ronald C. Wek, Ph.D., Co-Chair

May 3, 2017

_____

Jeffrey B. Travers, M.D., Ph.D.

_____

John J. Turchi, Ph.D.

_____

Matthew J. Turner, M.D., Ph.D.

ACKNOWLEDGEMENTS

I would like to acknowledge Sheree Wek and David Southern for their technical assistance and support. I would also like to thank my committee members for their time, thoughtful advice, and suggestions. Financial support for this work was supplied by the National Institute of Environmental Health Sciences (ES020866 to DFS/JBT and F31ES026517 to AEC), the National Institute on Aging (AG048946 to DFS/JBT), and the National Institute of General Medical Sciences (GM049164 to RCW). I would also like to thank Drs. Howard Edenberg and Mark Kaplan for use of laboratory equipment.

Ann E. Collier

HUMAN KERATINOCYTES UTILIZE THE INTEGRATED STRESS RESPONSE TO ADAPT TO ENVIRONMENTAL STRESS

Human skin, consisting of the outer epidermis and inner dermis, serves as a barrier that protects the body from an onslaught of environmental stresses. Keratinocytes in the stratified epidermis undergo sequential differentiation that consists of multiple layers of cells differing in structure and function. Therefore, keratinocytes must not only combat environmental stress, but need to undergo massive changes in gene expression and morphology to form a proper barrier. One mode by which cells cope with stress and differentiation is through phosphorylation of the α subunit of eukaryotic initiation factor 2 (eIF2α-P), which causes global inhibition of protein synthesis coincident with preferential translation of select gene transcripts. Translational repression allows stressed cells to conserve energy and prioritize pro-survival processes to alleviate stress damage. Since eIF2α kinases are each activated by distinct types of stress, this pathway is referred to as the Integrated Stress Response (ISR). We sought to identify the roles of the ISR in the keratinocyte response to the stresses associated with differentiation and ultraviolet B (UVB) irradiation.

In this thesis, we show that both general and gene-specific translational control in the ISR are activated following differentiation or UVB irradiation of human keratinocytes. ISR deficiency through genetic modifications or

pharmacological interventions caused severe divergence from the appropriate keratinocyte response to differentiation or UVB. Differentiation genes were selectively translated by eIF2α-P, and inhibition of the ISR diminished their induction during differentiation. Furthermore, loss of the eIF2α kinase GCN2 (*EIF2AK4*) adversely affected the ability of keratinocytes to stratify in three-dimensional cultures. Our analysis also revealed a non-canonical ISR response following UVB irradiation, in which downstream factors ATF4 (CREB2) and CHOP (DDIT3/GADD153) were poorly expressed due to repressed transcription, despite preferential translation in response to eIF2α-P. The ISR was cytoprotective during UVB and we found that eIF2α-P was required for a UVB-induced G1 arrest, cell fate determination, and DNA repair via a mechanism involving translational control of human *CDKN1A* (p21 protein) transcript variant 4 mRNA. Collectively, this thesis describes novel roles for the ISR in keratinocyte differentiation and response to UVB, emphasizing the utility of targeting translational control in skin disease therapy.

Dan F Spandau, Ph.D., Co-Chair

Ronald C. Wek, Ph.D., Co-Chair

TABLE OF CONTENTS

LIST OF TABLES

LIST OF FIGURES

ABBREVIATIONS

AD	Actinomycin D
ATF	Activating transcription factor
BiP	Binding immunoglobulin protein
CA	Calcium
CARE	C/EBP-ATF response element
CCND1	Cyclin D1
CDK	Cyclin dependent kinase
CDKN1A	Cyclin dependent kinase inhibitor 1A (p21)
CDS	Coding sequence
C/EBP	CCAAT enhancer binding protein
CHOP	C/EBP homologous protein
CHX	Cycloheximide
CTD	C-terminal domain
CTRL	Control
Diff	Differentiated
DOX	Doxycycline
eIF	Eukaryotic initiation factor
EIF2AK	Eukaryotic initiation factor 2 alpha kinase
eIF2α-P	Phosphorylated eukaryotic initiation factor 2 alpha
EdU	5-ethynyl-2'-deoxyuridine
ER	Endoplasmic reticulum
FBS	Fetal bovine serum

FLG	Filaggrin
GADD	Growth arrest and DNA damage inducible protein
GCN	General control nonderepressible
HisRS	Histidyl-tRNA synthetase-like domain
HRI	Heme-regulated eIF2α kinase
IVL	Involucrin
ISR	Integrated stress response
J/m^2	Joules per meter squared
KRT	Keratin
LOR	Loricrin
NER	Nucleotide excision repair
NMSC	Non-melanoma skin cancer
NT	No treatment
PBS	Phosphate buffered saline
PERK	PKR-like endoplasmic reticulum kinase
PI	Propidium iodide
PKR	Protein kinase R
p/m	polysome/monosome ratio
PP	Protein phosphatase
qPCR	quantitative polymerase chain reaction
SA β-gal	Senescence associated beta-galactosidase
Sal	Salubrinal
shRNA	Short hairpin RNA

TG	Thapsigargin
P_{Tk}	Thymidine kinase promoter
TM	Tunicamycin
Undiff	Undifferentiated
uORF	Upstream open reading frame
UPR	Unfolded protein response
UV	Ultraviolet
XBP	Xbox binding protein

CHAPTER 1. INTRODUCTION

1.1 Role of the keratinocyte in skin barrier function

Human skin, the largest organ in the body, serves as an interface between the external environment and internal organs. At this location, skin is a crucial defense system against a range of bodily insults including UVB, microorganisms, and water loss (Bikle *et al.*, 2012; Fuchs, 1990, 2007). As a result, skin has evolved multiple mechanisms of stress resistance to protect the life it encloses. One such mechanism is the formation of the epidermal barrier, which consists of distinct layers of keratinocytes ranging from basal proliferating cells to enucleated, terminally differentiated corneocytes (Figure 1). Skin diseases such as psoriasis, atopic dermatitis, and squamous cell carcinoma are often characterized by reduced barrier function, making the epidermis more permeable to exogenous factors (Bouwstra and Ponec, 2006; Menon *et al.*, 1994). Therefore it is crucial not only to understand how the skin responds to stress, but how a healthy epidermis is formed and maintained. A better grasp on how keratinocytes regulate differentiation could elucidate new therapeutic targets for skin diseases with diminished barrier function.

In order to form distinct epidermal layers, keratinocytes must undergo a tightly controlled differentiation process, which involves reprogramming of gene expression and cell morphology (Figure 1). Undifferentiated epidermal keratinocytes are attached to the cutaneous basement membrane, which separates the epidermis and the underlying dermis. Keratinocytes in the basal layer actively divide until select progeny receive a signal to exit from the cell

cycle, detach from the basement membrane, and migrate to the upper layers of the epidermis. During this process, cells begin to synthesize differentiation-specific proteins, including involucrin (IVL), loricrin (LOR), filaggrin (FLG), and various keratins (KRT1, KRT10) that are essential for changes in cell morphology and function (Abhishek and Palamadai Krishnan, 2016; Moll *et al.*, 1982; Steven *et al.*, 1990; Warhol *et al.*, 1985). A major regulator of the differentiation process is a natural calcium (Ca^{2+}) gradient that exists within the human epidermis (Bikle *et al.*, 2012). An increase in Ca^{2+} promotes cell-cell adhesions as well as intracellular signaling through selected pathways including activation of protein kinase C (PKC) and phosphoinositide 3-kinase (PI3K). Subsequent changes in transcriptional and epigenetic networks during keratinocyte differentiation are also well documented (Borowiec *et al.*, 2013), with an emphasis on induction of AP1, SP1, and C/EBP transcription factors (Eckert *et al.*, 2004). Interestingly, little is known about the contributions of translational control to keratinocyte differentiation.

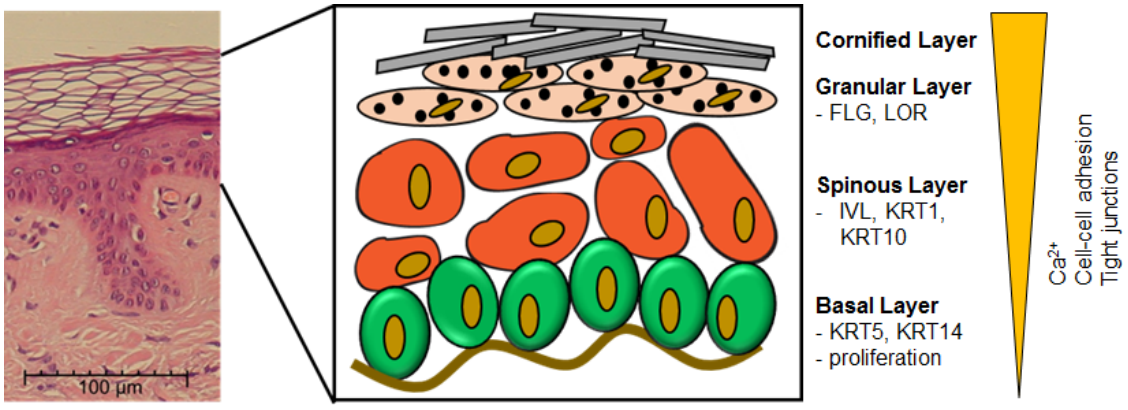

Figure 1. Human keratinocyte differentiation is required to form an intact epidermis. The human epidermis is the most superficial layer of skin and is

composed of four distinct layers of keratinocytes. The single basal layer consists of actively proliferating cells, which are attached to the dermis by the basement membrane (depicted as a brown line). Following division, some progeny remain in the basal layer as transient amplifying cells or stem cells while others receive a signal to differentiate, exit the cell cycle, and form the spinous layer. This process coincides with a change in gene expression including induction of IVL and KRT1 proteins as well as marked changes in morphology such as flattening and increased cell-cell adhesion. Lamellar bodies (depicted as black dots) appear in the granular layer, which secrete lipids to improve skin barrier function. Finally during cornification, a process distinct from apoptosis, cells become enucleated and are eventually sloughed from the skin during desquamation.

1.2 The keratinocyte response to UVB

Once an intact epidermal barrier is formed, it must have the ability to protect against environmental stress. One such stress is ultraviolet (UV) radiation. UV is a major risk factor in the development of non-melanoma skin cancer (NMSC), which is the most frequently diagnosed cancer in the United States (Melnikova and Ananthaswamy, 2005). UV comprises around 10% of the total light yield of the sun, with spectrums denoted UVA (315-400 nm), UVB (280-315 nm), and UVC (100-280 nm). Since UVC is completely absorbed by the earth's ozone layer, UVB irradiation is physiologically the most harmful to human health. The threshold of UVB exposure that is required to elicit a sunburn, or minimal erythemal dose (MED), varies from person to person and is dependent

partially on skin type. For example, for an individual with the minimum amount of natural pigmentation, a UVB dose of 300-400 J/m^2 is required to induce sunburn. Although the level of UVB reaching the surface of the earth varies with each season, geographical location, and weather conditions, this dose of UVB can be obtained within 15-20 minutes outside on a sunny day in the summer.

A proper cellular response to environmental UVB is crucial to avoid the onset of NMSCs. Human keratinocytes have evolved a variety of mechanisms to block the initiation of cancer by UVB including cell cycle regulation, senescence, DNA repair, and apoptosis (Figure 2). UVB introduces crosslinked covalent DNA adducts such as cyclobutane pyrimidine dimers and 6,4 photoproducts into genomic DNA, which must be resolved by nucleotide excision DNA repair (NER) (Cadet *et al.*, 2012; Shuck *et al.*, 2008). Unrepaired DNA can lead to mutagenesis, which can cause cancer if mutations persist in tumor suppressors or oncogenes. As a consequence of UVB-induced DNA damage, keratinocytes transiently arrest progression in the cell cycle during G1 to prevent DNA replication with damaged DNA (de Laat *et al.*, 1996; Ortolan and Menck, 2013). If the DNA damage is successfully repaired, cells can resume progression into S phase and complete the cell cycle. Prolonged arrest can lead to cellular senescence, which in keratinocytes functions to preserve the barrier function of the epidermis while ensuring that affected keratinocytes do not replicate damaged DNA (Lewis *et al.*, 2008). Finally, if the keratinocytes have been damaged irreparably, these cells will be removed from the epidermis by

apoptosis. Each of these processes function to eliminate potentially mutagenic cells that can develop into NMSCs (Campisi, 2005; D'Errico *et al.*, 2003).

Mammalian cells have evolved multiple checkpoint mechanisms that function in this cell fate determination. Expression of the cyclin dependent kinase (CDK) inhibitor *CDKN1A* (p21 protein) is enhanced in response to UV, and elevated levels of p21 protein function to inhibit the activity of cyclin/CDK complexes, which ultimately blocks cell progression from G1 to S phase (Brugarolas *et al.*, 1995; Deng *et al.*, 1995; Mandal *et al.*, 1998). Transcriptional expression of *CDKN1A* has been extensively characterized, with emphasis on direct regulation via p53 (Hill *et al.*, 2008). Additional *CDKN1A* regulatory mechanisms such as epigenetic modifications, mRNA stability, and protein degradation have also been described (Gartel and Tyner, 1999; Jascur *et al.*, 2005; Scholpa *et al.*, 2014). Of interest, little is known about regulation of *CDKN1A* expression via translation. Furthermore, investigations about translation regulation during CDKN1A-dependent processes, such as cell cycle regulation and senescence, have not been extensively studied.

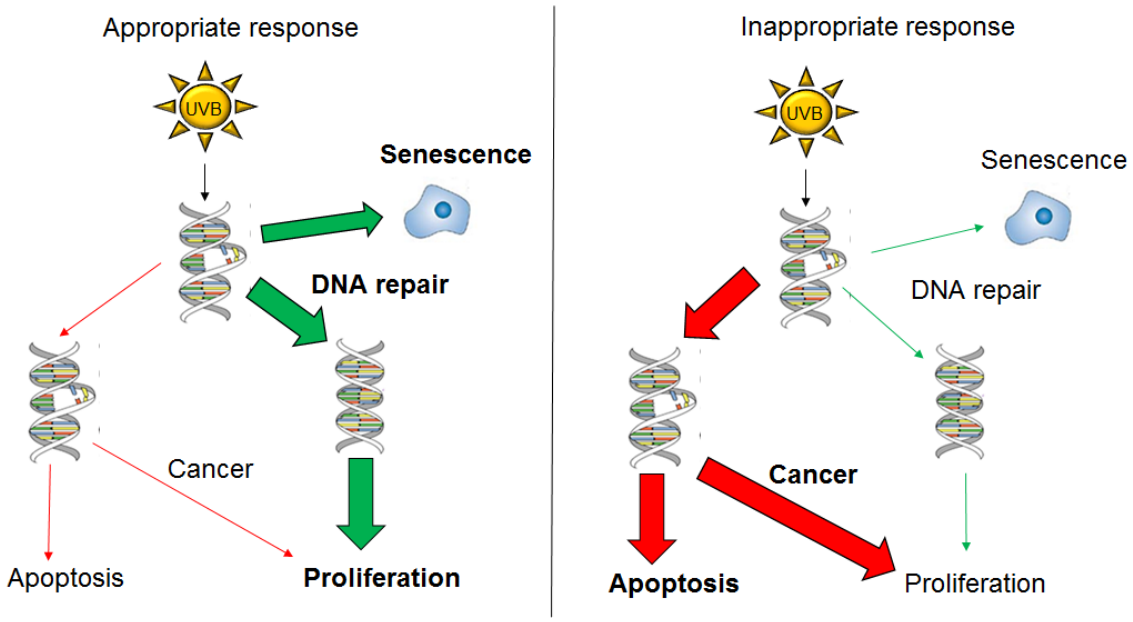

Figure 2. UVB irradiation activates a cascade of protective cellular functions. UVB has been shown to trigger multiple cell processes, including cell cycle arrest, DNA repair, senescence, and apoptosis. In order to allow time for DNA repair, cells must transiently halt the cell cycle and activate NER enzymes, which would remove DNA lesions. If repair of DNA is successfully completed, keratinocytes can re-enter the cell cycle and continue to proliferate. If the duration of the cell cycle arrest is too long, cells can induce senescence, which is an irreversible exit from the cell cycle. These cells are still metabolically active and can continue to aid in epidermal barrier function. Finally, if the DNA damage is too extensive, cells will undergo apoptosis. If cells enter S phase with DNA damage, this can also result in apoptosis by mitotic catastrophe. Keratinocytes can also transform into cancer cells if DNA damage leads to mutation of oncogenes or tumor suppressors that alter the propagation of daughter cells.

1.3 Eukaryotic Initiation Factor 2 and translational control

This thesis addresses the regulation of mRNA translation during the keratinocyte adaptations to stress. As mentioned above, keratinocytes must form an intact barrier through differentiation as well as activate signaling pathways to determine cellular fate when subjected to stresses such as UVB. Whereas transcriptional networks during these key keratinocyte processes are well studied, little is known regarding the role of translational control. This is a crucial gap in our knowledge, as recent studies have indicated that changes in mRNA expression only account for about 40% of functional protein levels (Schwanhausser *et al.*, 2011). One mechanism by which cells can modulate protein levels is through regulation of translation initiation, the rate-limiting and most highly regulated step in the translation process (Jackson *et al.*, 2010). A central mechanism directing translation initiation during stress or differentiation involves phosphorylation of the alpha subunit of eukaryotic initiation factor 2 (eIF2α-P) (Figure 3). eIF2α-P decreases initiation of global translation by a mechanism involving lowered eIF2α association with GTP and transport of the initiator tRNA to ribosomes (Baird and Wek, 2012; Jackson *et al.*, 2010; Wek *et al.*, 2006).

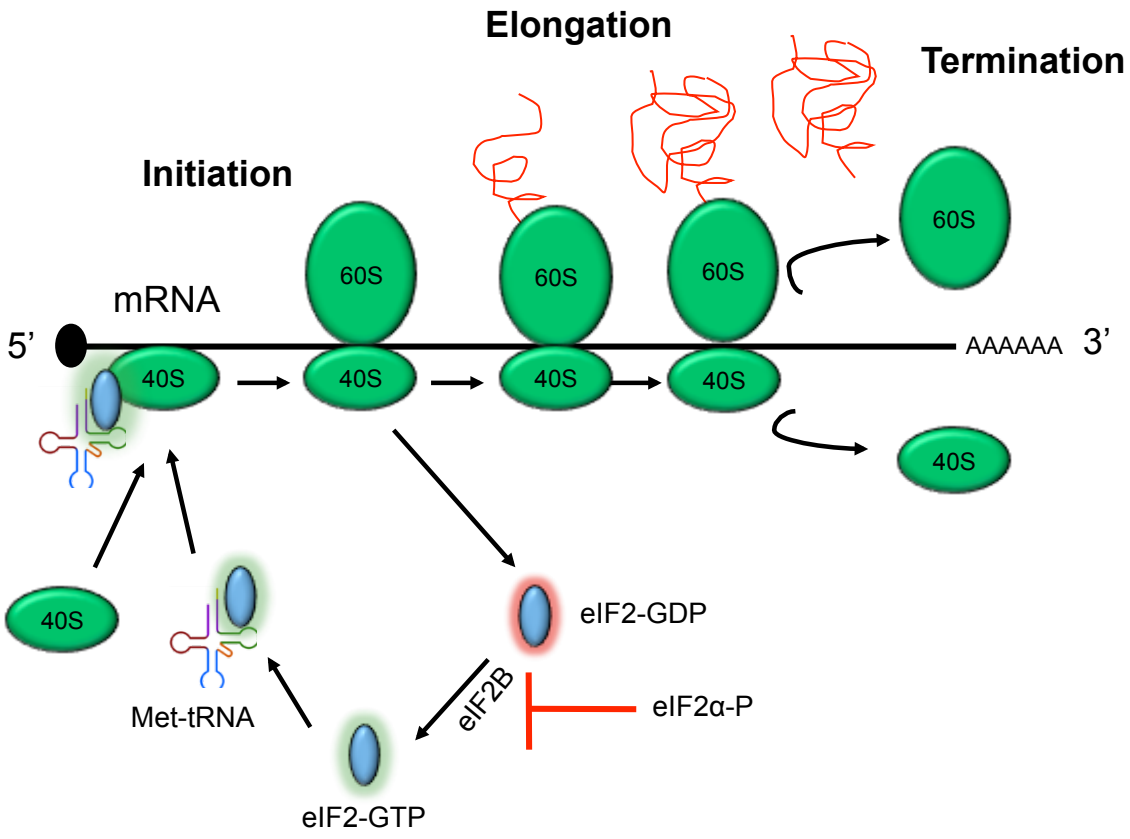

Figure 3. Phosphorylation of eIF2α represses the initiation phase of translation. Translation of mRNA involves three phases: initiation, elongation, and termination, which together that contribute to synthesis of a polypeptide (depicted as red line) via the joined small 40S and large 60S ribosomal subunits (depicted as green ovals). During normal cellular conditions, eIF2-GTP binds to the initiator tRNA and delivers it to the 40S ribosomal subunit. This 43S preinitiation complex can bind an mRNA at the 5' cap and then scan processively 5' to 3' until a start codon in optimal context is recognized and placed in the P site. Optimal start codons in eukaryotic organisms are defined by the Kozak context (gccRccAUGG, where R is a purine base and capital letters are highly conserved) (Kozak, 1989b). During this process, eIF2-GTP is hydrolyzed to eIF2-

GDP and released from the translation apparatus. In order to reactivate eIF2 for the next round of translation initiation, the guanine nucleotide exchange factor eIF2B must replace the GDP with a GTP. During stress conditions that activate the ISR, eIF2α-P becomes a competitive inhibitor for eIF2B, causing an overall decrease in delivery of initiator tRNA for the onset of translation initiation.

Four mammalian protein kinases phosphorylate serine-51 of eIF2α, each activated by distinct types of stress including amino acid starvation, oxidative stress, and ER stress (Figure 4). Because a collection of different stressors activates each eIF2α kinase, this pathway is referred to as the Integrated Stress Response (ISR) (Deng *et al.*, 2002; Harding *et al.*, 2003). In addition to repressing global translation in the ISR, eIF2α-P enhances translation of a subset of cytoprotective gene transcripts, such as activating transcription factor 4 (ATF4/CREB2), a transcriptional activator of ISR genes involved in alleviating stress damage (Harding *et al.*, 2000; Harding *et al.*, 2003; Vattem and Wek, 2004). Additionally downstream of ATF4 is C/EBP homologous protein (CHOP/GADD153/DDIT3), a critical transcription factor that can determine cell fate. Also downstream in the ISR is growth arrest and DNA damage-inducible protein 34 (GADD34/PPP1R15A), which facilitates the dephosphorylation of eIF2α-P and resumption of translation (Figure 4) (Connor *et al.*, 2001; Ma and Hendershot, 2003; McCullough *et al.*, 2001; Novoa *et al.*, 2001; Novoa *et al.*, 2003; Young *et al.*, 2015). Preferential translation of these transcripts relies on the sequence and structures of the 5’-leaders of the mRNAs, which are located

proximal to the coding sequence (CDS) and are required for recruitment of the translation machinery (Hinnebusch *et al.*, 2016; Young and Wek, 2016). Of note, GADD genes were discovered and named as such because they were induced in response to UVC irradiation and an alkylating agent in low glucose media (Fornace *et al.*, 1988). However it was later discovered that the induction was due to ER stress and nutrient deprivation, not DNA damage per se (Wang *et al.*, 1996).

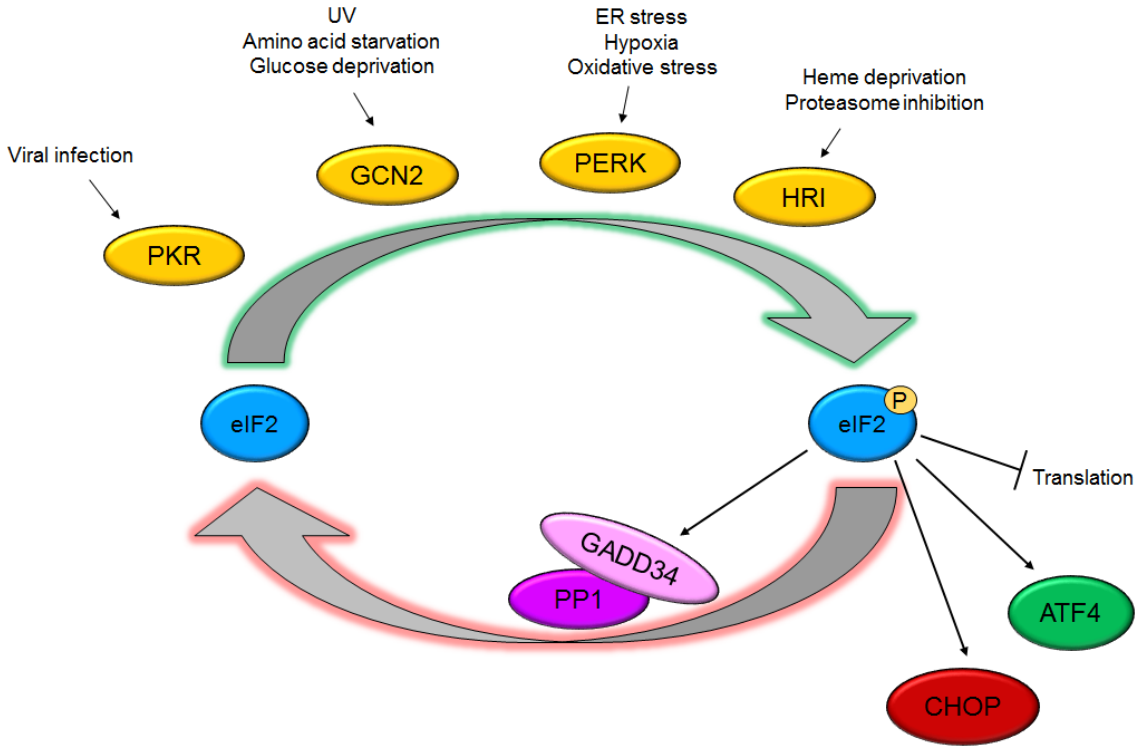

Figure 4. The Integrated Stress Response induces translational expression of a collection of transcription factors involved in cellular stress. The ISR consists of four eIF2α kinases, each of which are activated by specific types of stresses. eIF2α-P causes a global inhibition of translation initiation that serves to conserve energy and reprogram gene expression towards alleviation of stress.

eIF2α-P also induces translation of a cohort of transcription factors, such as ATF4 and CHOP, along with GADD34 that serves to direct protein phosphatase 1 (PP1) dephosphorylation of eIF2α-P. Therefore, GADD34 serves as a feedback inhibitor of the ISR.

Induction of *ATF4* and *CHOP* mRNA and protein during eIF2α-P facilitates transcriptional regulation of genes subject to the ISR. Importantly, ATF4 can form homodimers or heterodimers with several other bZIP transcription factors, including the C/EBP isoforms, FOS, JUN, NRF2, and CHOP. These families of transcription factors have been shown to have critical importance in the expression of keratinocyte differentiation or UVB response genes. ATF4 can bind to ISR target promoters via CARE elements, which contain half-sites for C/EBP and ATF transcription factors (Fawcett *et al.*, 1999; Kilberg *et al.*, 2009). Studies of ISR-dependent gene expression have classified target genes involved in diverse cellular processes including amino acid synthesis, protein degradation, cell redox status, autophagy, and mitochondrial function (Baird *et al.*, 2014; Fusakio *et al.*, 2016; Teske *et al.*, 2011b; Willy *et al.*, 2015). It has also been suggested that chronic stress that induces ATF4/CHOP can switch the ISR from its primary survival function to one that facilitates cell death. Therefore, the downstream consequences of ISR activation can be pro-survival or apoptotic, depending on the types and extent of stress. These ISR processes must be fine-tuned to avoid the onset of disease (Marciniak and Ron, 2006; Oslowski and Urano, 2011; Tabas and Ron, 2011; Wek and Anthony, 2009). For example,

during keratinocyte differentiation, activation of cell death signals can oppose the cornification process and cause aberrant formation of the epidermis. Similarly, cell fate determination following UVB must be carefully regulated to halt cell proliferation in the presence of damaged DNA.

1.4 Activation of eIF2α kinases in the ISR

As mentioned above, a myriad of environmental stress conditions can induce the ISR through activation of four different mammalian kinases (Figure 4). These kinases are GCN2 (EIF2AK4), known to respond to nutritional stress (Wek *et al.*, 2006), PERK (EIF2AK3/PEK), which responds to ER stress (Schroder and Kaufman, 2005; Walter and Ron, 2011), HRI (EIF2AK1), which is activated by heme limitation in erythroid cells (Han *et al.*, 2001; Han *et al.*, 2013), and PKR (EIF2AK2), which can protect against viral infection (Dey *et al.*, 2005; Garcia *et al.*, 2007). Malfunctions in these eIF2α kinases have been linked to diseases in a variety of organs and tissues, such as *EIF2AK4* in pulmonary veno-occlusive disease (Eyries *et al.*, 2014) and *EIF2AK3* in Wolcott-Rallison syndrome (Durocher *et al.*, 2006). These correlations indicate their critical function in human health. To facilitate the distinct stress conditions that activate each of the eIF2α kinases, there are unique regulatory domains that are juxtaposed to related protein kinase domains. These domains bind to nucleic acids, small molecules, and proteins, which can enhance or regulate the kinases during stress. The domain organization of GCN2 and PERK is outlined in Figure 5.

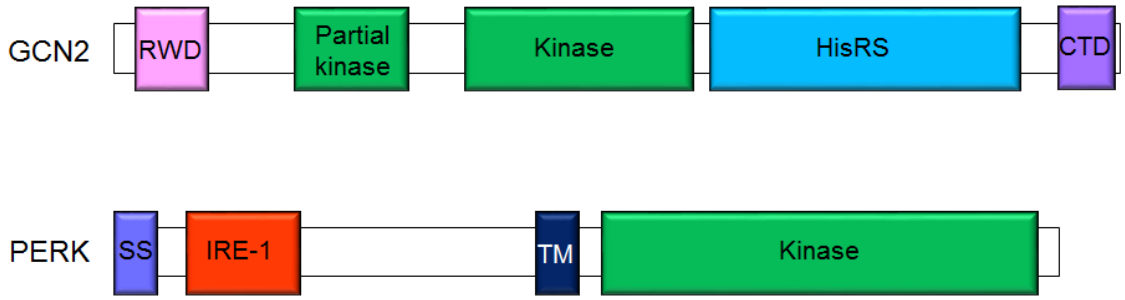

Figure 5. eIF2α kinases are activated by distinct types of stress. GCN2 includes an RWD domain, which can associate with the regulatory protein GCN1. An RWD domain is also present in the regulatory protein IMPACT, which competes with GCN2 for GCN1 binding. A partial kinase domain is also required for activation of the kinase domain. GCN2 features a histidyl tRNA synthetase-like domain (HisRS), which has the ability to bind uncharged tRNA that accumulates during deprivation for amino acids. As discussed in the text, this is a major known activating signal for GCN2. Finally GCN2 includes a carboxy terminal domain (CTD) that facilitates ribosome binding and stable dimerization between GCN2 polypeptides. PERK features a signal sequence (SS) on its amino terminus, which allows the eIF2α kinase to localize to the ER and a transmembrane (TM) domain that facilitates PERK placement in the ER membrane. The IRE-1 like domain is suggested to monitor unfolded proteins either by direct binding or association with protein chaperones.

The function of GCN2 has primarily been characterized during conditions of amino acid starvation, in which its mechanism of activation involves the binding of accumulated uncharged tRNAs to a histidyl-tRNA synthetase-like domain (HisRS) (Dong *et al.*, 2000; Wek *et al.*, 1995). Activation of human GCN2

is suggested to induce a conformational change that releases inhibitory interactions within the protein kinase domain, resulting in autophosphorylation in the activation loop at threonine 899 (Castilho *et al.*, 2014; Padyana *et al.*, 2005). Notably, GCN2 can also be activated by glucose deprivation, exposure to high salt, or other stresses not directly related to nutrient limitation (Averous *et al.*, 2012; Cai and Brooks, 2011; Dey *et al.*, 2010; Dey *et al.*, 2012; Eleftheriadis *et al.*, 2015; Yang *et al.*, 2000). The mechanism for GCN2 activation in response to these additional stress signals is not well understood, although some studies have implicated reduced tRNA charging and utilization of regulatory proteins.

Importantly, GCN2 has also been implicated in cellular differentiation. The processes of regulating GCN2 in differentiation are suggested to incorporate changes in tRNA charging, amino acid availability, and/or expression of GCN2 regulatory proteins depending on cell type and context. For example, during an immune response GCN2 has been shown to respond to the immunosuppressive enzyme indoleamine 2,3-dioxygenase (IDO), which blocks T-cell differentiation (Munn *et al.*, 2005). In this case, it was suggested that GCN2 is activated by tryptophan depletion caused by IDO activation. Other studies indicate that through GCN2, IDO suppresses T-cell differentiation by blocking key enzymes for fatty acid synthesis (Eleftheriadis *et al.*, 2015). Leucine deprivation has also been suggested to inhibit differentiation of myoblasts through GCN2 (Averous et al., 2012), and GCN2 is specifically inhibited by the protein IMPACT in differentiated neural cells to allow for high levels of translation (Pereira et al., 2005; Roffe et al., 2013). IMPACT can block GCN2 activation by competing for

binding with the activator protein GCN1 at the N-terminal RWD domain of GCN2 (Figure 5) (Sattlegger *et al.*, 2004). IMPACT is variably expressed among tissues, suggesting that this regulatory protein can differentially repress GCN2 in select cell types during stress or differentiation (Bittencourt *et al.*, 2008). Based on these observations, GCN2 is suggested to play critical roles in cellular differentiation among diverse tissues. However, there appear to be important differences in the mechanisms by which GCN2 and translational control can affect cell fates, owing to the fact that “differentiation” has alternative meanings across cell types.

Another key eIF2α kinase is PERK, which can be activated by accumulating levels of unfolded protein in the endoplasmic reticulum (ER stress) (Harding *et al.*, 1999; Shi *et al.*, 1998). PERK functions in the Unfolded Protein Response (UPR) in conjunction with other sensory proteins of ER stress, such as inositol requiring enzyme 1 (IRE1), which directs transcriptional gene expression through cytosolic splicing of x-box binding protein 1 (*XBP1*) mRNA that leads to the expression of an active XBP1(s) transcription factor (Schroder and Kaufman, 2005). PERK is a type 1 transmembrane protein positioned in the ER such that its N-terminus can monitor disruptions in protein homeostasis in this organelle. PERK can also respond to calcium dysregulation, oxidative damage, and an increased secretory load. PERK phosphorylation of eIF2α lowers the influx of nascent proteins into the ER and also induces changes in gene expression to enhance ER processing alongside ER-associated protein degradation (ERAD). This cascade of cellular events provides a mechanism for the removal and

breakdown of misfolded proteins to relieve ER stress. PERK has also been implicated in various diseases affecting a range of tissue types including diabetes, neuropathies, and cancers (Bobrovnikova-Marjon *et al.*, 2010; Delepine *et al.*, 2000; Malhi and Kaufman, 2011; Marciniak and Ron, 2006; Scheuner and Kaufman, 2008).

During activation, PERK dimerizes to facilitate autophosphorylation (Ma *et al.*, 2002). It has been suggested that activation of PERK occurs via decreased association with the ER chaperone binding immunoglobulin protein (BiP/GRP78) to the IRE-1 like domain in the luminal portion of PERK (Bertolotti *et al.*, 2000) (Figure 5). Alternatively, direct binding of misfolded proteins to the same luminal domain of PERK has also been proposed to be a critical activation signal of this UPR sensor.

1.5 Gene-specific translational control through upstream open reading frames

Together with repression of protein synthesis, eIF2α-P directs preferential translation of a subset of mRNAs during cellular stress. Mechanisms of expression of the downstream CDS can occur via secondary structures and upstream open reading frames (uORFs) located within the 5'-leader of induced mRNAs (Young and Wek, 2016). Essentially, these 5'-leaders function as bar codes by which ribosomes can recognize which transcripts are to be repressed or translated during eIF2α-P (Figure 6). The uORFs are defined by the presence of an in-frame initiation and termination codon with at least one codon in

between. uORFs were shown to be present in over 40% of human mRNAs and have been identified in ribosome profiling datasets as functional and recurrent sites of translation initiation (Baird *et al.*, 2014; Lee *et al.*, 2012). These same studies have also demonstrated the ability of non-canonical (non-AUG) initiation codons to serve as initiation sites in uORFs (Gao *et al.*, 2015; Kozak, 1989a, b; Lee *et al.*, 2012). Translation of an uORF occurs following 43S preinitiation complex binding to the 5' cap, followed by processive scanning 5' to 3' until the ribosome recognizes the first optimal initiation codon. After translation of the selected uORF, the 40S ribosomal subunit can retain association with the mRNA and scan once again for reinitiation of translation at a subsequent initiation codon. Alternatively, upon translation of the uORF, the ribosome can dissociate from the mRNA, resulting in sharply diminished translation of the CDS.

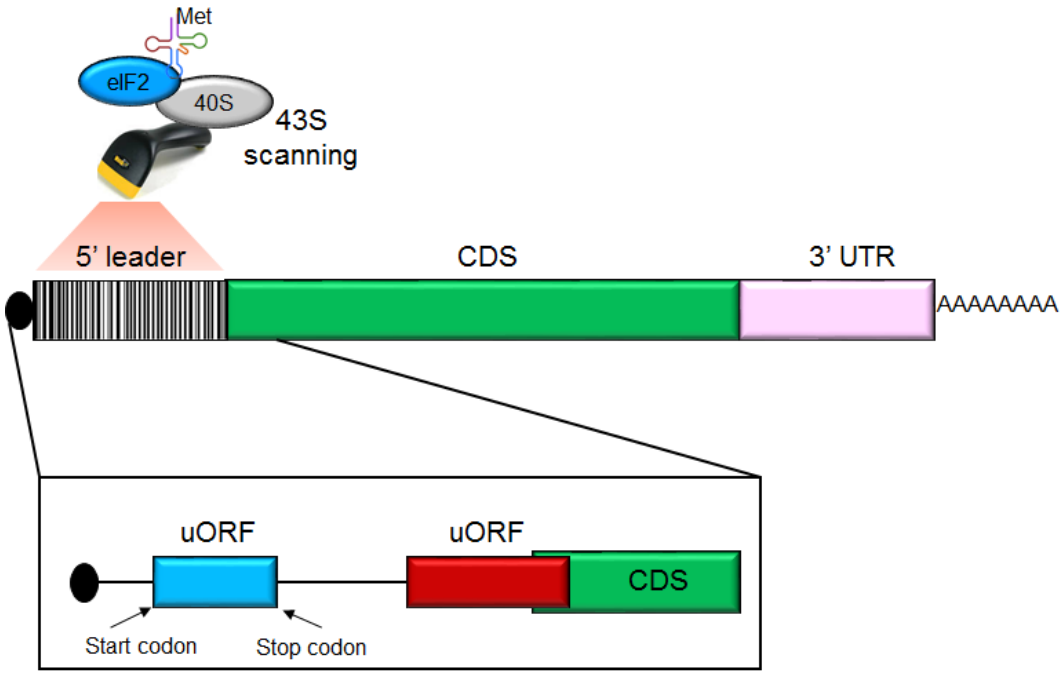

Figure 6. uORFs serve as barcodes for the gene-specific translational control. ISR-dependent mechanisms of translation control rely on the 5'-leaders of mRNAs. Following binding to the 5'- cap (depicted as a black circle), the 43S ribosomal preinitiation complex scans 5'- to 3'- along the mRNA until it encounters a start codon in optimal Kozak context. uORFs can be fully contained within the 5'-leader or overlap (in frame or out of frame) with the transcript CDS. uORFs can serve as dampeners or enhancers of downstream translation, depending on their arrangement and context. Therefore uORFs in the 5'-leader serve as a barcode to direct the translation machinery decision of whether a transcript should be translated or repressed during a given cellular condition. Importantly, translational control can also occur through association of RNA binding proteins to the 5'- or 3'- untranslated region (3'-UTR, depicted as a pink box).

Induction of eIF2α-P during stress decreases the rate of eIF2-GTP-Met-tRNA$_i^{Met}$ (eIF2 ternary complex) formation, which thereby affects how soon after completion of translation of an uORF a ribosome can reacquire the eIF2 ternary complex and reinitiate at the next start codon. If the uORF arrangement does not allow for reinitiation, either by overlapping out of frame or inducing a ribosome stall, it is considered inhibitory. Recent evidence also points to the existence of uORFs that enhance downstream translation by promoting reinitiation at the CDS or by facilitating a bypass of an inhibitory uORF (Palam *et al.*, 2011; Young *et al.*, 2016a; Young *et al.*, 2016b; Young *et al.*, 2015). Hence, depending on the nature and placement of uORFs in the 5'-leader of mRNAs, there can be preferential translation or dampening of mRNA translation during stress.

One of the most well understood mechanisms for uORF-mediated translation during stress is the delayed reinitiation model of mammalian *ATF4 (Hinnebusch, 2005; Vattem and Wek, 2004)*. The 5'-leader of the *ATF4* mRNA contains two uORFs: a 5'-proximal uORF1 that is 3 codons in length and a fifty-nine codon uORF2 that overlaps out-of-frame with the CDS and is therefore inhibitory. During unstressed conditions when eIF2-GTP is plentiful, translation initiates at uORF1 and rapidly reinitiates at the inhibitory uORF2; therefore there is minimal translation at the *ATF4* CDS. However, during stressed conditions eIF2α-P lowers the amount of eIF2-GTP-Met-tRNA$_i^{Met}$ delivered to ribosomes which delays reinitiation of the scanning ribosomes engaged with the *ATF4* mRNA. This delay will enhance ribosome bypass of the inhibitory uORF2. During the interval between the uORF2 initiation codon and the start codon for the *ATF4*

CDS, the scanning ribosome is suggested to reacquire the eIF2 ternary complex, allowing for reinitiation of translation of the CDS. Therefore, the distance between the uORFs and the CDS are critical for this mode of translational control. This mechanism is also central for *ATF5* translation in the ISR (Teske *et al.*, 2013).

Many other preferential translation mechanisms for ISR genes, including *CHOP*, *GADD34*, *EPRS*, and *IBTKα* have also been characterized previously in our laboratory (Baird *et al.*, 2014; Palam *et al.*, 2011; Young *et al.*, 2016a; Young *et al.*, 2016b; Young *et al.*, 2015). In these examples, a single inhibitory uORF appears to be sufficient for preferential translation in response to eIF2α-P. The basis for the uORF repressing effects includes the uORF being overlapping and out-of-frame with the CDS, ribosomal stalling during uORF translation, and an altered termination process during uORF translation. Precisely how the scanning ribosome bypasses the inhibitory uORFs during eIF2α-P is not yet understood, but the less than optimal sequences flanking the initiation codon of the bypassed uORFs appear to be essential.

Alternative mRNA splicing of human *CDKN1A* results in multiple transcript variants (variants 1-5). The p21 protein encoded in the *CDKN1A* gene functions to bind to and inhibit cyclin-dependent kinases, which triggers cell cycle arrest in response to environmental stresses (Deng *et al.*, 1995; Macleod *et al.*, 1995; Rigberg *et al.*, 1998). Of the five *CDKN1A* variants, only one (variant 3) encodes a unique isoform of the p21 protein. Variants 1, 2, 4, and 5 differ only in the sequences of the 5'-leaders of the respective mRNAs. This observation is important because alternative splicing, especially those altering the 5'-leaders of

mRNAs, can have major implications for translational control. Two *CDKN1A* variants (V1 and V4) have variations contained in the uORFs. V4 contains two uORFs: a 19-codon uORF1 with two non-canonical initiation codons, and a 48-codon uORF2 overlapping out-of-frame with the *CDKN1A* CDS. Of note, the non-AUG initiation sites in uORF1 were identified as functional sites of initiation in a previously published ribosome profiling dataset (Lee *et al.*, 2012). Additionally, a recent study described a mechanism for uORF-mediated translational control of the mouse *CDKN1A* transcript variant in response to amino acid deprivation (Lehman *et al.*, 2015). While providing evidence for ISR involvement in p21 protein expression, the mouse transcript variant bears no resemblance to the human variant, indicating species-specific differences in alternative splicing and translational control. This thesis will describe preferential translation of the *CDKN1A* V4 mRNA and its role in cell fate in response to UVB irradiation.

1.6 New roles for the ISR in the keratinocyte adaptation to stress

Little is known regarding the role of the ISR and translational control in the keratinocyte adaptation to stress. We propose that repression of global protein synthesis is a critical function during the process of keratinocyte differentiation and response to UVB irradiation. Induction of the ISR and accompanying translational control would allow keratinocytes to conserve energy and upregulate differentiation or UVB specific programs such as cell cycle control, DNA repair, apoptosis, and senescence. To address this hypothesis, we carried out polysome profiling analyses to analyze general and gene-specific translation.

Our data suggest that both keratinocyte differentiation and UVB irradiation cause a global inhibition of translation initiation coincident with eIF2α-P and preferential translation of stress-specific gene transcripts. Further, we show that loss of a functional ISR diminished proper keratinocyte differentiation and also altered cell fate in response to UVB, suggesting that the ISR is crucial in the proper keratinocyte adaptation to stress. We also demonstrate that, in response to stress, the ISR upregulated translation of human *CDKN1A* transcript variant 4 in a mechanism mediated by the mRNA 5'-leader. Taken together, this thesis provides new and important findings for translational control in the keratinocyte response to stress, and sheds light on additional regulatory processes of gene expression in human skin. Our results indicate that keratinocyte differentiation and UVB irradiation can act as two sides of the same coin; both processes require induction of the ISR but represent two distinct aspects of keratinocyte biology.

CHAPTER 3. EXPERIMENTAL PROCEDURES

2.1 Cell culture, treatments, and generation of stable cell lines

Normal human keratinocytes and fibroblasts were isolated from neonatal foreskin tissue as described previously (Kuhn *et al.*, 1999). N-TERT (Dickson *et al.*, 2000) and normal human keratinocytes were grown in EpiLife media (Invitrogen, Carlsbad, CA) supplemented with human keratinocyte growth supplement (HKGS, Invitrogen) and 1000U Penicillin-Streptomycin (Roche, Indianapolis, IN). Fibroblasts were grown in Dulbecco's Modified Medium (DMEM) supplemented with 10% fetal bovine serum (FBS). The collection of human skin biopsies was approved by the Indiana University School of Medicine Institutional Review Board. N-TERT keratinocytes were generated by overexpression the catalytic subunit of telomerase alongside a spontaneous loss of p16 expression (a gift from Dr. James Rheinwald, Harvard University) (Dickson *et al.*, 2000). Keratinocytes *in vitro* can be induced to differentiate by growing cells to confluence and switching to a growth media containing 2 mM Ca^{2+} and 2% FBS for 72 hours (Borowiec *et al.*, 2013). This calcium switch protocol is widely accepted as a means to initiate keratinocyte differentiation *in vitro* (Micallef *et al.*, 2009; Pillai *et al.*, 1990; Poumay and Pittelkow, 1995).

To construct 3D skin cultures, a collagen-fibril (collymer) matrix was created using a Standardized Oligomer Polymerization Kit (Geniphys, Zionsville, IN) according to the manufacturer's instructions. Briefly, Oligomer-PD was diluted to the desired concentration (2.25 mg/mL) in hydrochloric acid, followed by stepwise addition of sodium hydroxide and polymerization supplement which

facilitate polymerization by adjusting pH and ionic strength. While still on ice, primary fibroblasts were combined with the mix, and then added to a 3 μm transwell placed inside a well on a 6-well dish. This mixture was then incubated at 37°C for 10 minutes to induce polymerization. Following polymerization, 1.5 mL of 10% DMEM was added to the 6-well dish (underneath the transwell) and 1.5 mL of EpiLife was added on top of the transwell/polymerized matrix for 2 hours. $1.5x10^6$ primary human keratinocytes were then added to the top of each transwell and allowed to attach to the matrix overnight. The following morning, keratinocytes were moved to the air-liquid interface by removing any liquid from the top of the insert and replacing the bottom media with E media (Simpson *et al.*, 2010). Cells were allowed to stratify for 7 days prior to subsequent analysis.

Stable N-TERT knockdowns were produced using validated Mission shRNA clones as described previously (Teske *et al.*, 2011b). shRNA sequences are listed in Table 1 (Sigma-Aldrich, St. Louis, MO). The ATF4 knockdown cells and their wild-type counterparts were supplemented with extra amino acids and 55 μM β-mercaptoethanol due to an increased sensitivity of ATF4-depleted cells to oxidative stress (Harding *et al.*, 2003). Cells overexpressing GADD34 were created by transducing N-TERT keratinocytes with a lentivirus encoding a doxycycline-inducible full-length human *GADD34* gene with a C-terminal HA tag. This lentivirus was constructed by first PCR-amplifying the GADD34 coding sequence (Thermo Fisher, prepared from plasmid MHS6278-202828370) using the following primers:

F: 5’-GGGGACAAGTTTGTACAAAAAAGCAGGCTGC-3’-,

B: 5’-GGGGACCACTTTGTACAAGAAAGCTGGGTCCTA-3’-.

The resulting GADD34 PCR product was incubated with Donor Vector and BP Clonase enzyme mix (Invitrogen, #11789-020) to create the GADD34 entry vector, following the vendor's instructions. The GADD34 entry vector was then incubated with LR clonase mix (Invitrogen, #11791-020) and a p-LIX402 lenti vector (gift from David Root, Addgene plasmid # 41394, Cambridge, MA). Primers used to insert GADD34 into p-LIX402 were as follows:

pLIX R: 5’-phospho-CTTATCGTCGTCATCCTTGTAATC-3’-

pLIX F: 5’-phospho-GAAATGGAAGCCAAAGCTGAAGATTAA-3’-

GADD34 F: 5’-phospho-ATGGCCCCAGGCCAAGCACCCCAT-3’-

GADD34 R: 5’-phospho-TTATCAGCCACGCCTCCCACTGAG-3’-.

GADD34 insertion into p-LIX402 was confirmed by sequencing. Transduced cells were selected for stable expression with 1 µg/mL puromycin. Expression of GADD34 was induced by 24 hours of treatment with 1 µg/mL doxycycline that was confirmed by immunoblot. Cultured cells were treated with 2 µM tunicamycin, 10 µM actinomycin D, 0.1 µM thapsigargin, 0.1 µM halifuginone, or 50 µg/mL cycloheximide as indicated. All of these reagents were purchased from Sigma.

UVB irradiation of N-TERT keratinocytes was carried out using Philips FS20T12 UVB broadband light sources as described previously (Lewis et al., 2010). An IL1700 radiometer and a SED240 UVB detector (International Light, Newburyport, MA) were used to measure UVB intensity prior to each experiment

using a distance of 8 cm from the light source to the culture dish. Cells were always irradiated in EpiLife media, which blocks the small amount of UVC emitted from the broadband source, followed by normal incubation setting (37°C and 5% CO_2).

Gene Name	Clone ID	Target Sequence
ATF4	TRCN0000013575	GCCAAGCACTTCAAACCTCAT
CHOP	TRCN0000007265	CGAATGGTGAATCTGCACCAA
GCN2	TRCN0000300850	GCCTAACTGGTGAAGAAGTAT
GCN2	TRCN0000304216	CCGGCCCTAAAGAACTGTCGT
CDKN1A	TRCN0000287091	GACAGATTTCTACCACTCCAA
PERK	TRCN0000262380	GGAACGACCTGAAGCTATAAA
Luciferase Control	SHC007	CTTCGAAATGTCCGTTCGGTT

Table 1. shRNA clone names and sequences. Validated Sigma Mission shRNA clone numbers, along with the 5'- to 3'- sequences of the targeted genes.

2.2 Polysome profiling

Polysome analysis used 10 to 50% sucrose gradients containing 20 mM Tris-HCl (pH 7.5), 100 mM NaCl, 5 mM $MgCl_2$, and 50 µg/ml cycloheximide as described previously (Palam *et al.*, 2011; Teske *et al.*, 2011a). Gradients were made using a tilted tube rotation method on a gradient station equipped with a Piston Gradient Fractionator and a Gradient Master (BioComp, Fredericton,

Canada). Irradiated and control cultured keratinocytes were incubated in EpiLife media containing 50 µg/ml cycloheximide for 10 minutes at 37°C prior to harvest. Cells were rinsed twice with ice-cold phosphate buffered saline (PBS) containing 50 µg/ml cycloheximide and then lysed with 500 µl of cold lysis buffer containing 20 mM Tris (pH 7.5), 100 mM NaCl, 10 mM $MgCl_2$, 0.4% Nonidet P-40, 50 µg/ml cycloheximide, and an EDTA-free protease inhibitor cocktail tablet (Roche, Indianapolis, IN). Lysates were sheared with a 1 mL syringe and 23-gauge needle, incubated on ice for 10 minutes, and clarified at top speed in a table-top micro centrifuge for 10 minutes. Supernatants were added to the top of the gradients, which were then subjected to ultracentrifugation in a Beckman SW41Ti rotor at 40,000 rpm for 2 hours at 4°C. Polysome profiles and 14 sucrose fractions for each sample were collected with a Piston Gradient Fractionator and a 254 nm ultraviolet monitor with Data Quest software. To analyze specific mRNA transcript shifts following UVB irradiation, fractions were pooled into 7 samples and RNA was extracted from sucrose fractions via TRIzol Reagent LS (Invitrogen, Life Technologies). Firefly luciferase control RNA (Promega, Madison, WI) was added to each pooled sample before RNA isolation, so that the relative amounts of the transcript of interest to be standardized to an exogenous RNA control. To represent percentage total gene transcript for the seven fractions, the $2^{(-\Delta\Delta CT)}$ value for each fraction was divided by the $2^{(-\Delta\Delta CT)}$ value sum of all fractions.

2.3 Immunoblot analyses

For immunoblot analyses, cultured cells were washed with ice-cold PBS and lysed in a solution containing 50 mM Tris-HCl (pH 7.9), 150 mM NaCl, 0.1% SDS, 100 mM NaF, 17.5 mM glycerol phosphate, and 10% glycerol supplemented with protease inhibitors (100 μM phenylmethylsulfonyl fluoride, 0.15 μM aprotinin, 1 μM leupeptin and 1 μM pepstatin). Lysates were sonicated for 30 seconds and precleared by centrifugation at top speed in a microfuge for 10 minutes. Protein concentrations were measured using the Bio-Rad protein quantification kit for detergent lysis (Bio-Rad Laboratories, Inc.; Herculues, CA) and equivalent protein levels were subjected to electrophoresis by SDS/PAGE. Proteins were transferred to nitrocellulose membranes via cold wet transfer for 2 hours at 80 volts. Membranes were then incubated in PBS supplemented with 5% (w/v) nonfat dried milk for 30 minutes followed by overnight incubation with antibodies for phosphorylated eIF2α at serine 51, phosphorylated GCN2 at threonine 899, and KRT1 (Abcam #32157, #75836, and #93652, respectively); p53, phosphorylated p53 at serine 15, total GCN2, cleaved caspase-3, S6, S6-P, and p21 (Cell Signaling Technologies; Danvers, MA; #9282, #9284, #3302, #9661, #2217, #4858, and #2947, respectively); monoclonal antibody for total eIF2α (Scott Kimball. Pennsylvania State University College of Medicine, Hershey, PA); CHOP and IVL (Santa Cruz Biotechnology; Dallas, TX; sc-575 and 21748, respectively), ATF4 prepared against recombinant protein (Zhou et al., 2008), GADD34 (Proteintech #10449, Rosemont, IL), cyclin D1 (Millipore, Billerica, MA DCS-6), and β-actin (Sigma #A5441). Membranes were washed the

next day in PBS-Tween for 1 hour followed by 1 hour in milk supplemented with a secondary antibody tagged with horseradish peroxidase, followed by 1 hour in PBS-Tween. Proteins bound to antibody on the membrane were visualized by incubation in a chemiluminescent solution followed by exposure to x-ray film.

2.4 Measurement of mRNA levels by quantitative PCR

RNA was isolated from cultured keratinocytes using TRIzol reagent (Invitrogen, Life Technologies). Single-strand cDNA synthesis was conducted using the TaqMan reverse transcriptase kit (Applied Biosystems, Life Technologies). mRNA levels were measured by quantitative PCR (qPCR) using transcript-specific SYBR Green primers on a Realplex2 Master Cycler (Eppendorf, Hamburg, Germany). To measure the levels of target mRNAs, transcripts were normalized to luciferase control RNA (Promega). Statistical significance was calculated using the two-tailed student's t test. SYBR green primer sets are listed in Table 2. Quantification of *CDKN1A* transcript variants was carried out using cDNA generated from untreated N-TERT keratinocytes. PCR was performed for 35 cycles with gene-specific primers (CDKN1A V1/V4) using Bullseye Taq Polymerase (MIDSCI, St. Louis, MO). Synthesized DNAs were separated and visualized by electrophoresis using a 2% agarose gel supplemented with ethidium bromide. Representative bands were quantified by using ImageJ software.

Gene	Forward Sequence	Reverse Sequence
ATF4	TCAAACCTCATGGGTTCTCC	GTGTCATCCAACGTGGTCAG
CCND1	GAGGAAGAGGAGGAGGAGGA	GAGATGGAAGGGGGAAAGAG
CHOP	AGCCAAAATCAGAGCTGGAA	ACAAGTTGGCAAGCTGGCTCT
eIF4E	TGTGGCGCTGTTGTTAATGT	GCGTGGGACTGATAACCAAT
GCN2	AGGTCTAGGCGAGAACGTCA	CCACTGAAGGACCCACTCAT
GRP78	TAGCGTATGGTGCTGCTGTC	GGGAGGCAGTGGAGTTG
IVL	CCTCAGCCTTACTGTGAG	TTTGTCAGGGGTCTTTCACC
Luciferase	CCAGGGATTTCAGTCGATGT	AATCTCACGCAGGCAGTTCT
CDKN1A	CAGCAGAGGAAGACCATGTG	GGCGTTTGGAGTGGTAGAAA
CDKN1A V1	AGGCACTCAGAGGAGGCGCCA	GGTGACAAAGTCGAAGTTCCA
CDKN1A V4	TGTTTCTGCGGCAGGCGCCAT	CCGCCATTAGCGCATCACAGT
CDKN1A V1/V4	AGCAGCTGCCGAAGTCAGTTC	GGACATCCCCAGCCGGTTCTG
PERK	CTCAGCGACGCGAGTACC	TCCCAAATACCTCTGGTTTGCT
XBP1(s)	CTGAGTCCGAATCAGGTGCAG	ATCCATGGGGAGATGTTCTGG

Table 2. PCR primer sequences. The 5'- to 3'- sequences of primer pairs are listed for SYBR green quantification of the indicated gene transcripts.

2.5 Immunofluorescence and microscopy

Immunofluorescence was performed as described previously (Loesch et al., 2016). Tissues were fixed in formalin for 1 hour at room temperature. Tissue embedding and sectioning was performed by the Indiana University Histology Core. Briefly, specimens were dehydrated through a graded series of ethanol treatments (45 minutes per step), cleared in two changes of xylenes (45 minutes each) and infiltrated through 4 changes of melted paraffin (~60°C; 45 minutes each). The specimens were then embedded in melted paraffin and allowed to harden. Thin sections (4-12 μm) were cut using a rotary microtome equipped with disposable steel knives. Sections were flattened on a heated water bath, floated onto microscope slides and dried.

Paraffin embedded tissues were sectioned and deparafinized by two five minute incubations at room temperature fully submerged in HistoPrep Xylene (Thermo), followed by the subsequent 5 minute incubations in 100, 95, and 70% ethanol, all at room temperature. Sections were then heated at 95° for 20 minutes in 1X antigen retrieval solution, pH 9 (DAKO, Santa Clara, CA) and then allowed to cool on the bench top for an additional 20 minutes. Slides were washed in water three times followed by a five minute incubation in 2% Triton-X100. Slides were washed three more times and then blocked for one hour with Cas-Block (Thermo Fisher) at room temperature in a humidified chamber. Sections were then incubated with antibodies against eIF2α-P (Abcam, #32157), ATF4 (Cell Signaling Technologies, D4B8), CHOP or IVL (Santa Cruz Biotechnology, sc-575 and 21748, respectively), or Ki67 (Thermo SP6) in a

humidified chamber overnight at 4°. The following day, sections were washed three times by rocking in water at room temperature. Slides were then incubated with a secondary antibody conjugated to the desired fluorochrome (Invitrogen Molecular Probes, A31632 goat anti-rabbit 594nm, A31624 goat anti-mouse 594nm, or A31620 goat anti-mouse 488nm) for one hour in the dark. Sections were washed with water in the dark (covered with foil) two times, then incubated for 15 minutes in the dark with 1:1,000 DAPI (10mg/mL), and mounted onto coverslips using Immu-Mount (Thermo). Slides were imaged with a Nikon 80i microscope with Intensilight epifluorescence and Qimaging camera. Images were prepared using a 20X objective lens at 25°C. Qimaging and Nikon Elements software were used for data acquisition.

2.6 Cell cycle analyses

S phase labeling was accomplished using a Click-iT EdU Alexa Fluor 488 Imaging Kit (Life Technologies) following the manufacturer's instructions. N-TERT keratinocytes were synchronized in G1 by removing growth factors from the media for 48 hours, followed by recovery by adding growth factors back to the media for 8 hours. Following UVB, cells were labeled with 10 μM EdU for 1 hour and then cells were removed from culture dishes by trypsinization. The cells were then fixed with 4% paraformaldehyde, permeabilized, and added to the Click-iT Plus reaction cocktail to detect EdU incorporation according to the manufacturer's instructions. Following incubation with the reaction cocktail, cells were collected by centrifugation (10 minutes at 750 xg) and resuspended in a

500μL solution of FxCycle PI/RNase Staining Solution (Life Technologies) in the dark for 30 minutes. EdU staining and DNA content were measured on an Attune Acoustic Focusing Flow Cytometer (Life Technologies) using a 530/30 BL1 or 574/26 BL2 filters, respectively. Live cells were gated based on forward (FSC) and side (SSC) scattering light area. 100,000 live events were captured and characterized for each sample. Appropriate cell populations were calculated using Attune Cytometric software and presented as a percentage of total live cells.

2.7 DNA repair assays

To measure relative amounts of thymine dimers over time, cultured cells were scraped from dishes in PBS, pelleted, and genomic DNA was isolated using a Wizard DNA Purification Kit (Promega, Madison, WI). 0.5 μg of genomic DNA was diluted in 50 μL TE solution, then added to 50 μL of denaturing solution (0.5 M NaOH, and1 M NaCl), and heated at 70°C for 10 min. Samples were then placed on ice for 5 min, followed by addition of 100 μL ice cold 0.2X SSC. DNA slot blotting was performed using the 48-well Convertible Filtration Manifold System (Life Technologies part #14323C). A sheet (dimensions dependent on the number of wells utilized) of Gene Screen Plus Hybridization Transfer Membrane (Perkin Elmer, Waltham, MA) was soaked in a wetting solution (0.4 M Tris-HCl, pH 7.5) and applied on top of the filtration manifold system. Wells in the manifold system were uniformly washed with a total of 200 μL of wetting solution and 0.5 μg of each sample (prepared earlier) was loaded per well to bind to the

membranes inserted on top of the manifold. A vacuum was used to facilitate the application of the DNA to the filer through each well. The membrane was removed from the manifold then soaked in a neutralization buffer (0.5 M NaCl and 0.5 M Tris-HCl, pH 7.5) for 10 min and allowed to dry overnight at 37°C. The membrane was then blocked in 5% milk for 30 min, followed by a one hour incubation in 5% milk containing a 1:2000 dilution of a thymine dimer antibody (KTM53; Kamiya Biomedical, Seattle, WA). The membranes were washed three times for 15 min in PBS-Tween, followed by incubation in 5% milk containing a 1:5000 dilution of an HRP-conjugated anti-mouse IgG (Cell Signaling Technology, Danvers, MA). The membrane was again washed three times followed and the bound antibody complex was detected by chemiluminescence (GE Healthcare, Pittsburgh, PA). Relative amounts of DNA repair were calculated by using densitometry and ImageJ software. The amount of DNA repair at each collection time was calculated as a percent of thymine dimers at 15 minutes post-UVB, at which repair was considered 0%.

To perform a host-cell reactivation assay, N-TERT keratinocytes were transfected with 1 µg undamaged or damaged PGL3 control plasmid alongside 50 ng Renilla transfection control (Promega) into each well of a 6-well dish containing 50,000 cells. The damaged plasmid was irradiated with 600 J/m^2 UVB. Luciferase assays were then performed as described in Chapter 2.9.

2.8 Cell death and senescence assays

To measure senescence-associated β-galactosidase, N-TERT keratinocytes were washed twice in PBS followed by fixation in a solution of 2% formaldehyde/0.2% gluteraldehyde at room temperature for 10 minutes. Cells were again washed twice with PBS and then incubated with staining solution (50 mM sodium chloride, 25 mM sodium phosphate dibasic, 7 mM citric acid, 5 mM potassium ferricyanide, 5 mM potassium ferrocyanide, 2 mM magnesium chloride, and 1 ng/ml 5-bromo-4-chloro-3-indolyl-β-d-galactoside, pH 6.0) for 16 hours at 37°. The staining solution was then removed, cells were changed to PBS, and photographs were taken using bright field microscopy.

Caspase-3 activity was measured using a synthetic fluorogenic substrate (DEVD-AMC, Alexis Biochemicals, San Diego, CA). Cultured keratinocytes scraped from culture dishes were pelleted and suspended in caspase lysis buffer (50 mM PIPES pH 7.0, 50 mM KCl, 5 mM EGTA, 2 mM MgCl2, and 1 mM DTT) and subjected to three rounds of freeze-thawing (-80°C to 42°C). Cellular debris was removed by centrifugation at top speed in a microfuge for 3 minutes. 50 µL of cell lysate was added to 55 µL of caspase-3 reaction buffer (100 mM HEPES, pH 7.5, 10% sucrose, 0.1% CHAPS, 10 mM DTT, 0.1 mg/mL bovine albumin, and 50 µM DEVD-AMC substrate) and incubated at 37°C for 45 minutes. Release of the fluorescent AMC moiety was measured using a Hitachi F2000 spectrophotofluorimeter (excitation, 380 nm; emission, 460 nm). The fluorescence intensity was converted to pmoles of AMC by comparison to the fluorescent intensity of standards of AMC (7-amino-4-methylcoumarin; Molecular

Probes, Eugene, OR). The specific activity of caspase-3 was determined following measurement of the total protein concentration of the cell lysates (Bio-Rad Protein Assay Reagent).

Trypan blue assays were performed using a TC20 Automated Cell Counter (BioRad). 10 µL of cell suspension was added to 10 µL of 0.4% Trypan Blue Dye (BioRad). 10 µL of the mixture was added to a counting slide and live cells were detected, quantified, and reported by the cell counter.

2.9 Luciferase assays and plasmid constructs

P_{Tk}-*CDKN1A*-Luc reporters were constructed by inserting a cDNA fragment encoding the wildtype or mutated 5'-leader of *CDKN1A* V1 or V4 inserted into *Hin*dIII and *Nc*oI sites located between the P_{Tk} promoter and luciferase CDS in a derivative of PGL3 plasmid (Vattem and Wek, 2004). The uORF fusion constructs were made by inserting cDNA fragments between *HindIII* and *NarI* sites on the same PGL3 plasmid. The fusions were designed to ensure removal of the start codon of the luciferase CDS. 1 µg of each construct along with 50 ng of a Renilla transfection control plasmid (Promega) were co-transfected into 50,000 N-TERT keratinocytes for 24 hours using Fugene-6 (Promega) according to manufacturer instructions. Cells were collected following treatment with either 100 J/m^2 UVB or 0.1 µM TG for 6 hours. Dual luciferase assays were carried out as described by the Promega instruction manual on a 20/20 luminometer (Turner Biosystems, Sunnyvale, CA). Changes made in mutated constructs are outlined in Table 3.

Gene construct	Description of Mutation
CDKN1A V4 uORF1 ΔATG	AGG**ATG**CGT to AGG**AGG**CGT
CDKN1A V4 uORF1 ΔCTG1	GTG**CTG**CGT to GTG**CGG**CGT
CDKN1A V4 uORF1 ΔCTG2	TTT**CTG**CGG to TTT**CGG**CGG
CDKN1A V4 uORF2 ΔGTG	CTT**GTG**GAG to CTT**GGG**GAG
CDKN1A V4 uORF2 ΔCTG	GAG**CTG**GGC to GAG**CGG**GGC

Table 3. Description of luciferase reporter mutations. The 5'- to 3'-sequences of the mutations introduced into the P_{Tk}-CDKN1AV4-Luc reporter. Δ indicates a single nucleotide change from T to G was made for the indicated initiation codon. Bold indicates the affected initiation codon.

CHAPTER 3. RESULTS: HUMAN KERATINOCYTE DIFFERENTIATION REQUIRES TRANSLATIONAL CONTROL BY THE EIF2α KINASE GCN2

3.1 Translation initiation is repressed during keratinocyte differentiation

To determine the regulatory importance of control of translation initiation in keratinocyte differentiation, undifferentiated and differentiated keratinocyte lysates were prepared and subjected to sucrose gradient ultracentrifugation to measure protein synthesis as judged by polysome profiling. The polysome assay determines the amount of ribosomal loading on mRNA at a fixed point in time. Differentiated keratinocytes were compared with subconfluent, proliferating cultures of keratinocytes defined here as undifferentiated (Figure 7a). Keratinocyte differentiation substantially decreased the level of cellular mRNAs bound to heavy polysomes coincident with an increase in mRNAs associated with 80S monosomes, indicating repression of translation initiation (Figure 7b). Translational efficiency can be quantified by determining the ratio of mRNA bound to polysomes and monosomes (p/m); larger p/m values correspond to increased translation. The p/m of differentiated keratinocytes was decreased by six-fold compared to undifferentiated controls. To determine if translational control also impacted the elongation phase of protein synthesis, polysome profiling analyses were performed without the addition of cycloheximide (CHX). If differentiation also lowered the elongation phase of translation, omission of CHX should not significantly change the levels of measured polysomes. However in the absence of CHX, differentiated keratinocytes showed a further decrease in polysomes accompanied by increased levels of monosomes (Figure 7b, blue

line), verifying that the repression of protein translation occurred predominantly at the initiation stage.

While the use of *in vitro* two-dimensional cell culture is a powerful tool to study keratinocytes, this culture condition may not fully represent how intact three-dimensional (3D) skin undergoes differentiation. Therefore, 3D organotypic skin equivalents were constructed using primary keratinocytes (Figure 7c) and analyzed by polysome profiling. A monolayer of undifferentiated primary keratinocytes seeded on collagen-fibril/fibroblast matrix, the initial step in constructing a skin equivalent (Figure 7d, green line), displayed levels of translation similar to that of a keratinocyte monolayer grown on a plastic dish. However, after seven days of growth at the air-liquid interface, fully stratified skin equivalents revealed sharply lowered levels of transcripts bound to heavy polysomes coincident with increased numbers of mRNAs associated with 80S monosomes (Figure 7d, red line), indicating a repression of translation initiation similar to keratinocytes differentiated in monolayers. Collectively, these results indicate that keratinocyte differentiation is concomitant with lowered translation initiation in a 3D tissue.

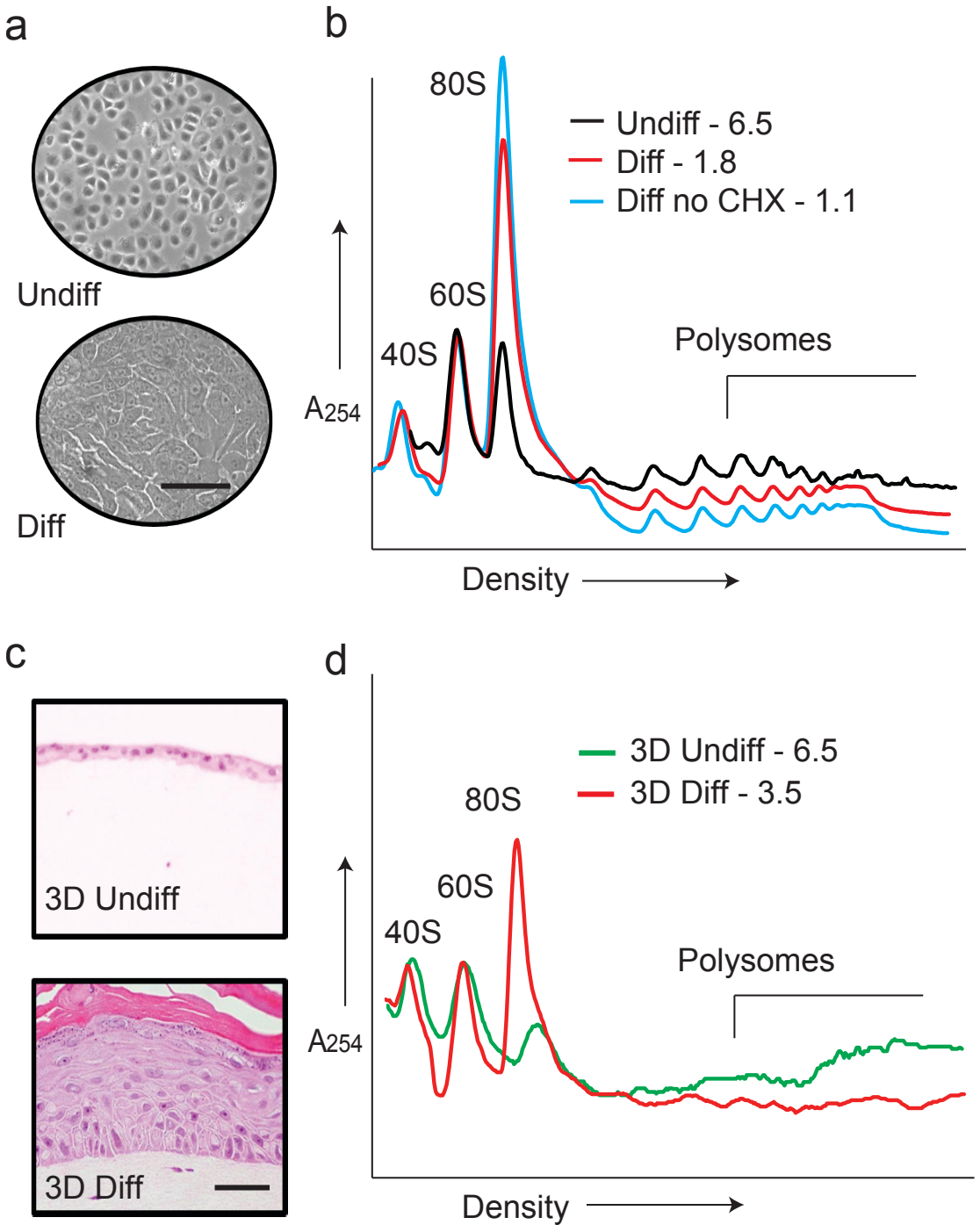

Figure 7. Global translation initiation is repressed during keratinocyte differentiation. (a) Phase-contrast images of undifferentiated (Undiff) and differentiated (Diff) N-TERT keratinocytes generated by switching confluent N-

TERT keratinocytes to a media containing 2mM Ca^{2+}/2% FBS for 72 hours. Polysome profiles for these conditions are shown in (b). No CHX (blue line) indicates that cycloheximide was omitted from the protocol. (c) 3D organotypic cultures were fixed at Day 0 (3D Undiff) and 7 (3D Diff) after raising to the air-liquid interface and stained with H&E. Polysome profiles generated for these conditions compared to an undifferentiated monolayer control are shown in (d). For all polysome profiles, ratio of polysomes to monosomes (P/M) is indicated to the right of each sample label. Scale bars = 50 μm.

3.2 The ISR is activated in differentiated keratinocytes

To determine whether the ISR is induced in differentiating keratinocytes, eIF2α-P was measured in both undifferentiated and differentiated cells. Levels of eIF2α-P were nearly 9-fold higher in differentiated keratinocytes as compared to undifferentiated cells (Figure 8a and b). Of importance, there were increased amounts of the differentiation-specific proteins IVL and KRT1. As a control, keratinocytes were also treated with tunicamycin (TM), a potent inducer of ER stress and the eIF2α kinase PERK. While eIF2α-P was increased following treatment with TM, there were no detectable IVL and KRT1 proteins, indicating that eIF2α-P alone cannot induce keratinocyte differentiation. As expected, *IVL* mRNA was significantly elevated with keratinocyte differentiation but not with exposure to TM (Figure 8c). Importantly, eIF2α-P occurred early during differentiation (within 24 hours), was detected concurrently with the induction of IVL, and was sustained over the course of the experiment (Figure 8d).

To address whether eIF2α-P occurs during keratinocyte differentiation *in vivo*, full-thickness human skin was obtained from surgical abdominoplasty procedures. The tissue was fixed, paraffin embedded, sectioned, and stained with antibodies to measure eIF2α-P, ATF4, or CHOP (Figure 8e), which are subject to preferential translation in the ISR. Fluorescence marking the increased presence of each of these ISR markers was increased specifically in the suprabasal layers of the epidermis, which contain differentiated keratinocytes. By comparison, these protein markers were not visible in the single layer of basal keratinocytes. These results indicate that eIF2α-P and translational control are induced selectively in differentiated keratinocytes, *in vivo* and *in vitro*.

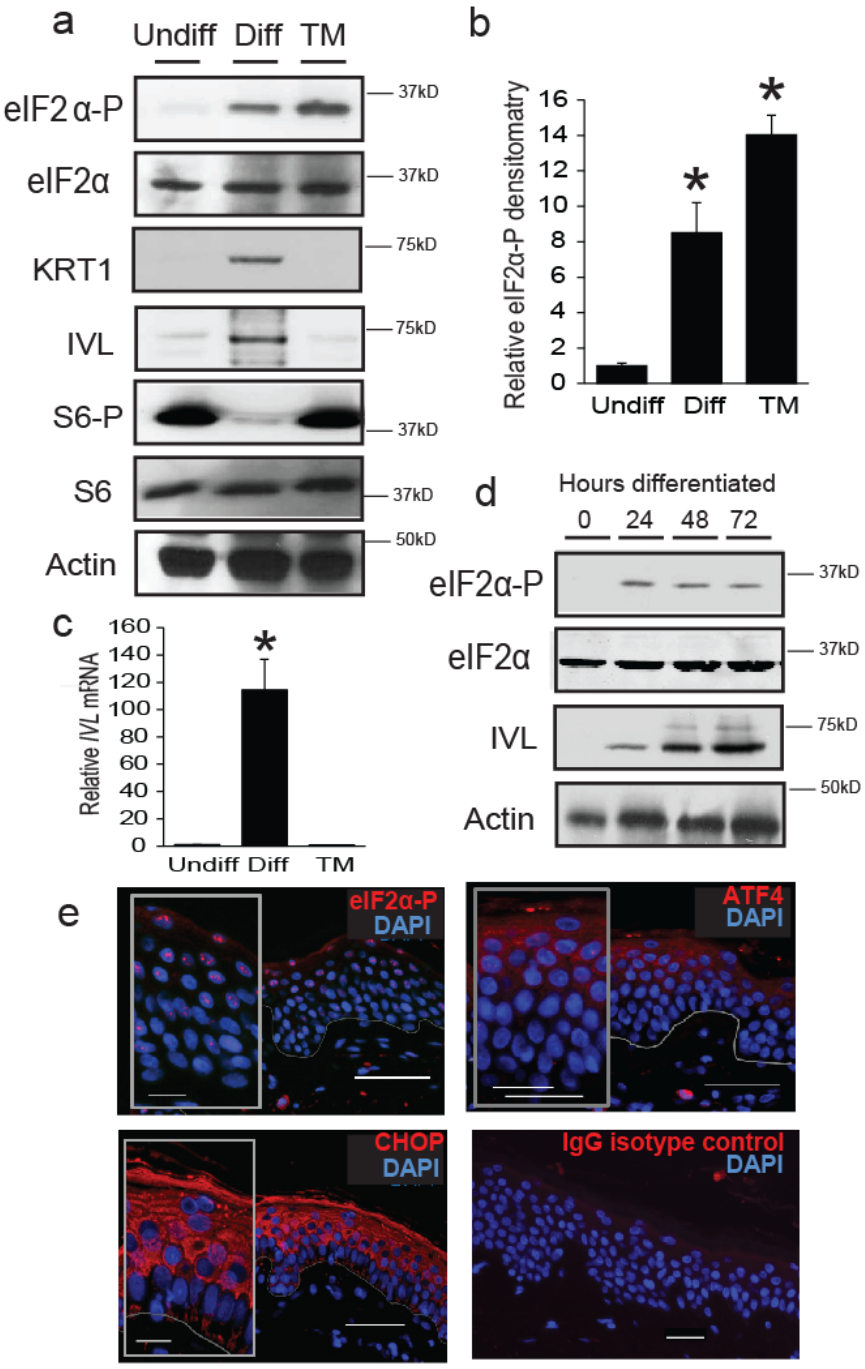

Figure 8. The ISR is activated in differentiated keratinocytes. (a) Undifferentiated (Undiff), differentiated (Diff), and tunicamycin (TM)-treated N-TERT keratinocytes were subjected to immunoblot analysis to measure levels of the indicated proteins. Levels of eIF2α-P as measured by densitometry are

indicated in (b). Alternatively, RNA was collected from samples and mRNA levels were measured for *IVL* (c). Keratinocyte differentiation was also monitored for the indicated number of days and lysates were subjected to immunoblot analysis (d). Full-thickness skin was stained for antibodies against eIF2α-P, ATF4, CHOP, or an IgG isotype control (e). The basement membrane is demarcated with a gray line. Scale bars in panels D and F are: large image = 50 μm, inset = 25 μm. *, $p<0.05$. Error bars represent mean +/- SD of three separate experiments.

3.3 Gene-specific translational control during keratinocyte differentiation

In addition to global translation repression, eIF2α-P leads to enhanced translation of specific mRNA transcripts, such as *ATF4* and *CHOP*. To investigate if gene-specific translational control occurs during keratinocyte differentiation, fractions were collected from polysome profiles and levels of specific mRNAs were measured by qPCR. The percent of total *ATF4* and *CHOP* mRNAs present in heavy polysomes (fractions 5-7) was increased by 18% and 27%, respectively, during differentiation of keratinocytes *in vitro* (Figure 9a and b), indicative of preferential translation during eIF2α-P. Average polysome (fractions 5-7) over monosome (fractions 1-3) values are indicated for each gene transcript to further illustrate changes in polysome association during differentiation. Importantly, *IVL* transcripts also shifted 27% toward heavy polysomes during differentiation (Figure 9c). By comparison, *eIF4E* mRNA showed a 12% shift away from heavy polysomes towards monosomes (Figure 9d), which is representative of the large number of genes that are subject to

translation repression in the ISR. These results show that individual mRNAs including canonical ISR markers and keratinocyte differentiation-specific transcripts are bound to heavy polysomes despite global repression of translation that occurred during keratinocyte differentiation (Figure 7b).

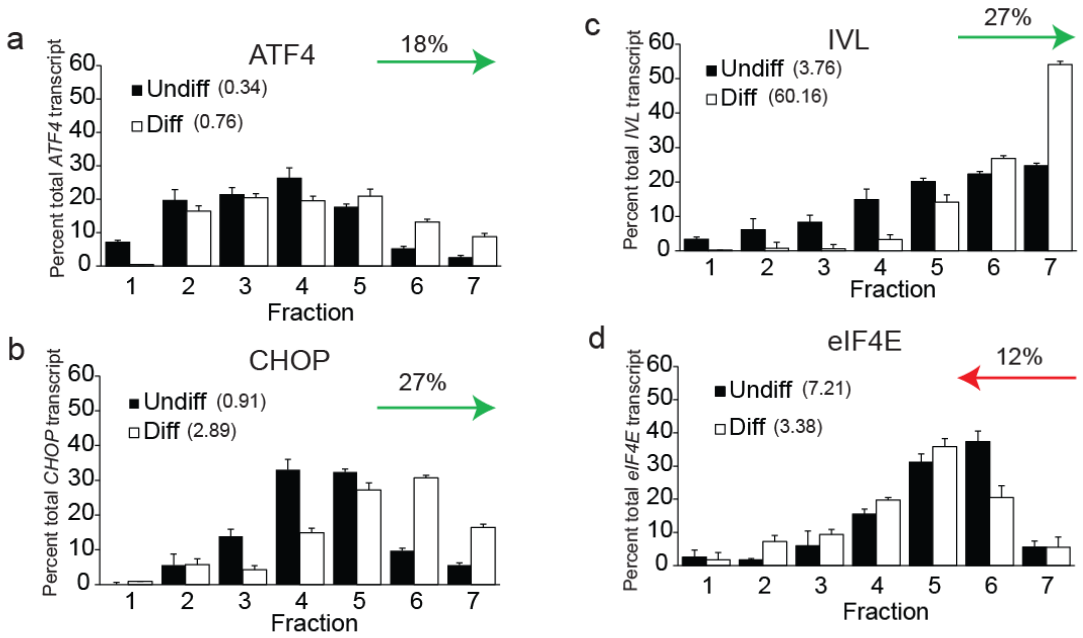

Figure 9. Gene-specific translational control during keratinocyte differentiation. RNA was isolated from sucrose fractions taken from polysome profiles in Figure 7b and used to generate cDNA. qPCR was used to measure mRNA levels of (a) *ATF4*, (b) *CHOP*, (c) *IVL*, or (d) *eIF4E* in each fraction. Levels of mRNA were normalized to a spike-in luciferase transcript, and represented as a percent total for each mRNA so as to omit changes in gene transcript levels. Arrows represent shifts towards (green) or away from (red) heavy polysomes (fractions 5-7), and the total percentage of each gene transcript that shifts during differentiation are indicated next to each sample label. Error bars represent mean +/- SD of three separate experiments.

3.4 Inhibition of the ISR response suppresses keratinocyte differentiation

To determine whether eIF2α-P plays a critical role in keratinocyte differentiation, we utilized a doxycycline-inducible (DOX) system to overexpress GADD34 in N-TERT keratinocytes. Elevated levels of GADD34 lead to robust dephosphorylation of eIF2α, which will halt the ISR and relieve global translational repression. When GADD34 was overexpressed in differentiated keratinocytes, polysome profiling analyses revealed a shift to heavy polysomes alongside a decrease in monosome association (Figure 10a). These findings are consistent with GADD34 relieving translation repression in response to keratinocyte differentiation. Importantly, GADD34-induced dephosphorylation of eIF2α reduced the amount of IVL protein over 2-fold in keratinocytes compared to differentiated controls (Figure 10b and c). Overexpression of GADD34 also decreased the levels of KRT1 protein, indicating a widespread effect on expression of differentiation proteins. Elevated levels of GADD34 lowered the polysome association and resulting p/m ratio for *ATF4* and *CHOP* mRNAs (Figure 10d), and *IVL* transcript (Figure 10e) compared to differentiation in the absence of DOX. By contrast, the p/m value for *eIF4E* was significantly increased upon GADD34 overexpression (Figure 10d). Of note, DOX-reduced levels of eIF2α-P led to a 2-fold reduction in *IVL* mRNA levels during keratinocyte differentiation compared to the differentiated control, suggesting that translational control also contributed directly or indirectly to the increase in *IVL* transcript (Figure 10f). These results indicate that differentiation-specific protein expression is dependent on eIF2α-P and the induction of the ISR.

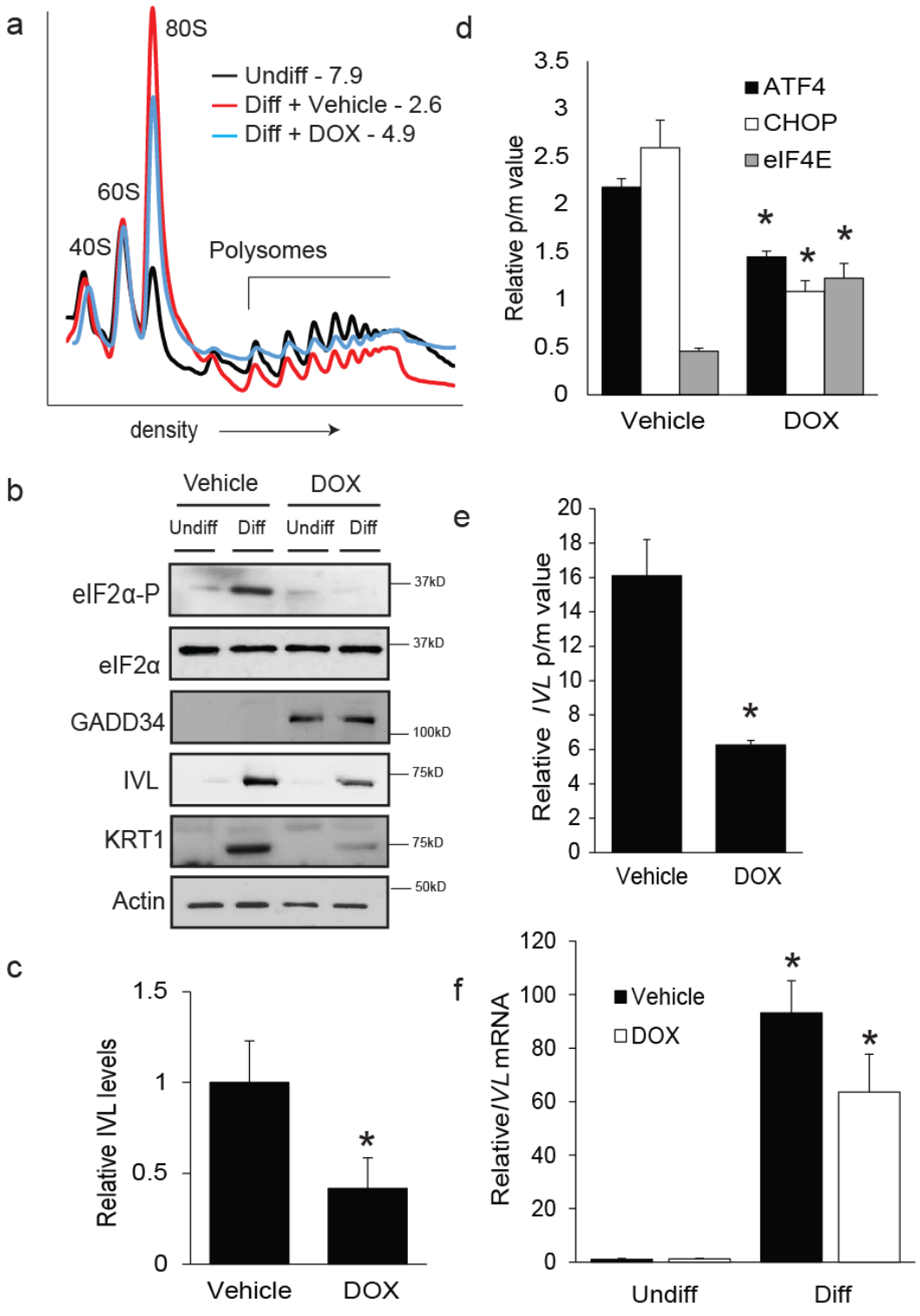

Figure 10. Inhibition of the ISR suppresses keratinocyte differentiation. (a) Polysome profiles were generated for undifferentiated (Undiff), differentiated

(Diff+Vehicle), and differentiated during GADD34 overexpression (Diff+DOX) N-TERT keratinocytes grown in monolayer culture. p/m ratios are listed beside each sample. (b) Alternatively, lysates were subjected to immunoblot analysis to measure the levels of the indicated proteins. Measurement of IVL protein is indicated in (c). (d) P/M values are displayed for the indicated gene for each respective treatment group. (f) Alternatively, total RNA was isolated from cells and qPCR was performed to measure levels of *IVL* mRNA. *, $p<0.05$. Error bars represent mean +/- SD of three separate experiments.

3.5 Loss of GCN2 abrogates differentiation gene expression and epidermal formation

eIF2α kinases are activated in response to distinct stress signals (Baird and Wek, 2012) (Figure 4). In the case of PERK, accumulating levels of unfolded protein in the ER directly or indirectly activates this eIF2α kinase, which is a transmembrane protein situated in this organelle. PERK functions in the UPR in conjunction with other sensory proteins, such as inositol requiring enzyme 1 (IRE1), which directs gene expression through cytosolic splicing of x-box binding protein 1 (*XBP1*) mRNA that leads to the expression of an active XBP1(s) transcription factor. To determine if there is ER stress and activation of the UPR during keratinocyte differentiation, levels of mRNA encoding *XBP1*(s) or the ER chaperone binding immunoglobulin protein (BiP/*GRP78*/HSPA5) were measured by qPCR. Keratinocyte differentiation led to lower amounts of both *XBP1*(s) and *GRP78* mRNAs, suggesting that there is minimal activation of the UPR (Figure

11a and b). In contrast, both UPR markers were robustly induced in keratinocytes treated with TM. While TM also enhanced PERK expression, there was no induction during keratinocyte differentiation, suggesting that PERK was not activated by this type of stress (Figure 11d).

Since the UPR was not appreciably induced during keratinocyte differentiation, we next tested whether PERK or GCN2 was responsible for differentiation-induced eIF2α-P. Knockdown of GCN2 or PERK were created in N-TERT keratinocytes using shRNA against either gene (Figure 12c and a). PERK knockdown had no effect on differentiation-induced eIF2α–P, IVL, or KRT1 protein expression (Figure 12d and e). By comparison, depletion of GCN2 caused a decrease in differentiation-induced eIF2α-P compared to control (shCTRL) (Figure 12b and c). Loss of GCN2 also caused a sharp decrease (5-fold) in IVL and KRT1 protein induced upon differentiation (Figure 12e). Of interest, loss of GCN2 caused a decrease in differentiation-induced *IVL* mRNA expression compared to control (shCTRL) (Figure 12d), which was also observed with overexpression of GADD34 in these keratinocytes (Figure 10f). These results suggest that the ISR can affect both the translation and total mRNA levels of key gene transcripts involved in keratinocyte differentiation.

To test whether lowered levels of *IVL* mRNA in differentiated GCN2-depleted keratinocytes was due to an increase in *IVL* transcript decay, we assayed the stability of *IVL* mRNA. Differentiated keratinocytes were treated with actinomycin D (AD), an inhibitor of transcript synthesis, and harvested at different times following addition of the drug (Figure 12e). There was no significant

difference between *IVL* mRNA degradation in shCTRL compared to shGCN2 keratinocytes upon differentiation, suggesting that the decrease in *IVL* mRNA levels in shGCN2 cells is due to lowered transcription of the *IVL* gene. To examine whether GCN2 is directly activated by keratinocyte differentiation, levels of GCN2 phosphorylated on threonine 899 (GCN2-P) were measured by immunoblot. Activation of GCN2 leads to auto-phosphorylation on this residue, releasing auto-inhibitory molecular interactions that enhance GCN2 phosphorylation of the eIF2α kinase. Keratinocyte differentiation caused an increase in GCN2-P similar that seen with halofuginone (HF) a known GCN2 activator that inhibits charging of $tRNA^{Pro}$ (Figure 12f). As predicted, the ER stress inducer TM did not induce GCN2-P.

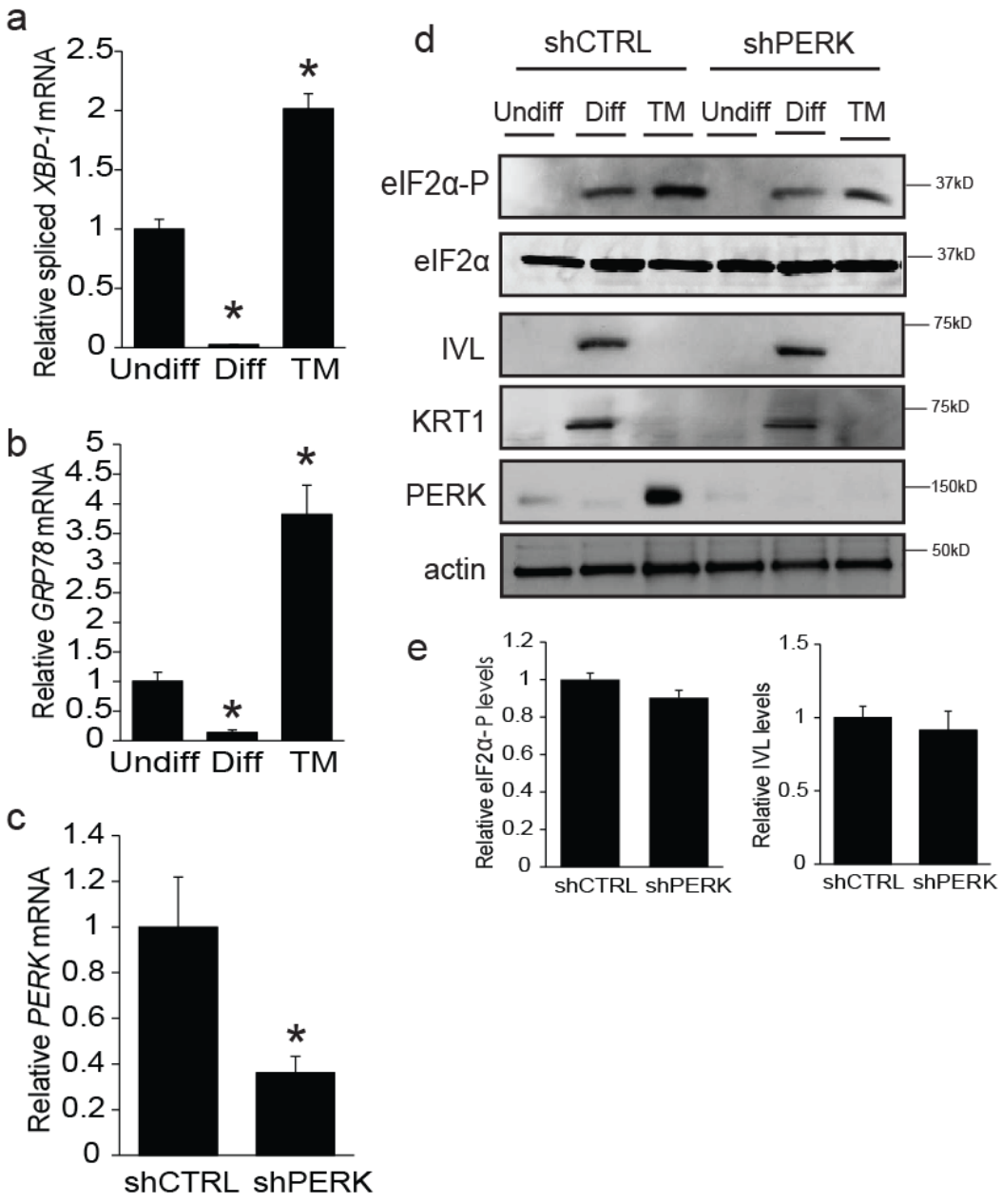

Figure 11. PERK and the UPR are dispensable for keratinocyte differentiation. RNA was collected from undifferentiated (Undiff), differentiated (Diff), or tunicamycin (TM)-treated N-TERTs and mRNA levels were measured for (a) *XBP1*(s) and (c) *GRP78*. (c) PERK mRNA knockdown efficiency was measured by qPCR. (d) Lysates were collected from shPERK or shCTRL cells following the same treatments used in a and b, and then subjected to immunoblot

analysis to measure the indicated proteins. Measurement of IVL and eIF2α-P protein expression are indicated in (e). *, $p<0.05$. Error bars represent mean +/- SD of three separate experiments.

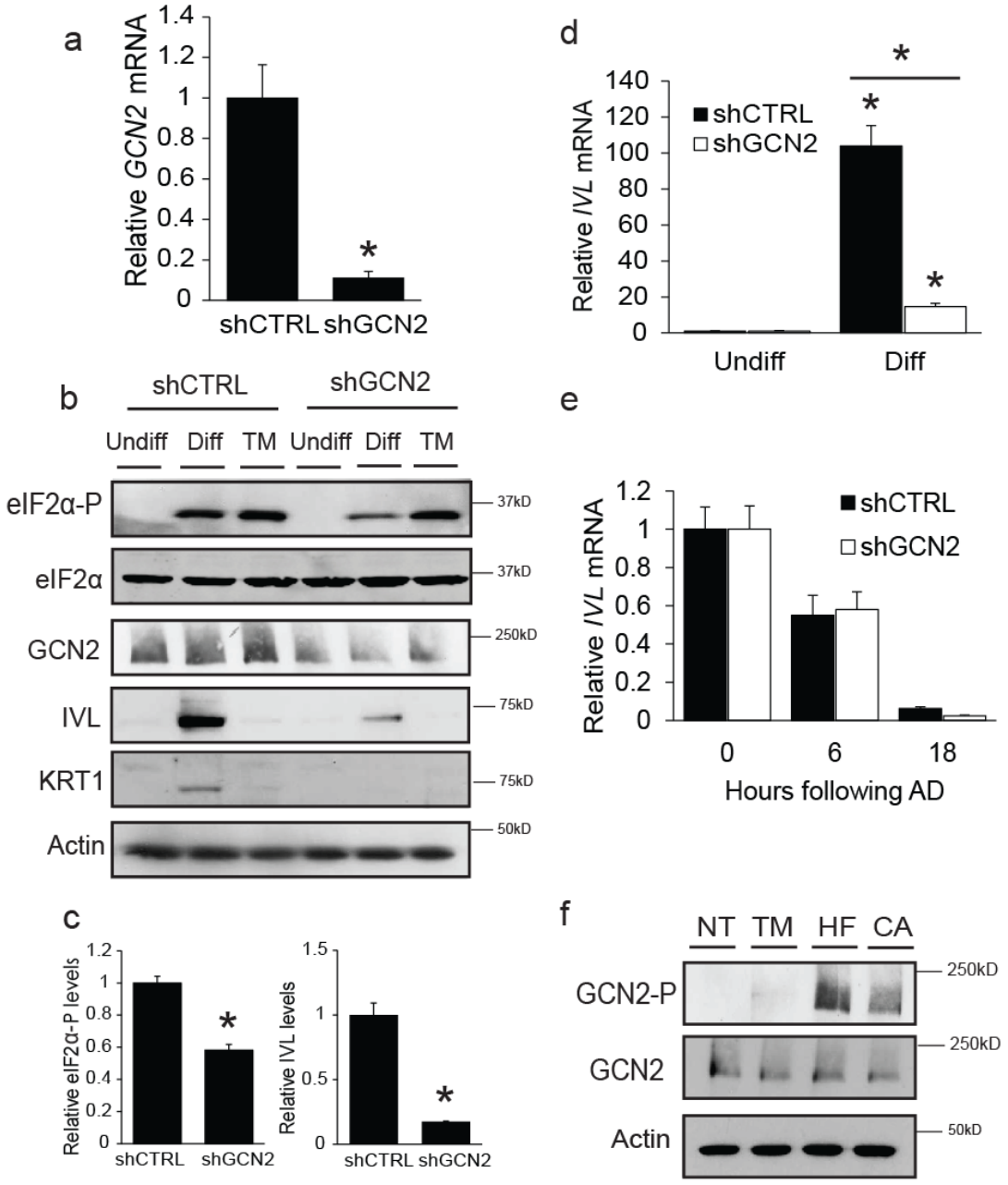

Figure 12. Loss of GCN2 abrogates involucrin expression. (a) The efficiency of the GCN2 mRNA knockdown was measured by qPCR. (b) Undifferentiated (Undiff), differentiated (Diff), or tunicamycin (TM)-treated N-TERT keratinocytes with control (shCTRL) or shGCN2 were subjected to immunoblot analysis to measure the indicated proteins. Measurement of IVL and eIF2α-P protein are

indicated in (c). (d) RNA was also isolated from these shCTRL and shGCN2 cells and *IVL* mRNA levels were measured by qPCR. (e) An mRNA half-life assay was performed by treating shCTRL or shGCN2 cells, which had been allowed to differentiate for 24 hours, with 10 μg/mL actinomycin D (AD). RNA was isolated from each sample after the indicated number of hours, and qPCR was performed to measure levels of *IVL* mRNA. (f) Activation of GCN2 as measured by immunoblot analyses following differentiation or a 6 hour treatment with 2 μM TM or 100 nM halifuginone (HF). *, $p<0.05$. Error bars represent mean +/- SD of three separate experiments.

Given the influence of GCN2 knockdown on differentiation in monolayer keratinocytes, we next addressed the impact of the loss of GCN2 on epidermal differentiation and formation of an intact, stratified tissue. 3D organotypic cultures were constructed using primary keratinocytes expressing shGCN2 or shCTRL. After seven days of induced differentiation, skin equivalents were sectioned and stained with hematoxylin and eosin (H&E) or antibodies against eIF2α-P, IVL, or Ki67, a well-characterized marker of cell proliferation (El-Abaseri *et al.*, 2006). There was a striking difference in histology of the shCTRL and shGCN2 skin equivalents, as noted by disorganization of the keratinocytes and decreased cornification compared to the control (Figure 13a). As expected, there was decreased immunofluorescence detected using antibodies against IVL protein or eIF2α-P (Figure 13b and c). These findings are consistent with those observed in monolayer tissue culture (Figure 12b). Of interest, there was an increase in Ki67

positive cells in the basal layer, indicating higher numbers of actively proliferating cells, which can be indicative of hyperplasia (Figure 13d). Furthermore, immunofluorescence analysis with an IgG isotype control indicated that these results are not a consequence of non-specific antibody detection (Figure 13e). Relative GCN2 knockdown efficiency is indicated in Figure 13f. These results indicate that GCN2 is required for proper expression of IVL during keratinocyte differentiation and as a consequence is critical for proper formation of an intact epidermis.

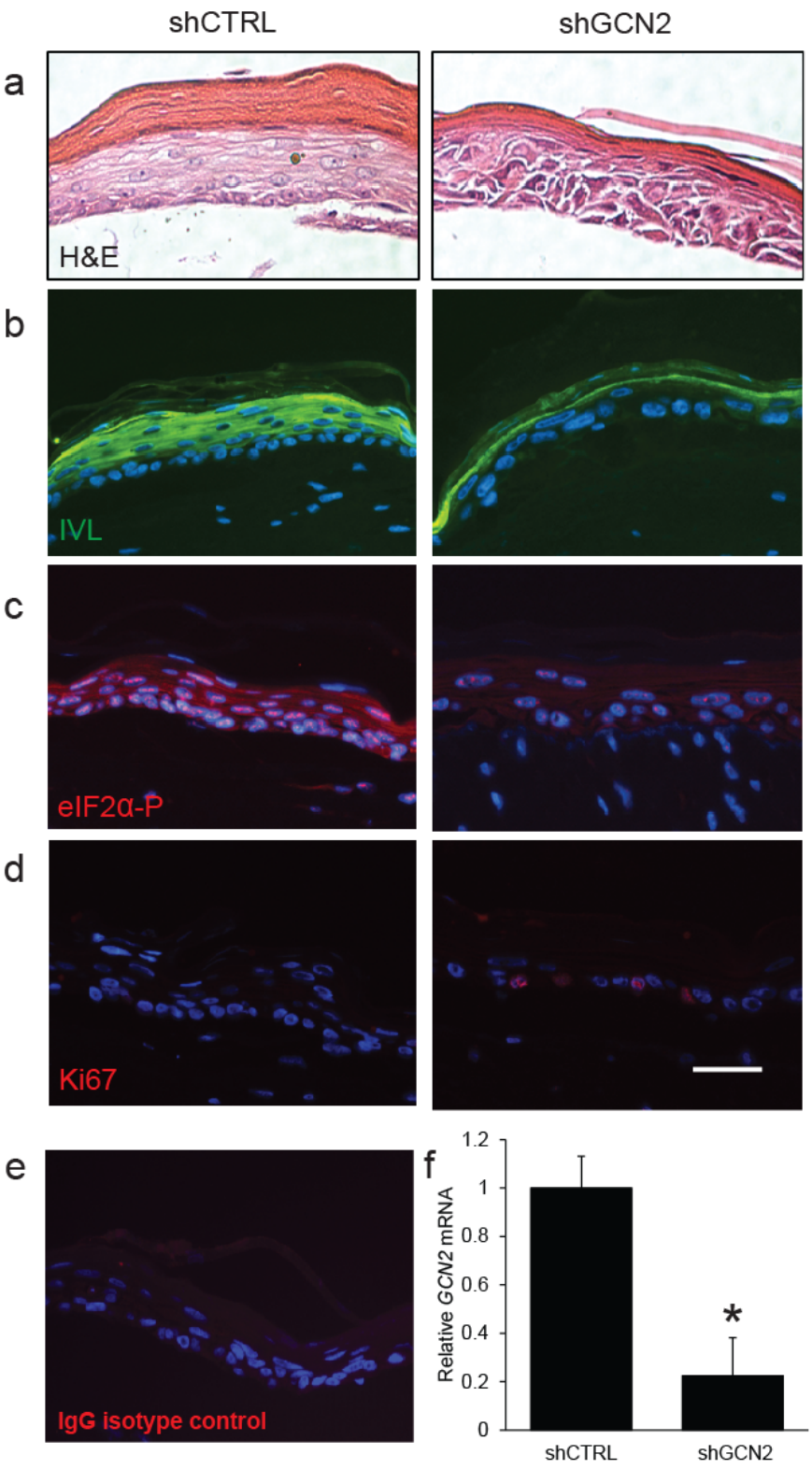
shCTRL
shGCN2
a
H&E
b
IVL
c
eIF2α-P
d
Ki67
e
IgG isotype control
f
Relative GCN2 mRNA
1.2
1
0.8
0.6
0.4
0.2
0
*
shCTRL
shGCN2

Figure 13. GCN2 is required for proper epidermal differentiation. 3D organotypic cell cultures were made using shCTRL and shGCN2 primary human keratinocytes that were seeded on a collagen-fibroblast matrix and raised to the air-liquid interface in order to differentiate and stratify. After 7 days the cell cultures were fixed, sectioned and stained with (a) H&E or antibodies against (b) eIF2α-P, (c) IVL, (d) Ki67, or (e) an IgG isotype control. Prior to 3D culture, GCN2 mRNA was measured to verify knockdown efficiency (f). Scale bar = 25μm. *, $p<0.05$. Error bars represent mean +/- SD of three separate experiments.

CHAPTER 4. RESULTS: TRANSLATIONAL REPRESSION PROTECTS HUMAN KERATINOCYTES FROM UVB-INDUCED APOPTOSIS THROUGH A DISCORDANT eIF2α KINASE STRESS RESPONSE

4.1 UVB irradiation induces eIF2α-P and global repression of translation initiation in human keratinocytes

Results in Chapter 3 showed that formation of the human epidermis is dependent on activation of the ISR. We next sought to determine the role of the ISR in the keratinocyte response to an environmental stress. To determine how UVB irradiation affects translational control in human keratinocytes, N-TERT and primary human keratinocytes were irradiated with a range of UVB doses. UV doses are measured in Joules per meter squared (J/m^2) which is a quantification of the energy emitted by UV over an area. In our laboratory, 50-600 J/m^2 is equal to about 30-90 minutes of sunlight exposure during the summer. One, three, and six hours post-irradiation, cell lysates were harvested and subjected to sucrose gradient ultracentrifugation to measure the level of protein synthesis as judged by polysome analyses. UVB irradiation of both N-TERT and primary keratinocytes substantially decreased the amount of cellular mRNAs bound to large polysomes coincident with an increase in mRNAs associated with 80S monosomes, indicating repression of translation initiation in a dose and time-dependent manner (Figure 14a, 15a and b). A pattern of reduced p/m ratio was observed following increasing doses of UVB in both N-TERT and primary human keratinocytes (Figure 14a and b). UVB doses as low as 50 J/m^2 and as soon as 1 hour post-UVB treatment yielded decreased p/m values, indicating that

translational repression occurs following both high and low (non-apoptotic) doses of UVB at times prior to any induction of apoptosis (Figure 15a and b).

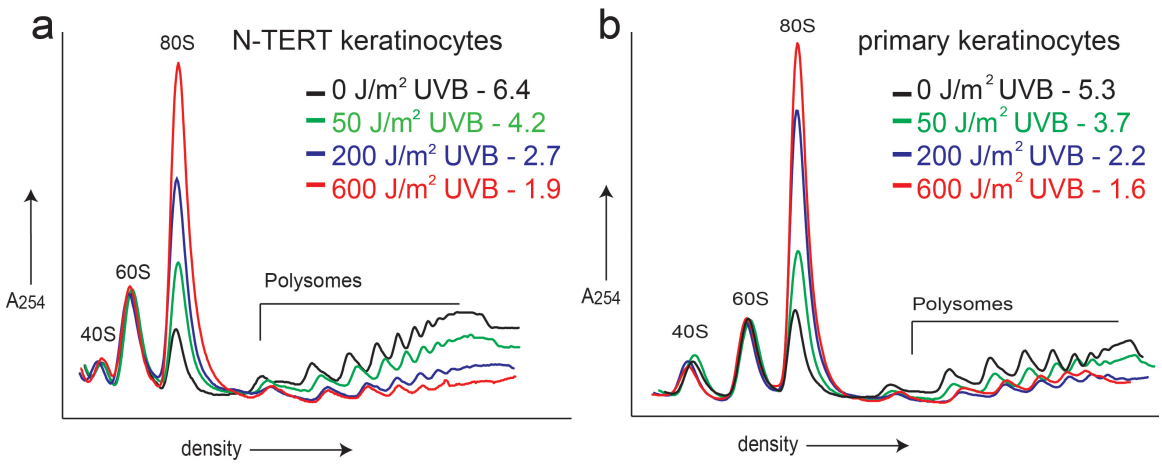

Figure 14. UVB irradiation decreases global translation initiation in human keratinocytes. Keratinocytes were irradiated with the indicated dose of UVB. Lysates from N-TERT (a) or primary human keratinocytes (b) were harvested 6 hours following UVB and subjected polysome profiling. P/M ratios are indicated next to each dose.

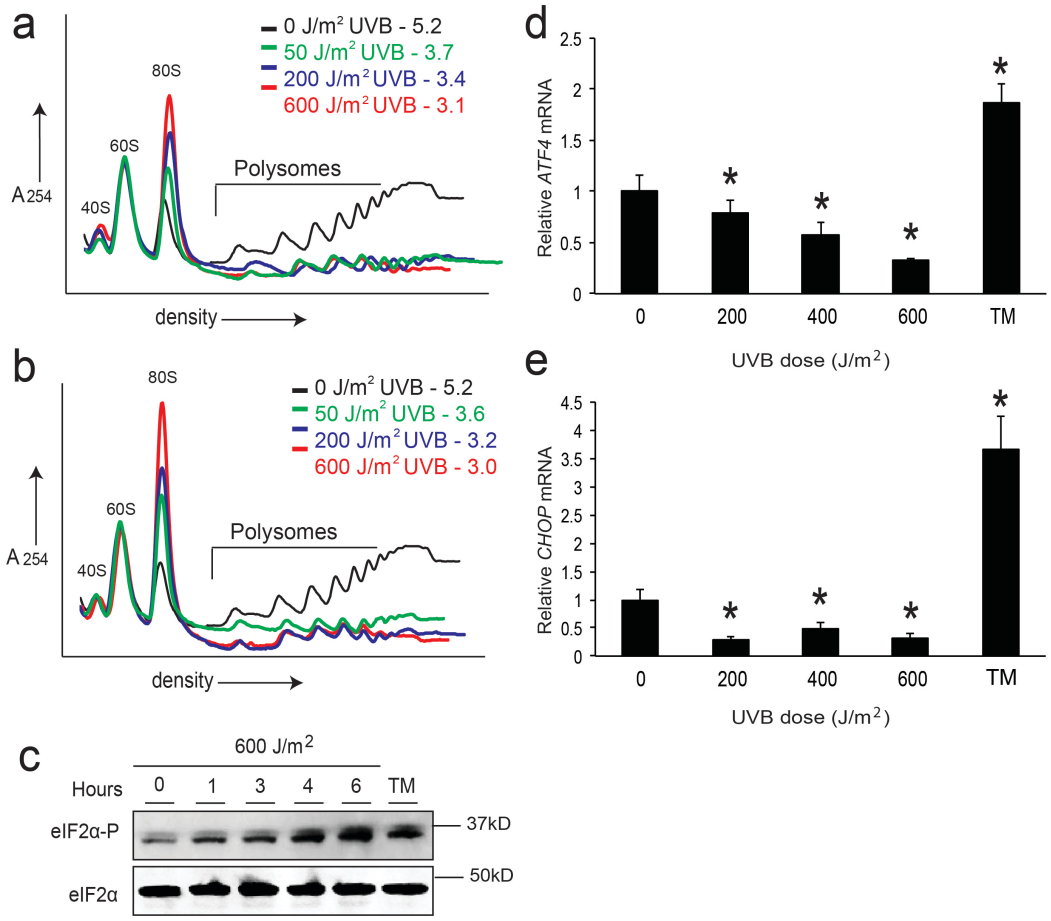

Figure 15. UVB elicits translational control at short time points and low doses. N-TERTs were irradiated with the indicated dose of UVB and subjected to polysome profile analysis at 1 (a) or 3 hours (b) of following irradiation. (c) N-TERTs were irradiated with 600 J/m^2 UVB and harvested for immunoblot analysis following the indicated incubation time. Alternatively, cells were treated with TM and harvested after 6 hours. N-TERTs were irradiated with the indicated dose of UVB or 2 μM TM, harvested after 6 hours, and total levels of *ATF4* (d) and *CHOP* (e) mRNA were measured by qPCR. *, p<0.01. Error bars represent mean +/- SD of three separate experiments.

To investigate the levels of eIF2α-P in response to UVB irradiation, we treated cultured N-TERTs with increasing doses of UVB. Six hours post-irradiation, cells were harvested and subjected to immunoblot analyses. Increasing doses of UVB resulted in enhanced eIF2α-P in a dose-dependent manner (Figure 16a), with a maximal response of a 4-fold increase in eIF2α-P following 600 J/m^2 UVB. eIF2α-P occurred as early as 1 hour post-UVB and continued to increase with time, indicating that the trigger for activation of this pathway is something recognized or produced over time (Figure 15c). Levels of eIF2α-P were enhanced following UVB exposure at levels similar to that seen with TM treatment. As a control for the keratinocyte UVB response, we showed that increasing doses of UVB led to increased phosphorylation of p53 at serine-15.

We next addressed the effects of global repression of translation initiation at the individual gene transcript level. Keratinocytes were irradiated with 0 or 600 J/m^2 UVB, followed by polysome analyses. Transcript levels were then measured by qPCR in the gradient fractions using oligonucleotide primers specific for genes not involved in the ISR, including β-2 microglobulin (*B2M*), β-actin (*ACTB*), and *EIF4E* (Figure 16b). Total levels of each transcript decreased in UVB-irradiated fractions compared to non-irradiated controls (Figure 16c). Furthermore the percent of each mRNA, independent of changes in total transcript levels, shifted from heavy polysomes towards small polysomes in UVB irradiated keratinocytes compared to non-irradiated controls (Figure 16d). These results support the idea that the translation of mRNAs genome-wide is reduced in response to UVB

irradiation in human keratinocytes, with significant translation repression among a range of genes.

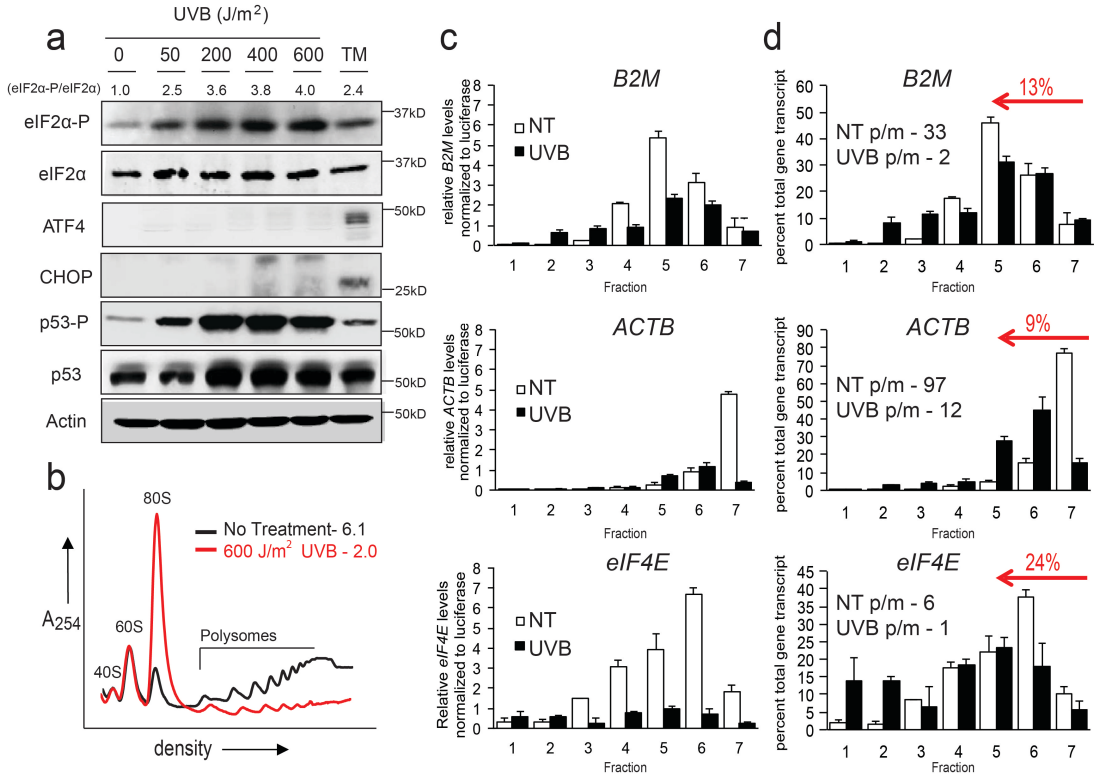

Figure 16. UVB irradiation induces eIF2α-P and gene-specific translational control in the absence of ATF4 and CHOP protein expression. N-TERT keratinocytes were irradiated with the indicated doses of UVB. (a) 6 hours following UVB lysates were prepared and indicated proteins were measured by immunoblot analyses. As controls, cells were subjected to ER stress elicited by TM. Levels of eIF2α-P normalized to total eIF2α protein are indicated below each dose. (b) 6 hours following 600 J/m^2 UVB lysates were subjected to polysome profiling. (c) Levels of the indicated gene transcripts from fractions collected in (b) were measured by qPCR. (d) mRNA levels are presented as a percent of total

gene transcript to illustrate a shift towards lower polysomes, which is quantified and indicated in red. Error bars represent mean +/- SD of three separate experiments.

4.2 UVB irradiation induces robust eIF2α-P in the absence of preferentially translated downstream effectors

In the ISR, enhanced eIF2α-P is typically accompanied by increased expression of ATF4 and CHOP proteins. However, despite a robust induction of eIF2α-P following either high or low doses of UVB irradiation, the amounts of ATF4 and CHOP protein detected were minimal (Figure 16a). In contrast, there were increased levels of ATF4 and CHOP proteins in response to ER stress. Therefore it appears that the ISR is being activated in a non-canonical fashion in keratinocytes exposed to UVB, as ATF4 and CHOP are known downstream targets of eIF2α-P in response to many stressors not limited to ER stress.

Previous work showed that *ATF4* is preferentially translated during ER stress via mechanisms involving upstream open reading frames (uORFs) in the 5'-leader of the mRNA (Vattem and Wek, 2004). We investigated whether *ATF4* is preferentially translated as a result of UVB irradiation, even though we observed no UVB-dependent induction of ATF4 protein. To address this question, relative levels of *ATF4* mRNA were measured by qPCR in each fraction collected by sucrose gradient ultracentrifugation from N-TERT keratinocytes irradiated with 0 or 600 J/m^2 doses of UVB (Figure 16b). Total levels of *ATF4* transcript were decreased in UVB-irradiated sucrose fractions compared to non-

irradiated controls (Figure 17a). Interestingly, despite apparently lowered amounts of total *ATF4* transcript, the percent of *ATF4* mRNA among gradient fractions shifted 50% towards heavy polysomes in UVB irradiated keratinocytes compared to non-irradiated controls (Figure 17b). This finding suggests that if *ATF4* mRNA is available following UVB, the transcript can be preferentially translated in response to eIF2α-P. To further test whether *ATF4* can undergo preferential translation following UVB irradiation, we transfected N-TERT keratinocytes with a plasmid encoding the 5'-leader of *ATF4* mRNA inserted between a constitutive P_{Tk} promoter and a luciferase CDS (Vattem and Wek, 2004). Therefore, any transcriptional regulation is removed and translation can be regulated through uORFs present in the 5'-leader. Luciferase activity increased significantly in cells treated with TM as well as UVB, indicating that preferential translation of *ATF4* can occur in response to both treatments (Figure 17c).

Given the diminished induction of ATF4 protein expression observed in response to UVB irradiation, we measured *ATF4* and *CHOP* mRNA expression at one, three, and six hours following UVB irradiation. Whereas treatment with TM led to an increase in both *ATF4* and *CHOP* mRNA over time, UVB caused a significant lowering of both transcripts following a UVB dose of 600 J/m^2 (Figure 17d and e). This significant decrease in *ATF4* and *CHOP* mRNA levels was also seen following lower doses of UVB irradiation (Figure 15d and e). It is possible that the decrease in *ATF4* following UVB could be a result of a UVB-induced increase in *ATF4* mRNA decay. To investigate this idea, we treated N-TERTs

with 0 or 600 J/m^2 UVB irradiation followed by AD for an additional 1, 2, or 4 hours. *ATF4* mRNA levels were then measured by qPCR. The half-life of *ATF4* mRNA was about 4 hours in both control and irradiated keratinocytes (Figure 17f), indicating that the lowered *ATF4* transcript levels in response to UVB are not a result of increased mRNA decay. These results suggest that while *ATF4* can be preferentially translated during UVB-irradiation in human keratinocytes, lowered steady-state *ATF4* mRNA levels resulting from decreased *ATF4* transcription occur in response to UVB and prevent appreciable induction of ATF4 protein.

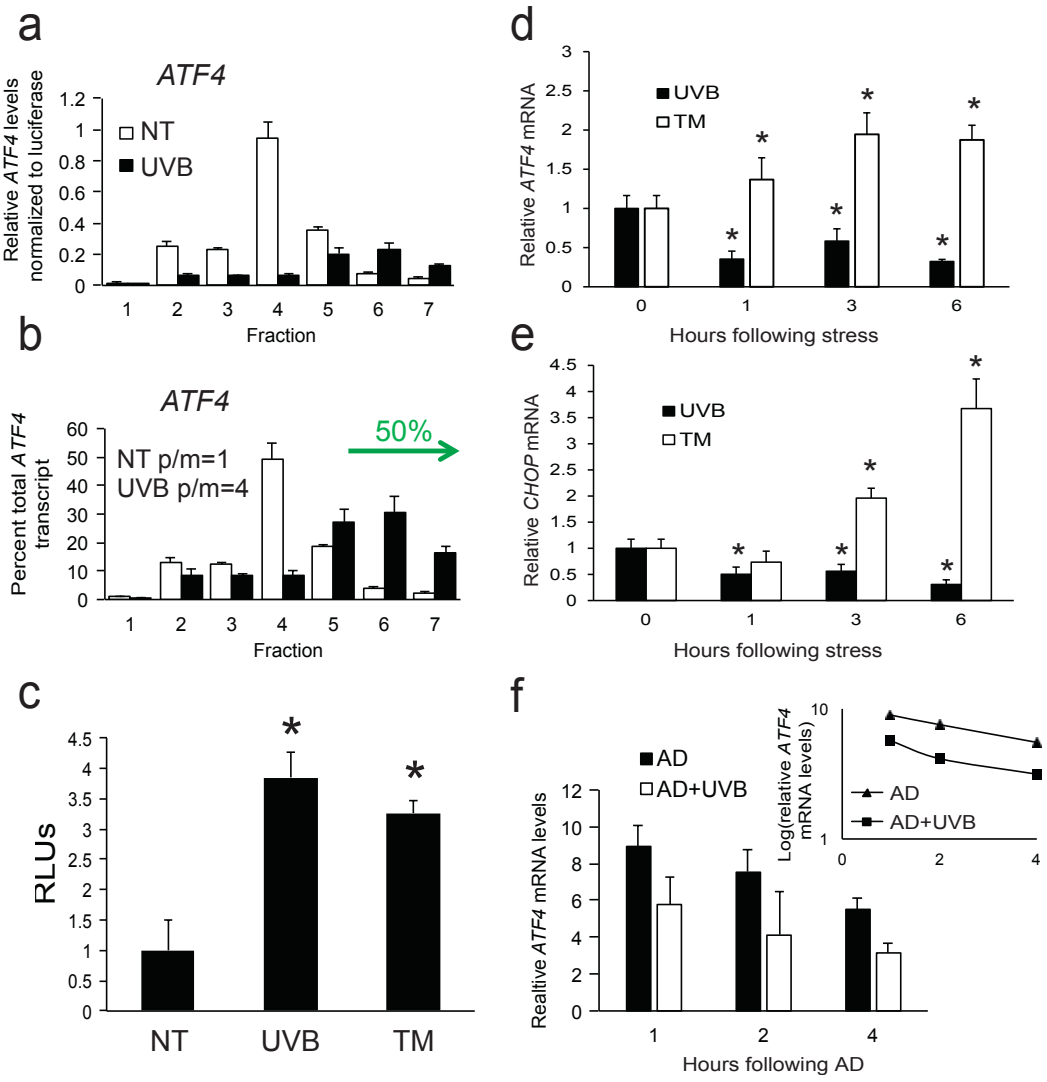

Figure 17. UVB irradiation causes both preferential translation and transcriptional repression of *ATF4*. (a) Total RNA was isolated from sucrose gradient fractions collected in Figure 16b, and levels of *ATF4* mRNA were measured by qPCR. (b) *ATF4* mRNA is presented as a percent of total gene transcript. (c) N-TERTs were co-transfected with P_{Tk}-*ATF4*-Luc and Renilla plasmids and luciferase activity was measured 6 hours following treatment. Activity is represented as relative light units (RLU). Total levels of *ATF4* (d) and *CHOP* (e) mRNAs following treatment with 600 J/m^2 of UVB or TM were

measured by qPCR at the indicated time following UVB. (f) N-TERTs were exposed to 0 or 600 J/m^2 UVB, and following 1 hour cells were treated with 20 μM AD for an additional 1, 2, or 4 hours. *ATF4* mRNA was measured by qPCR. *, $p<0.05$. Error bars represent mean +/- SD of three separate experiments.

4.3 Repression of downstream ISR effectors provides protection from UVB-induced apoptosis

We hypothesized that the discordant ISR triggered by UVB in which ATF4 and CHOP are repressed during eIF2α-P provides a survival advantage in human keratinocytes. To test this idea, we utilized a derivative of the drug salubrinal, Sal-003 (Sal), a potent inhibitor of eIF2α dephosphorylation (Boyce et al., 2005). Cells treated with Sal demonstrate enhanced eIF2α-P and forced expression of ATF4 and CHOP protein in the absence of exogenous cell stress. N-TERT keratinocytes were pretreated with Sal for 6 hours prior to UVB irradiation. Pretreatment increased ATF4 and CHOP protein levels in both untreated and irradiated keratinocytes in contrast to cells treated with UVB alone, which showed increased eIF2α-P but no ATF4 or CHOP protein (Figure 18a). Combined treatment of Sal and UVB also caused a significant increase in apoptosis as measured by caspase-3 specific activity at 6 hours post-irradiation when compared to UVB irradiation alone (Figure 18b). Similar results were observed in primary human keratinocytes (Figure 19a). Enhanced apoptosis associated with Sal pretreatment was seen as early as 3 hours post-UVB, at which point there is no significant induction of caspase-3 activity by UVB alone

(Figure 19b). The negative effects of Sal in combination with 600 J/m^2 dose UVB was lost at 8 hours (Figure 19b), indicating that Sal is most likely accelerating the onset of apoptosis at higher doses of UVB. N-TERT keratinocytes collected at three and six hours post-UVB showed a 0 and 4% increase, respectively, in Annexin V-positive cells compared to untreated controls, whereas cells pretreated with Sal showed a 38 and 25% increase, respectively. Annexin V staining revealed that the increases in caspase-3 activity with Sal pretreatment presented in figures 18 and 19 is indeed a result of increased apoptotic cells. These results indicate that combined treatment of Sal and UVB, which induced expression of ATF4 and CHOP, is deleterious to cell survival.

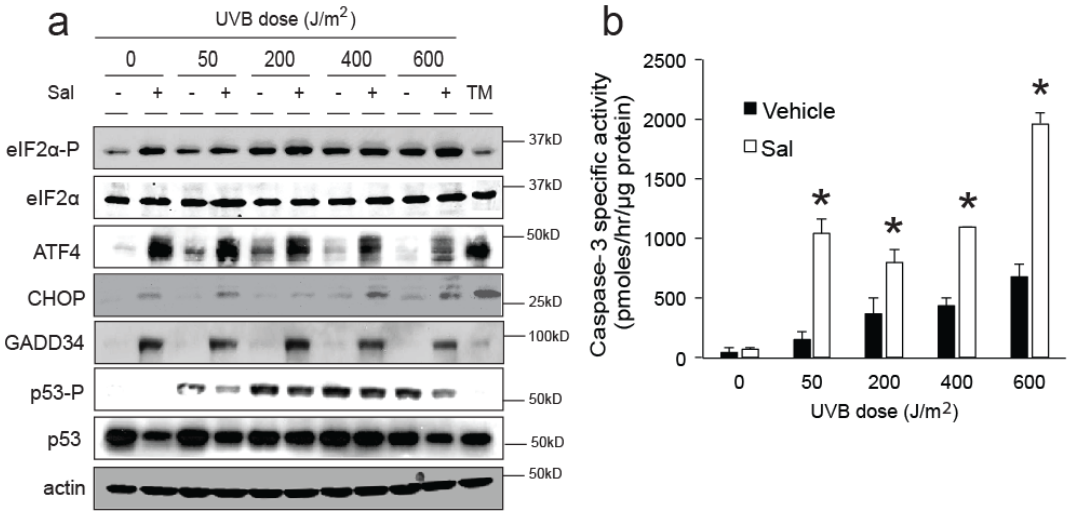

Figure 18. Expression of ISR downstream effectors sensitizes cells to UVB-induced apoptosis. (a) N-TERT keratinocytes were pretreated with 10 μM salubrinal-003 (Sal) for 6 hours prior to irradiation with the indicated dose of UVB. Alternatively, cells were subjected only to Sal, UVB, TM, or no treatment. Cells were harvested 3 hours post-irradiation and the indicated proteins were

measured by immunoblot analyses. (b) Caspase-3 specific activity was also measured in cells following exposure to UVB. Asterisks indicate a significant difference between groups treated with UVB alone versus a combined treatment of UVB and Sal. *, p<0.01. Error bars represent mean +/- SD of three separate experiments.

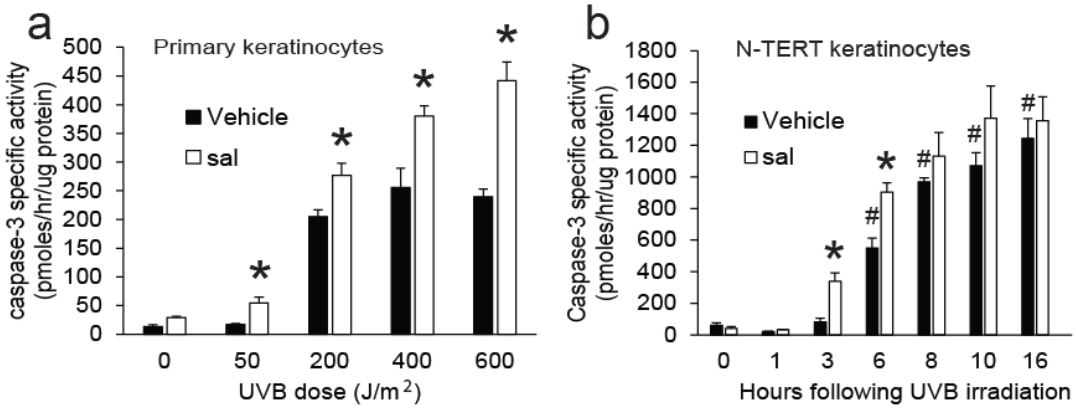

Figure 19. Expression of ISR downstream effectors sensitizes cells to UVB-induced apoptosis in primary keratinocytes. (a) Primary human keratinocytes were pretreated with Sal or vehicle for 6 hours and then irradiated with the indicated dose of UVB. 6 hours following UVB, cells were assayed for caspase-3 activity. (b) N-TERTs were pretreated with Sal or vehicle for 6 hours prior to irradiation with 600 J/m^2 UVB and assayed for caspase-3 activity at the indicated times post-UVB. *, p<0.01 compared to UVB alone at the indicated dose, #, p<0.01 compared to no treatment group. Error bars represent mean +/- SD of three separate experiments.

It is possible that the negative effects of combining Sal and UVB are a result of something unrelated to the ISR. Therefore to investigate the relative importance of Sal-induced *ATF4* expression, we used shRNA to stably knock down expression of ATF4 in N-TERT keratinocytes. By knocking down *ATF4*, we prevented its ability to be induced by treatment with Sal. Knock down of ATF4 resulted in about 80% reduction in basal *ATF4* mRNA (Figure 20a) and substantial lowering in the induction of ATF4 protein by TM, Sal, and combined treatment of Sal and UVB (Figure 20b). The caspase-3 activity of shATF4 keratinocytes was not significantly different between cells treated with UVB alone and cells pretreated with Sal prior to UVB irradiation (Figure 20c). Therefore, the knock down of ATF4 ablated the pro-apoptotic effects of combining Sal with UVB. These results suggest that the increase in UVB-induced cell death with Sal pretreatment is due to induced expression of ATF4. The N-TERT cells knocked down for ATF4 did experience a modest, albeit significant, increase in caspase-3 activity when treated with UVB alone, which may be a consequence of ATF4 triggering the expression of genes having anti-oxidation functions (Harding et al., 2003).

The ATF4 target gene *CHOP* is considered to be a potent pro-apoptotic transcription factor whose expression is induced at the transcriptional and translational level during canonical induction of the ISR (Teske et al., 2013). We used shRNA to carry out a similar analysis of keratinocytes knocked down for CHOP expression. Lentiviral delivery of shCHOP resulted in about a 60% reduction in basal *CHOP* mRNA (Figure 19d) as well as the loss of induced

expression by TM, Sal, and combined treatment of Sal and UVB (Figure 20e). Depletion of CHOP provided even greater relief from apoptosis in response to combined Sal and UVB treatment than was previously seen in ATF4 depleted cells; shCHOP cells treated with Sal and UVB actually had significantly less caspase-3 activity than those treated with UVB alone (Figure 20f). CHOP depleted cells also showed some protection from UVB exposure compared to control cells, which can be attributed to basal levels of the pro-apoptotic CHOP in keratinocyte controls. These results suggest that expression of downstream ISR effector CHOP, whose expression is transcriptionally enhanced by ATF4, is deleterious to keratinocyte survival in response to UVB irradiation.

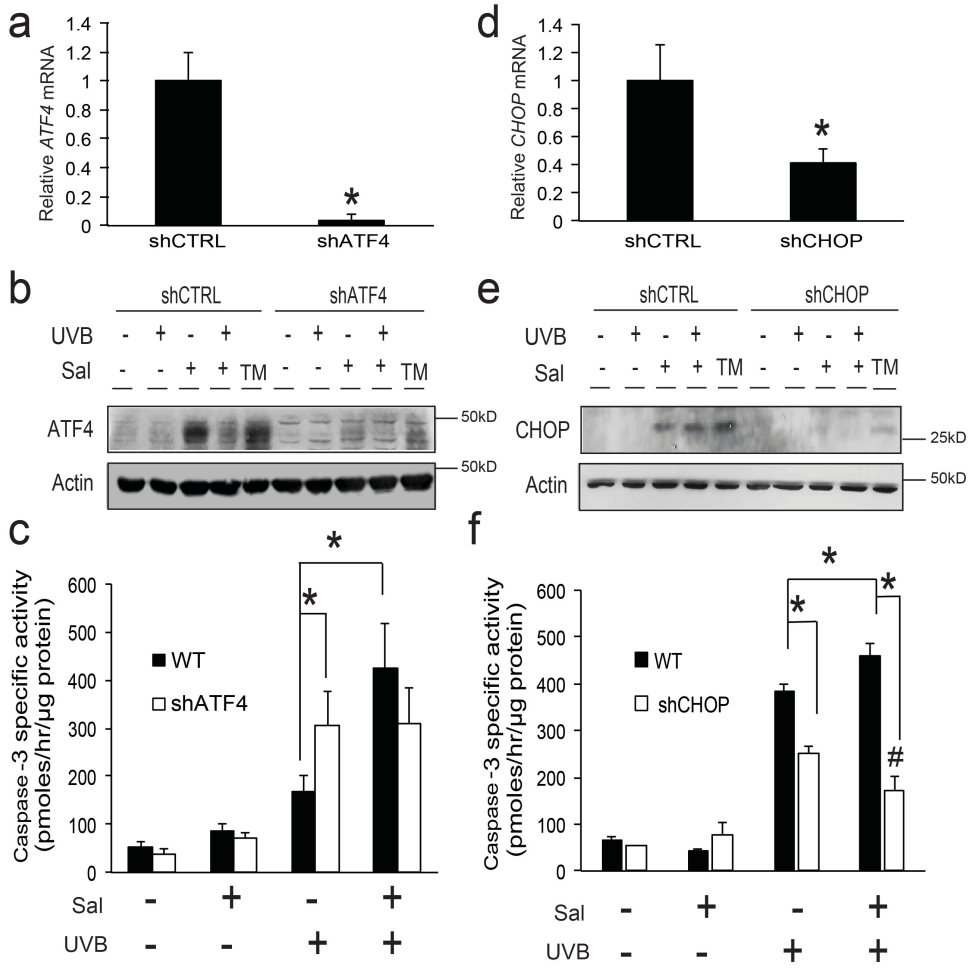

Figure 20. Loss of ATF4 or CHOP protects cells from apoptosis during combined Sal and UVB treatments. Total RNA was isolated from shCTRL, shATF4 (a), or shCHOP (d) cells and analyzed for expression of *ATF4* or *CHOP* mRNAs to validate knockdown efficiency. shCTRL, shATF4 (b), or shCHOP (e) cells were pretreated with 10 µM Sal for 6 hours prior to irradiation with 600 J/m^2 UVB. Lysates were subjected to immunoblot analysis 3 hours post-UVB. (c) shCTRL and shATF4 cells were assayed for apoptosis by measuring the induction of caspase-3 specific activity 6 hours post-irradiation. (f) shCTRL and shCHOP cells were separately assayed for caspase-3 specific activity. *, $p<0.05$,

#, $p<0.05$ relative to UVB alone. Error bars represent mean +/- SD of three separate experiments.

4.4 Translational control elicited by eIF2α-P provides resistance to UVB-induced apoptosis

To address the contribution of the ISR to UVB-dependent translation control and keratinocyte survival in response to UVB, we utilized two strategies to inhibit the ISR. We first exploited an inducible GADD34 overexpression system as described in Chapter 3. Treatment of keratinocytes overexpressing GADD34 with DOX for 24 hours caused a partial restoration of large polysomes coincident with a decrease in monosomes when treated with UVB (Figure 21a), as well as blocked induction of eIF2α-P by both TM and UVB (Figure 21b). Importantly, induced expression of GADD34 caused an increase in UVB-induced caspase-3 activity (Figure 21c). Secondly, we used ISRIB, a pharmacological inhibitor of eIF2-dependent translational repression (Sidrauski et al., 2013). Cells were pretreated with ISRIB for 1 hour prior to UVB irradiation and assayed for changes in polysome profiles or caspase-3 activity. ISRIB caused a substantial restoration of large polysomes in keratinocytes treated with UVB, coincident with a decrease in monosomes (Figure 21d). Pharmacological inhibition of the ISR also significantly increased apoptosis in response to UVB irradiation, indicating that eIF2α-P indeed provides protection to keratinocytes in response to both high and low doses of UVB (Figure 21e). Further investigation into the effects of ISR inhibition *in vivo* will provide evidence to support the testing of ISR

pharmacological agents in combination with UVB light therapy or as preventative treatment for skin disease.

As described above, eIF2α-P causes both a general repression of translation initiation as well as preferential translation of certain mRNAs. Previous studies have shown that the global reduction in protein synthesis elicited by ER stress provides a survival advantage to cells (Han et al., 2013; Harding et al., 2000b). Since *ATF4* expression did not provide protection from UVB-induced apoptosis, we hypothesized that an alternative explanation for eIF2α-P lies in the importance of global translation repression. To investigate the contribution of general repression of protein synthesis to the survival function of the ISR following UVB irradiation, we co-treated GADD34-overexpressing keratinocytes with both DOX and CHX, a potent inhibitor of translation elongation, and assayed for apoptosis. Whereas overexpression of GADD34 had a negative impact on ability of keratinocytes to survive UVB-induced stress, co-treatment with CHX rescued this phenotype (Figure 21f). This suggests that reduced survival of eIF2α-P-deficient cells following UVB exposure is in part due to their inability to repress protein synthesis levels globally.

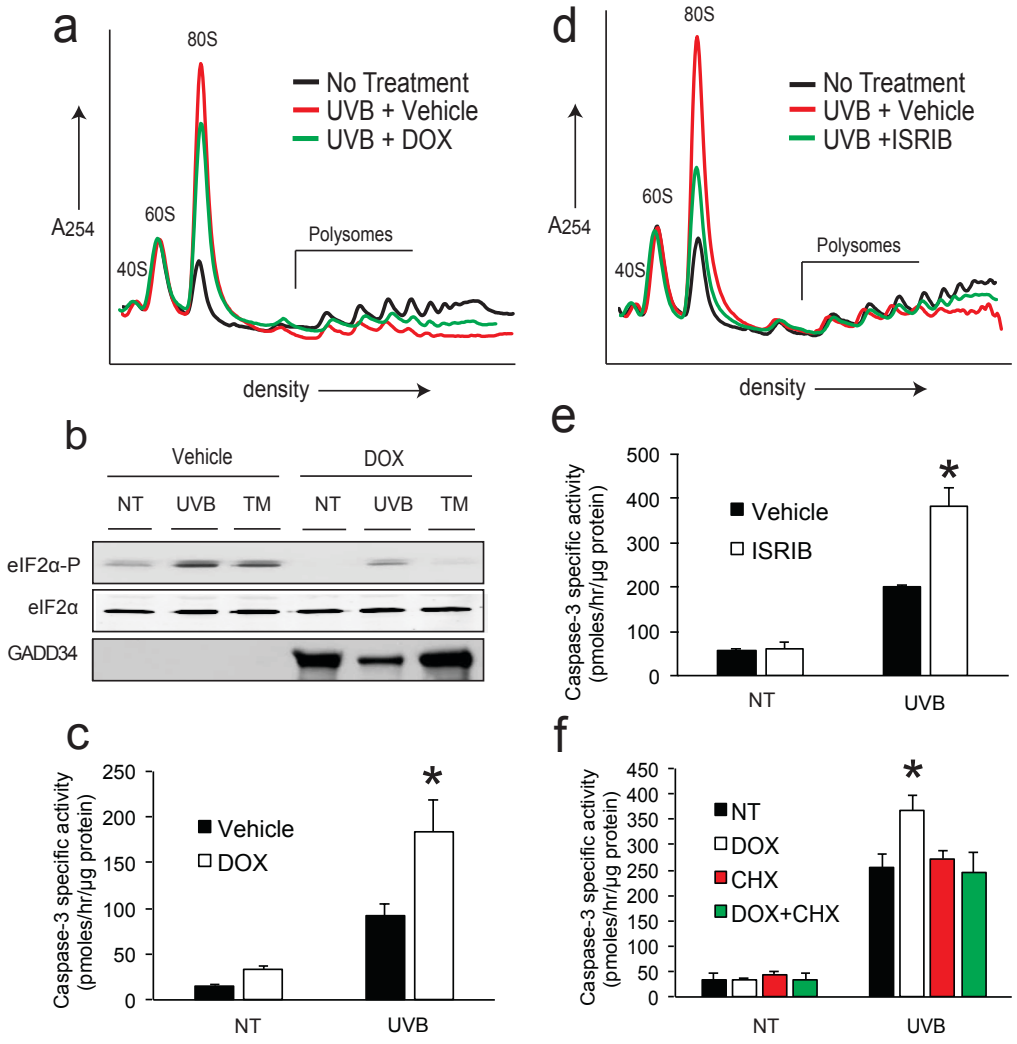

Figure 21. eIF2α-P dependent translation repression provides resistance to UVB-induced apoptosis. GADD34 overexpressing keratinocytes were treated with DOX for 24 hours to induce GADD34 expression prior to irradiation with 600 J/m^2 UVB and characterized by (a) polysome profile analysis, (b) immunoblot analysis, or (c) measurements of caspase-3 specific activity. N-TERTs were pretreated with ISRIB for 1 hour and subsequently irradiated with 600 J/m^2 UVB and subjected to (d) polysome profile analysis or (e) caspase-3 specific activity. (f) Keratinocytes expressing GADD34 were treated with vehicle, 24 hours of DOX

treatment, 30 minutes CHX, or a combination of 24 hours DOX followed by 30 minutes CHX. Cells were then irradiated with 0 or 600 J/m^2 UVB and assayed for induction of caspase-3 activity. *$p<0.01$. Error bars represent mean +/- SD of three separate experiments.

CHAPTER 5. RESULTS: TRANSLATIONAL CONTROL OF A HUMAN *CDKN1A* mRNA SPLICE VARIANT REGULATES THE FATE OF HUMAN KERATINOCYTES SUBJECTED TO UVB IRRADIATION

5.1 Loss of eIF2α-P decreases G1 arrest and DNA repair in response to UVB

Results presented in Chapter 4 delineated a mechanism for a non-canonical ISR response to UVB. However, the reasons for ISR protection from UVB-induced cell death are still unknown. To address this question, we used a low dose (100 J/m^2) of UVB, which retains cell viability and facilitates the study of cell cycle control and DNA repair. In order to investigate the effects of eIF2α-P deficiency on low dose UVB-irradiated keratinocytes, we again utilized the N-TERT keratinocyte cell line with a DOX-inducible GADD34 overexpression to thwart the ISR. Exposure to 100 J/m^2 UVB alone caused a sharp decrease in translation initiation as measured by an increase in the population of mRNAs associated with 80s monosomes and decreased levels of mRNAs bound to heavy polysomes as visualized by polysome profiling (Figure 22a). The p/m ratio decreased from 6.5 to 1.1 with UVB. This dose of UVB also elicited a robust increase in eIF2α-P (Figure 22b). GADD34 overexpression triggered by addition of DOX partially restored heavy polysomes (Figure 22a, blue line) as well as diminished UVB-induced eIF2α-P (Figure 22b).

We next sought to determine whether inhibition of the ISR regulated the keratinocyte cell cycle in response to UVB. To determine the effect of eIF2α-P inhibition on G1 arrest triggered by UVB, N-TERT keratinocytes were

synchronized in G1 as described in the methods and highlighted in Figure 22c. Cells were then irradiated with 100 J/m^2 UVB, cultured for the indicated number of hours, and labeled with both EdU and propidium iodide (PI). 6 hours following UVB, cells containing a fully functional ISR displayed only 9% of live cells in S phase while 74% remained in G1 (Figure 22c). By comparison, in DOX-treated cells following UVB, the number of cells in S phase was doubled (20%) and the G1 fraction was only 47%. These findings indicate that cells deficient for eIF2α-P display a lower percentage of cells in G1 and corresponding higher levels in S phase following UVB compared to control cells that present with a fully functional ISR. This trend was also observed 8 hours following UVB treatment. However by 10 hours post-UVB exposure, both control and DOX-treated cells were at steady-state cell cycle proportions.

Since cell cycle arrest is important to allow time for DNA repair of UVB-induced DNA damage, we next measured the levels of DNA repair in control and DOX-treated cells following UVB. At both 6 and 12 hours following 100 J/m^2 UVB, DOX-treated cells showed significantly lower levels of DNA repair as measured by loss of thymine dimers (Figure 22e). To determine if this effect was due to changes in capacity for NER per se, we performed a host-cell reactivation assay. Briefly, luciferase plasmid DNA was irradiated outside of the cell and then transfected into vehicle or DOX treated GADD34 overexpression N-TERTs, followed by measurement of luciferase activity. There was no significant difference in luciferase activity for the exogenously UVB-damaged luciferase plasmid DNA relative to the undamaged control in either control or DOX-treated

keratinocytes (Figure 22f). There was also no difference in repair of the plasmid DNA when cells were also irradiated with UVB prior to transfection. These results suggest that loss of translational control through eIF2α-P diminishes a UVB-induced G1 arrest in keratinocytes, resulting in decreased levels of DNA repair.

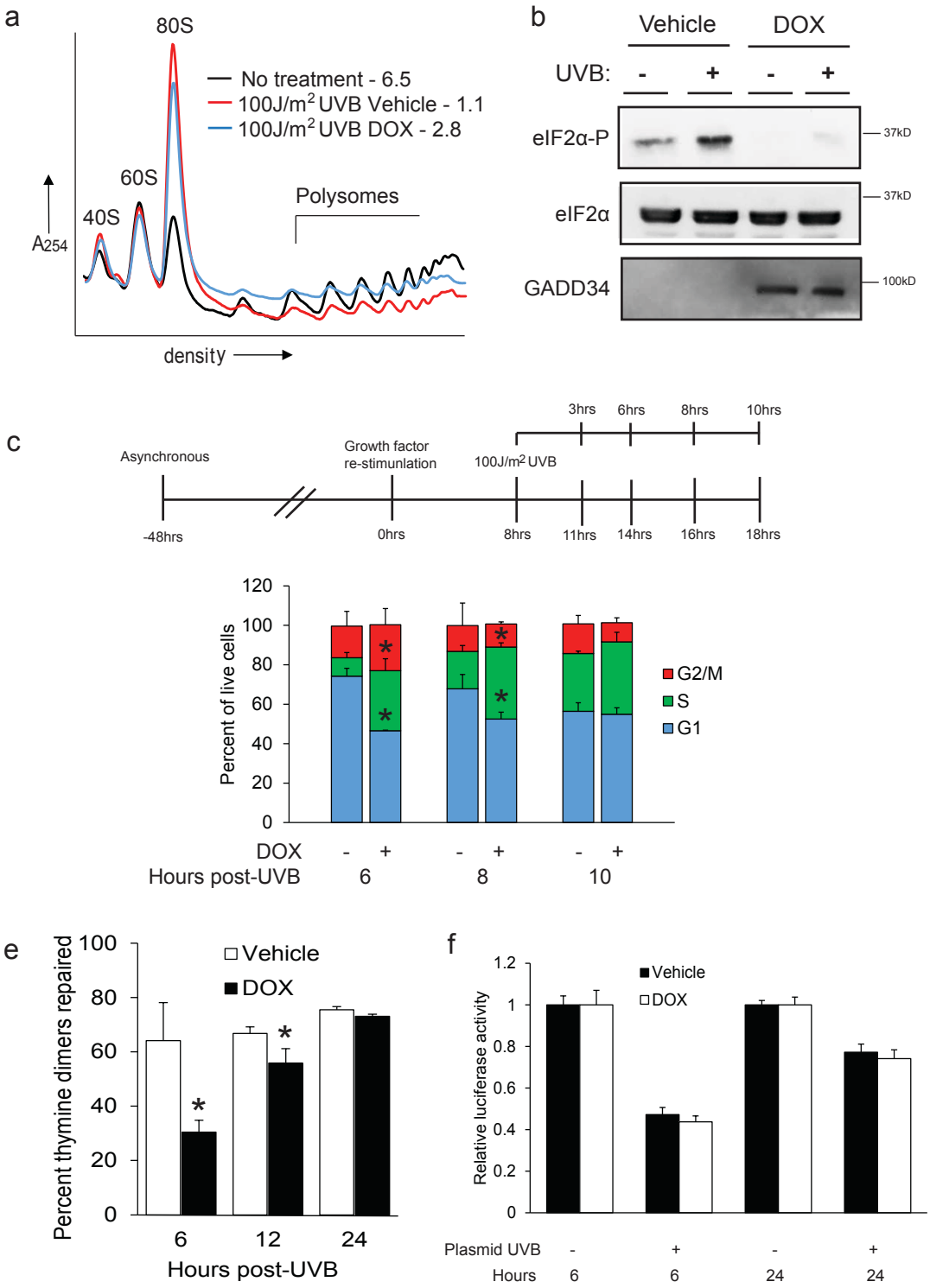

Figure 22. Loss of eIF2α-P diminishes G1 arrest and DNA repair following UVB. N-TERT keratinocytes were treated with 0 or 100 J/m^2 UVB or irradiated during GADD34 overexpression (DOX). Lysates were collected at 8 hours post-

UVB and subjected to (a) polysome profiling or (b) immunoblot analysis. P/M ratios for each sample are indicated in next to sample labels. Alternatively, cells were synchronized in G1 as described in (c) followed by irradiation with 100 J/m^2 UVB. At the indicated times post-UVB cells were co-stained with EdU and PI to measure cell cycle phases via flow cytometry or (d) subjected to immunoblot analysis for thymine dimer content. DNA repair rate is represented as percent decrease in thymine dimers from 15 minutes post-UVB. (e) A host-cell reactivation assay was performed at the indicated times post-transfection by measuring luciferase activity of an undamaged or UVB irradiated plasmid in untreated or irradiated N-TERTs. *p<0.05. Error bars represent mean +/- SD of three separate experiments.

5.2 Loss of eIF2α-P switches keratinocyte fate towards apoptosis following UVB

Since DOX-treated cells exhibited decreased cell cycle arrest following 100 J/m^2 UVB, we hypothesized that there would also be consequences of diminished levels of eIF2α-P on cell fate. 100 J/m^2 UVB is known to induce senescence in cultured human keratinocytes, which serves as a mechanism of protection from carcinogenesis (Lewis *et al.*, 2008). Losing the ability to senescence in response to UVB can lead to UVB-induced DNA damage in proliferative keratinocytes (Lewis *et al.*, 2010). In order to measure the effects of eIF2α-P deficiency on cellular senescence, we quantified the activity of a well-characterized marker, senescence-associated β-galactosidase (SA β-gal). While

UVB treated control cells displayed a 40% increase in SA β-gal activity, there was minimal change in senescence following UVB in DOX-treated cells (Figure 23a and b). DOX-treated keratinocytes also had significantly higher levels of UVB-induced caspase-3 activity compared to irradiated cells with a fully functional ISR, indicating higher levels of apoptosis (Figure 23c). This increase in cell death equated to about a 20% reduction in total cell population as measured by staining with trypan blue (Figure 23d). Taken together, these results indicate that eIF2α-P deficiency shifts cells away from senescence and towards apoptosis in response to UVB.

Since DOX-treated keratinocytes have a shortened cell cycle arrest and a decrease in the induction of senescence in response to UVB, we hypothesized that *CDKN1A* (p21 protein) levels may be regulated by the ISR. As noted in the introduction, enhanced p21 protein expression leads to inhibition of cyclin-dependent protein kinases and G1 arrest. *CDKN1A* is known to be induced by UV irradiation, and its primary function is to inhibit the progression from G1 to S phase of the cell cycle as well as to initiate cellular senescence (Brugarolas et al., 1995). To measure changes in *CDKN1A* expression we measured p21 protein levels following UVB exposure in vehicle and DOX-treated keratinocytes. In the control cells, UVB induced an increase in p21 protein (Figure 23e). However, lowered eIF2α-P levels by DOX diminished the UVB-induced p21 protein levels by over 50% at 6, 8, and 10 hours following UVB treatment. Therefore, in response to UVB irradiation, total p21 protein induction is dependent on eIF2α-P. DOX treatment also had no effect on cyclin D1 protein

levels (Figure 23e), which is another cell cycle regulator reported to be subject to translational control during ER stress. These results indicate that the ISR facilitates induced p21 protein expression upon UVB irradiation.

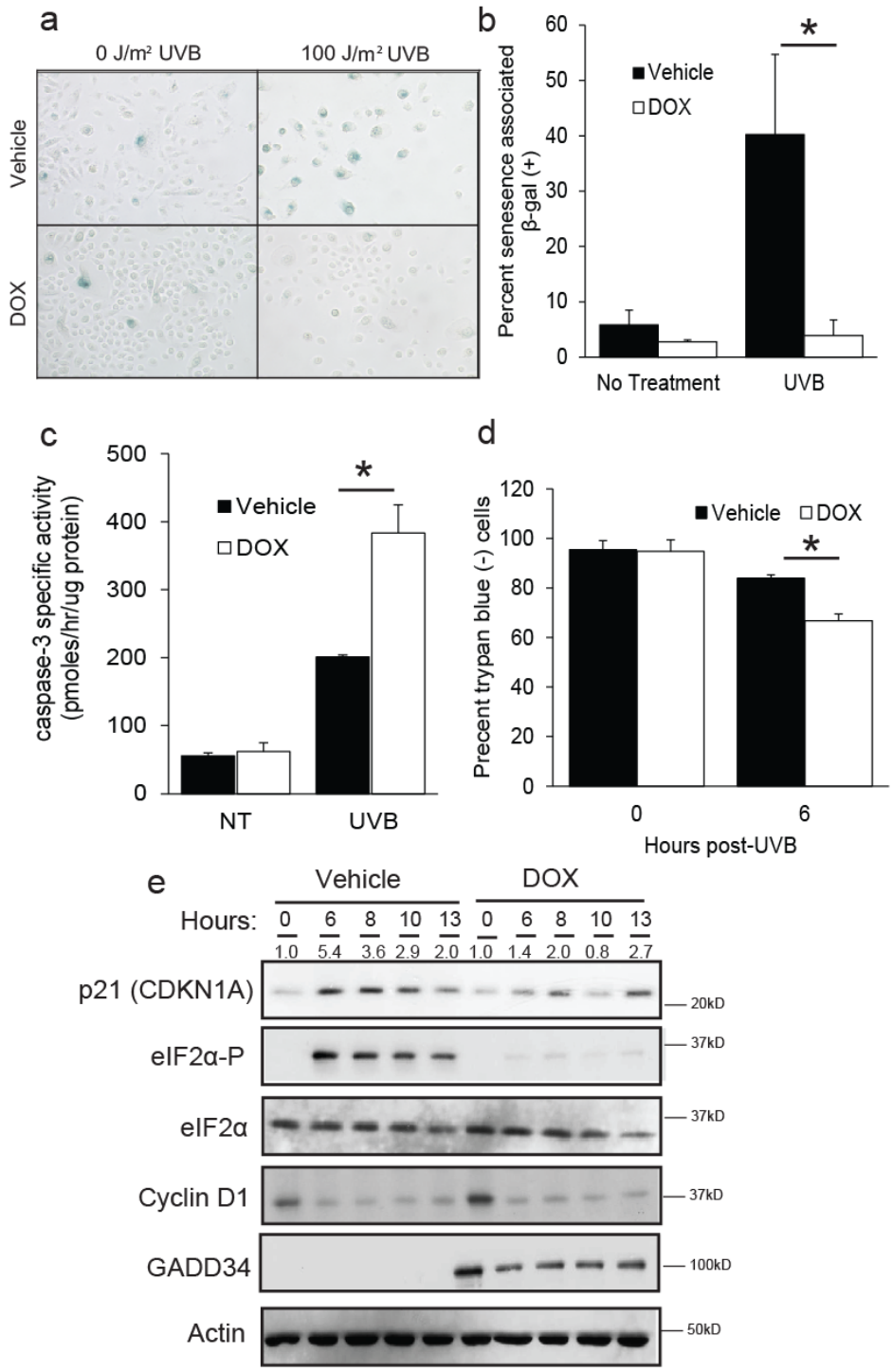

Figure 23. Loss of eIF2α-P switches cell fate away from senescence and towards apoptosis following UVB. (a) N-TERT keratinocytes were treated with 0 or 100 J/m^2 UVB and maintained in culture for 72 hours. Cells were then fixed

and stained for senescence-associated β-galactosidase activity. Senescent cells (dark blue) are quantified in (b). Alternatively, cells were collected at 6 hours post-UVB and assayed for (c) caspase-3 specific activity or (d) trypan blue to measure relative cell death. (e) Lysates were also collected at the indicated times post-UVB and subjected to immunoblot analysis to measure levels of the indicated proteins. Relative levels of p21 protein are shown above the immunoblot panels. *, $p<0.05$. Error bars represent mean +/- SD of three separate experiments.

5.3 UVB-induced *CDKN1A* translation is dependent on eIF2α-P

Since inhibition of the ISR diminished p21 protein expression, we wished to address whether *CDKN1A* is preferentially translated following UVB. We therefore measured changes in ribosome association of the *CDKN1A* mRNA via sucrose gradient centrifugation and polysome profiling (Figure 22a). In response to N-TERT exposure to UVB, total *CDKN1A* mRNA shifted 19% towards heavy polysomes fractions (5-7) compared to control cells not subjected to irradiation (Figure 24a). Of note, the 19% shift of *CDKN1A* mRNA toward heavy polysomes was diminished to only 3% when UVB irradiation was combined with DOX treatment, indicating that the preferential translation of *CDKN1A* is dependent on eIF2α-P. These changes are comparable to shifts for the ISR regulator *ATF4* mRNA following 100 J/m^2 UVB exposure (Figure 24b). We have shown previously that *ATF4* is preferentially translated in response to eIF2α-P during

diverse stresses, including high doses of UVB. These findings indicate that *CDKN1A* is subject to preferential translation in response to UVB and eIF2α-P.

Human cells express multiple *CDKN1A* transcript variants which differ only by their 5'-leader sequences. Variants 1 and 4 (denoted V1 and V4, respectively) contain 5'-leaders with sufficient length to be regulated by eIF2α-P. *CDKN1A* V4 mRNA contains two putative uORFs with one predicted canonical codon and two noncanonical start codons. Importantly, the noncanonical initiation codons have been identified in ribosome profiling studies as functional sites of initiation (Lee *et al.*, 2012). The 5'-leader of V1, which is considered the major expressed splice variant, contains 3 upstream noncanonical CUG start codons in poor context which have not been identified as functional sites of initiation. We therefore sought to determine which individual *CDKN1A* mRNA splice variants were preferentially translated in response to eIF2α-P. *CDKN1A* V4 displayed an 18% shift toward heavy polysomes following UVB (Figure 24c), whereas V1 displayed a negligible 3% shift (Figure 24d). V4 translation also appeared to be dependent on eIF2α-P, as DOX treatment reversed the preferential translation of V4, shifting instead 6% away from polysomes towards monosomes compared to no treatment. DOX treatment had no effect on V1 polysome association. Consistent with our immunoblot analysis, cyclin D1 polysome association exhibited negligible changes in response to UVB with or without DOX treatment (Figure 24e). These results indicate that an individual *CDKN1A* transcript variant 4 is subject to preferential translation in response to eIF2α-P and UVB.

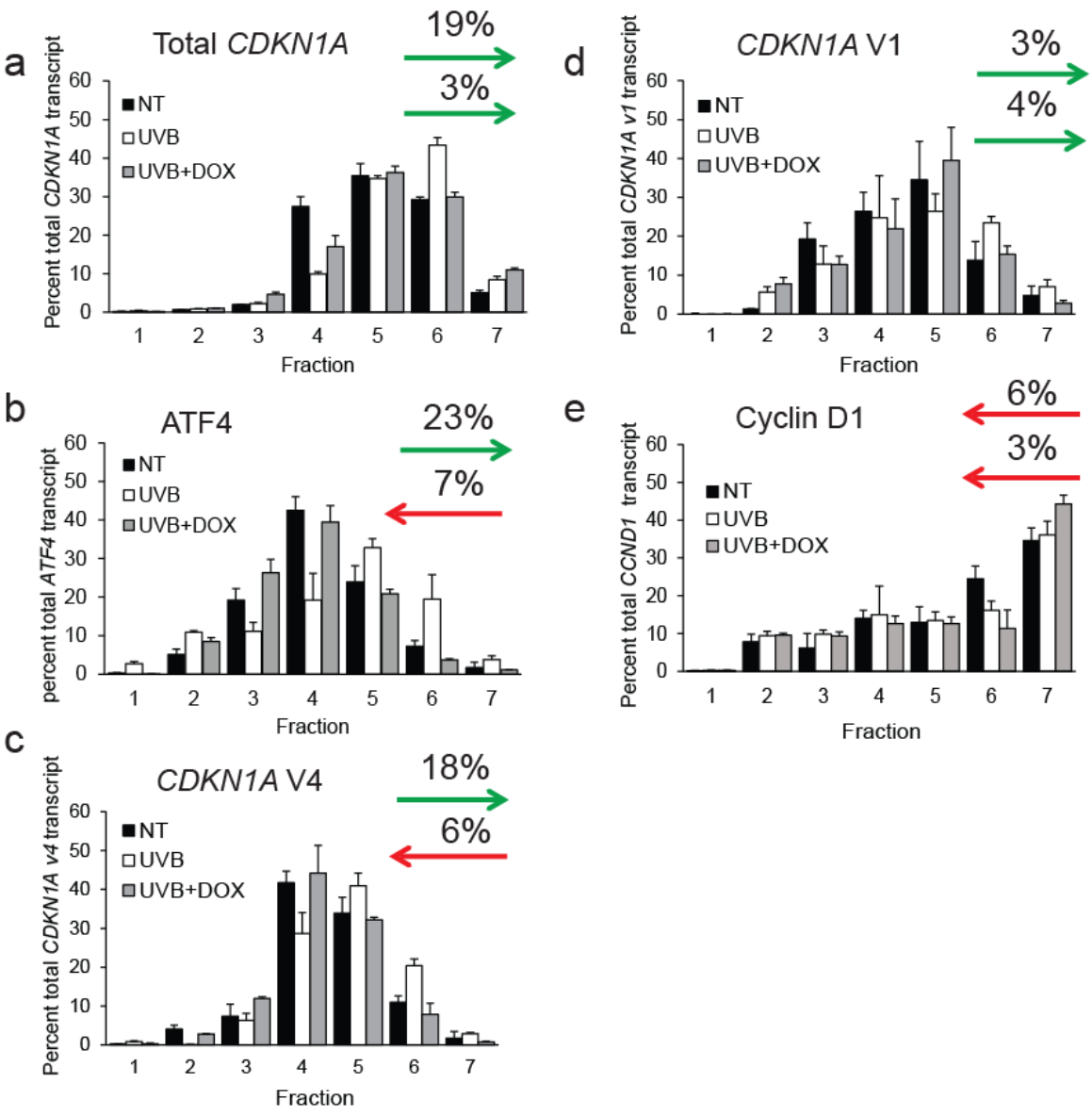

Figure 24. Human *CDKN1A* splice variant 4 is preferentially translated following UVB. DOX treated N-TERT cells that overexpressed GADD34 were irradiated with 0 or 100 J/m^2 UVB and compared to control keratinocytes. Lysates were collected at 8 hours post-UVB and subjected to polysome profiling. qPCR was performed on RNA isolated from sucrose gradient fractions to measure mRNA levels of the indicated genes. mRNA levels are represented as a percent of total gene transcript to discount any changes in transcription. Arrows

represent the percent of each transcript that shifts toward or away from heavy polysomes (fractions 5-7). Error bars represent mean +/- SD of three separate experiments.

To address whether mRNA changes of specific *CDKN1A* transcript variants could be responsible for the ISR induction of p21 protein, we performed qPCR to measure mRNA levels of each individual *CDKN1A* variant at various times following UVB exposure. While total *CDKN1A* and both transcript variants 1 and 4 were induced in response to UVB over time, neither the total *CDKN1A* nor splice variants showed any altered induction of mRNA levels with GADD34 overexpression (Figure 25a, b, and c). These results indicate that diminished p21 protein in DOX-treated cells was not due to decreased induction of *CDKN1A* mRNA. To determine the relative abundance of each variant in keratinocytes, we performed PCR using primers that recognize both variants. Distinct bands for each variant were separated by agarose gel electrophoresis and visualized by staining with ethidium bromide. Both variants were present in N-TERT keratinocytes, and V1 appears to be roughly 40% more abundant than V4 (Fig. 25d). It is of note that this method of transcript quantification likely does not take into account the PCR preference for shorter transcripts, as V1 is shorter than V4. Since our data suggest that the ISR is required for *CDKN1A* expression following UVB, we wished to determine if loss of *CDKN1A* mimics the cell death phenotype associated with eIF2α-P deficiency. We created N-TERT keratinocytes stably expressing shRNA against *CDKN1A* or control and treated the cells with 0 or 100

J/m^2 UVB. Keratinocytes depleted for *CDKN1A* showed increased UVB-induced cell death as measured by increased cleaved caspase-3 (Figure 25e), as well as increased apoptotic cell populations as measured by flow cytometry (Figure 25f). These results suggest that loss of the ISR mimics the behavior of keratinocytes deficient for *CDKN1A*.

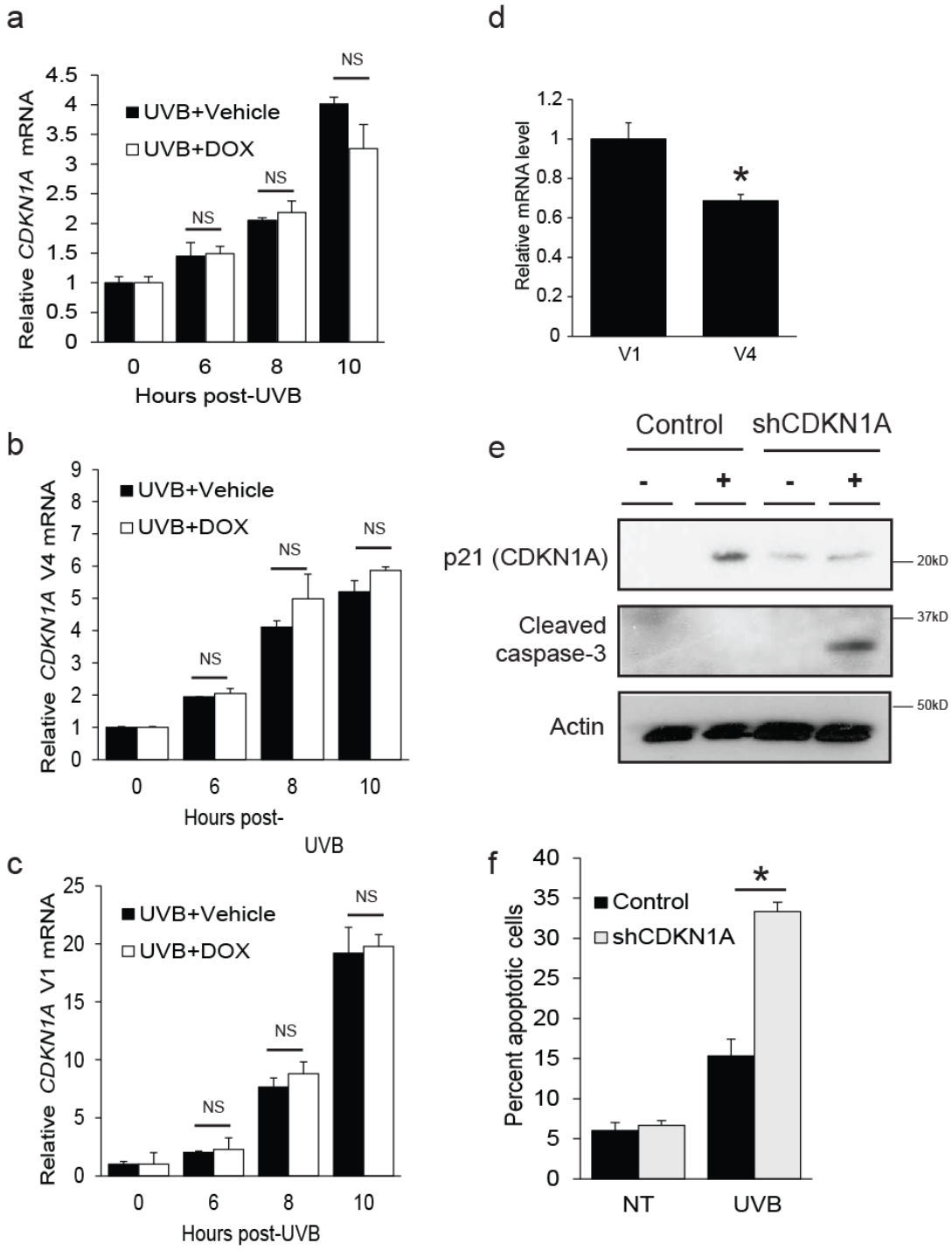

Figure 25. Loss of *CDKN1A* mimics ISR deficiency. Vehicle or DOX treated N-TERT keratinocytes overexpressing GADD34 were irradiated with 0 or 100 J/m^2 UVB. Lysates were collected from cells at the indicated times following UVB

treatment. (a) Total *CDKN1A*, (b) *CDKN1A* V4, or (c) V1 mRNAs were measured by qPCR. Primers that recognize both V1 and V4 were used to perform PCR on N-TERT keratinocytes to determine relative transcript abundance. PCR product bands separated using an agarose gel for each variant are quantified in (d). To investigate the effects of *CDKN1A* loss on cell death, control and *CDKN1A* knockdown N-TERTs were irradiated with 0 or 100 J/m^2 UVB. Lysates were collected at 8 hours post-UVB and subjected to (e) immunoblot analysis or (f) PI staining to measure DNA content and relative cell death. *, $p<0.05$. Error bars represent mean +/- SD of three separate experiments.

5.4 The 5'-leader of *CDKN1A* V4 mRNA directs preferential translation in response to eIF2α-P

We next wished to test whether translational control of *CDKN1A* V4 is mediated through the 5'-leader and involves uORFs. We inserted the cDNA segments encoding the 5'-leader for either *CDKN1A* V1 or V4 between a minimal thymidine kinase promoter (P_{Tk}) and firefly luciferase CDS (Figure 26a). The arrangement of these reporter constructs was similar to other ISR transcripts tested for preferential translation (Vattem and Wek, 2004; Young *et al.*, 2016a; Young *et al.*, 2016b). Given that UVB can have a general deleterious effect on mRNA levels (Gyenis *et al.*, 2014; Williamson *et al.*, 2017), we measured the mRNA for the P_{Tk}-CDKN1AV4-Luc following treatment with UVB or TG, a known inducer of ER stress. Notably, treatment with UVB caused an over 50% decrease in the luciferase reporter mRNA levels. While UVB is known to enhance *CDKN1A*

transcription, it is not known to induce transcription with a Tk promoter. We next measured luciferase activity of P_{Tk}-CDKN1AV4-Luc normalized to changes in mRNA levels. Luciferase activity of *CDKN1A* V4 increased 2-fold following treatment with either UVB or TG, indicating preferential translation is mediated through the V4 5'-leader (Fig. 26a).

We wished to determine the underlying mechanism for *CDKN1A* preferential translation in response to eIF2α-P. In order to circumvent the complication caused by UVB on P_{Tk}-CDKN1AV4-Luc mRNA in our analysis of preferential translation in response to eIF2α-P, we elected to carry out our experiments using TG, which did not affect levels of endogenous *CDKN1A* or reporter mRNA levels (Figure 26b). Of interest, treatment of N-TERT cells with TG led to an increase in p21 protein levels (Figure 26c), further supporting its usefulness as a tool to study *CDKN1A* translational control. *CDKN1A* V4 and V1 as well as *ATF4* luciferase reporters were treated with TG and collected after 6 hours. While V4 luciferase activity increased with TG to a similar degree as *ATF4*, there was no change in reporter activity for V1 in response to stress (Figure 26d). This indicates that *CDKN1A* V4, but not V1, is subject to preferential translation mediated by its 5'-leader. To determine whether uORFs in *CDKN1A* V4 mRNA are indeed translated, we created in-frame fusions between the 5'-proximal uORF1 and uORF2 with the firefly luciferase CDS. These constructs did not contain the luciferase translation start site, so any quantifiable luciferase activity will be due to initiation at the in-frame uORF. The fusion of both uORF1 and uORF2 had measureable luciferase activity, suggesting functional

initiation codons for each uORF (Figure 26e). Mutation of possible initiation sites in ORF1 and ORF2 fusions, along with less frequent initiation codons (CUG and GUG) caused a substantial decrease in luciferase activity, indicating that each start codon is functional and required for translation of each uORF.

To determine the relative contribution of each uORF and initiation codons to preferential translation for *CDKN1A* V4, we performed a series of mutational analyses using variations of the P_{Tk}-CDKN1AV4-Luc. Importantly, the increase in P_{Tk}-CDKN1AV4-Luc reporter activity with TG was abolished during GADD34 overexpression (Fig. 26f), suggesting that the translation control mediated by the 5'-leader is dependent on eIF2α-P. Mutation of the AUG in uORF2 caused a significant increase in basal reporter activity, indicating that uORF2 serves to repress downstream translation. This mutation, however, had no effect on the increase in reporter activity seen with TG treatment. Mutation of the uORF1 CUG caused a decrease in basal reporter activity, but again had no effect on induction. Mutation of both the uORF1 GUG and CUG showed similar results. This result is consistent with uORF1 acting as a moderate enhancer of downstream translation, with the GUG being the primary initiating codon. There was no significant change in mRNA levels for P_{Tk}-CDKN1AV4-Luc throughout the experiment, suggesting the changes in luciferase activity are a result of translational control We therefore propose a model in which uORF1 promotes reinitiation of downstream translation at the CDS during unstressed conditions. Translation can also initiate at uORF2 in unstressed conditions causing a bypass

of the *CDKN1A* CDS. During stress, delayed reinitiation of translation after uORF1 causes a bypass of uORF2 and allows translation of the *CDKN1A* CDS.

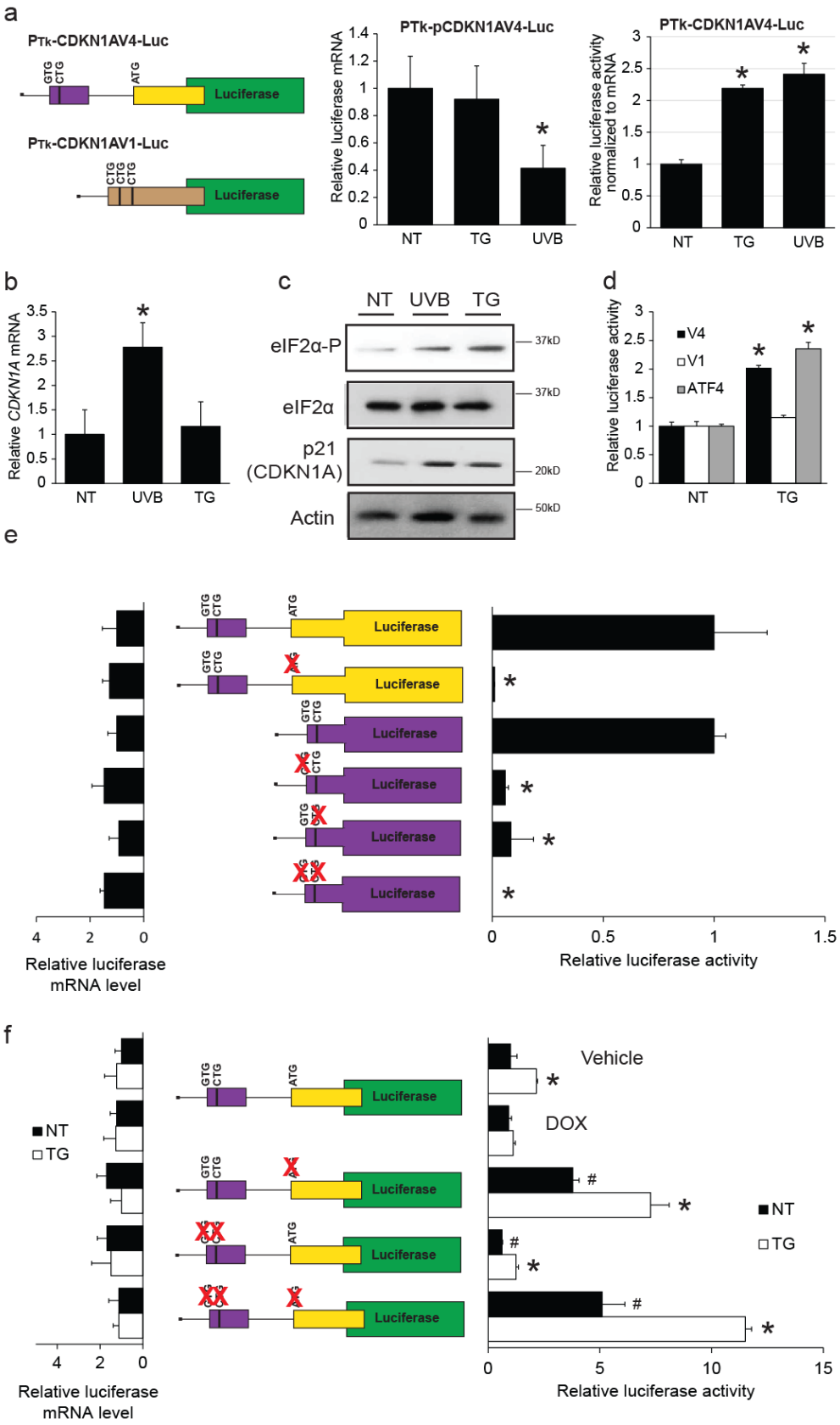
a
PTk-CDKN1AV4-Luc
GTG
CTG
ATG
Luciferase
PTk-CDKN1AV1-Luc
CTG
CTG
CTG
Luciferase
PTk-pCDKN1AV4-Luc
Relative luciferase mRNA
NT
TG
UVB
PTk-CDKN1AV4-Luc
Relative luciferase activity normalized to mRNA
NT
TG
UVB
b
Relative CDKN1A mRNA
NT
UVB
TG
c
NT
UVB
TG
eIF2α-P
37kD
eIF2α
37kD
p21 (CDKN1A)
20kD
Actin
50kD
d
Relative luciferase activity
V4
V1
ATF4
NT
TG
e
Luciferase
Relative luciferase mRNA level
Relative luciferase activity
f
NT
TG
Luciferase
Relative luciferase mRNA level
Vehicle
DOX
NT
TG
Relative luciferase activity

Figure 26. The 5'-leader of *CDKN1A* V4 mRNA directs preferential translation in response to eIF2α-P. N-TERTs were transfected with a P_{Tk}-CDKN1AV4-Luc reporter represented graphically in (a), followed by treatment with TG or 100 J/m^2 UVB and measurement of mRNA or luciferase activity. Luciferase activity in (a) is normalized to reporter mRNA levels. Untransfected N-TERTs were also collected at 6 hours after stress and lysates were subjected to (b) qPCR to measure levels of endogenous *CDKN1A* mRNA or (c) immunoblot analyses. (d) N-TERTs were transfected with either *CDKN1A* V4, V1, or an *ATF4* luciferase reporters, collected 6 hours following TG treatment, and measured for luciferase activity. (e) N-TERTs were transfected with the indicated fusion construct and measured for luciferase activity at 24 hours following transfection. (f) N-TERTs were transfected with the indicated P_{Tk}-CDKN1AV4-Luc reporter followed by treatment with TG for 6 hours and measurement of luciferase activity. Relative amounts of luciferase mRNA as measured by qPCR are shown to the left in Figures e and f. *, $p<0.05$, #, $p<0.05$ compared to untreated P_{Tk}-CDKN1AV4-Luc. Error bars represent mean +/- SD of three separate experiments.

CHAPTER 6. DISCUSSION

6.1 Activation of the ISR in keratinocyte-specific stress conditions

This thesis focused on the role of translational control through the ISR in human keratinocyte differentiation and adaptation to UVB irradiation. Without a tightly controlled response to environmental changes, keratinocytes can contribute to skin diseases such as psoriasis, atopic dermatitis, or NMSCs among others (Bikle *et al.*, 2012; Bouwstra and Ponec, 2006; Menon *et al.*, 1994). Mechanisms of translational control have been well described in response to environmental challenges such as ER, nutritional, and oxidative stress in other cell types (Castilho *et al.*, 2014; Harding *et al.*, 2003). The ISR has also been shown to be vital in response to a variety of stressors with dysregulation contributing to diseases such as diabetes, fatty liver, and cancer (Eyries *et al.*, 2014; Malhi and Kaufman, 2011; Marciniak and Ron, 2006; Scheuner and Kaufman, 2008). However, little is known about the activation, role, or mechanisms of the ISR in key keratinocyte processes. This thesis demonstrates that not only is the ISR activated in response to stress and differentiation processes in human keratinocytes, but also is crucial for their proper cellular responses. Loss of ISR regulation during keratinocyte differentiation or UVB irradiation produces an aberrant cellular proliferation response, further demonstrating its previously unrecognized importance in keratinocyte biology. Collectively, this thesis describes a dual role for the ISR in stress and differentiation in skin, further emphasizing the critical importance for translational control in both tissue homeostasis and adaptation to environmental insults. We

propose that differentiation and environmental stress are two sides of the same coin in keratinocytes. While differentiation is a developmental aspect of skin biology and UVB is an external stimulus, both responses elicit and require translational control using similar mechanisms to maintain healthy skin function.

6.2 Translational control during keratinocyte differentiation

Results from Chapter 3 showed that translational control through GCN2 phosphorylation of eIF2α is required for epidermal differentiation (Figure 27). eIF2α-P represses global translation initiation coincident with preferential translational control of genes such as *IVL* during keratinocyte differentiation (Figures 8-10). Loss of either eIF2α-P or GCN2 abrogated this translation regulation as well as caused a decrease in differentiation and accompanying induced expression markers (Figure 11 and 13). IVL protein levels were decreased sharply in eIF2α-P deficient and GCN2 knockdown cells compared to controls. The significance of GCN2 was further demonstrated when depletion of GCN2 resulted in disorganized epidermal formation and decreased squamous layers in 3D organotypic culture (Figure 14). Of importance, loss of PERK did not have any detectable effect on differentiation-induced eIF2α-P (Figure 12d), supporting the idea that ER stress and induction of the UPR are not critical. Furthermore, we did not see any changes in IRE1-directed splicing of *XBP1* mRNA, a hallmark feature of the UPR (Figure 12a). These results show an importance for GCN2 and translational control in normal epidermal formation, as well as point to potential involvement of this signaling pathway in diseases with

impaired keratinocyte differentiation such as psoriasis, squamous cell carcinoma, and atopic dermatitis.

Another major finding described in Chapter 3 was the dependence of the expression of differentiation-specific genes on activation of the ISR. Regulation of the keratinocyte differentiation marker *IVL* has previously been characterized at the transcriptional level, with extensive focus on promoter elements that control *IVL* mRNA levels (Eckert et al., 2004). To our knowledge, this is the first report of *IVL* regulation at the translational level, as we saw a 27% percent shift of *IVL* mRNA toward heavy polysomes during keratinocyte differentiation (Figure 8c). The resistance of transcripts such as *IVL* to global translation inhibition by eIF2α-P ensures appropriate protein expression during keratinocyte differentiation. Lowered general translation would reduce energy and nutrient expenditure and dramatically alter the proteome during the differentiation process. It is noteworthy that total *IVL* mRNA levels were also decreased both in eIF2α-P deficient and GCN2 knockdown keratinocytes compared to controls (Figures 10f and 12d). This finding indicates that mRNA induction of *IVL* is partially dependent on the ISR. This increase in mRNA may involve the well characterized transcriptional increases in *IVL*.

Our laboratory and others have previously characterized a cohort of eIF2α-P-dependent transcription factors, which include ATF3, ATF5, C/EBPβ, and NF-κB (Calkhoven *et al.*, 2000; Deng *et al.*, 2004; Dey *et al.*, 2012; Jiang and Wek, 2005; Jiang *et al.*, 2004; Jiang *et al.*, 2003; Teske *et al.*, 2013; Zhou *et al.*, 2008). The *IVL* promoter contains canonical AP1, SP1, C/EBP, and CRE binding

sites, all of which have shown to have some effect on *IVL* transcription (Adhikary *et al.*, 2005; Banks *et al.*, 1998; Crish *et al.*, 2006). It is anticipated that GCN2/eIF2α-P controls the activity of a transcription factor(s) that modulates *IVL* transcriptional expression, which can also contribute to keratinocyte differentiation. Such transcription factors include Jun, Fos, and C/EBP family members, which also have been implicated in response to cellular stress such as UV (Wisdom *et al.*, 1999). Not only do these factors control transcription of differentiation genes, but also have targets in cell cycle and apoptosis pathways and have been shown to be overexpressed in various cancers (Eferl *et al.*, 2003; Vogt, 2002). Therefore the connection between GCN2 and differentiation-induced transcription factors could implicate the ISR in additional cell signaling cascades.

Importantly, general and gene-specific translational control can also occur during inhibition of mammalian target of rapamycin (mTOR) signaling. Our preliminary data suggest that mTOR signaling is also inhibited during keratinocyte differentiation (Figure 8a), and previous work indicates that GCN2 can facilitate sustained mTOR repression during amino acid deprivation (Anthony *et al.*, 2004; Ye *et al.*, 2015). Therefore GCN2 may also be required for inhibition of mTOR signaling during keratinocyte differentiation, and that this could contribute to translational regulation of genes such as *IVL*. GCN2 is known to be activated during amino acid starvation through binding of uncharged tRNAs to an aminoacyl-tRNA synthetase-like domain (Dong *et al.*, 2000; Wek *et al.*, 1989; Wek *et al.*, 1995; Zaborske *et al.*, 2009), however the activating signal during

keratinocyte differentiation is currently unknown. Previous research has reported that the composition of tRNAs can be altered in different layers of mouse skin (Zhao *et al.*, 2005), suggesting that the dynamics of tRNA expression and subsequent aminoacylation may also be an activating signal of GCN2 during human keratinocyte differentiation. Since accumulation of uncharged tRNAs is a known GCN2 activator, we hypothesize that there is a decrease in tRNA charging during keratinocyte differentiation, likely coinciding with decreased free amino acids.

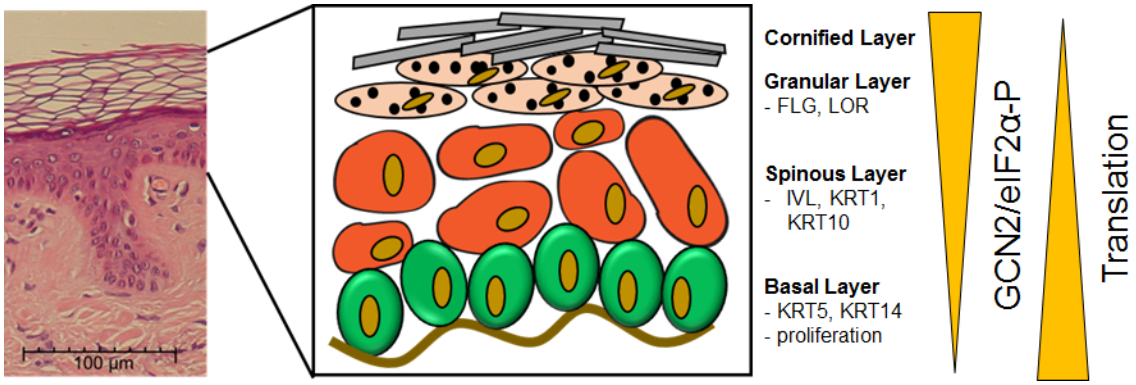

Figure 27. Model: Human keratinocyte differentiation requires translational control by the eIF2α kinase GCN2. As human keratinocyte differentiate, cells undergo a major change in both gene expression and morphology. Chapter 3 demonstrates that translation initiation is repressed during keratinocyte differentiation both *in vitro* and *in vivo* through the ISR. During this process eIF2α phosphorylation is induced by GCN2. Loss of this eIF2α kinase or the phosphorylation event itself caused a reduction in differentiation gene expression and altered morphology in 3D culture. Taken together, these results implicate

translational control through the ISR as a major regulator of gene expression changes in keratinocyte differentiation.

6.2 Non-canonical ISR mechanisms in response to UVB

The results in Chapter 4 addressed the importance of the ISR in the response of human keratinocytes to UVB irradiation. First, we show that UVB represses global and individual transcript translation initiation in a dose-dependent manner (Figure 14-16). Second, the ISR response to UVB does not involve appreciable induced expression of ATF4 and its downstream target CHOP in keratinocytes (Figure 16). *ATF4* mRNA was preferentially translated in response to UVB irradiation (Figure 17). However, *ATF4* and *CHOP* mRNA levels were significantly reduced (Figures 15 and 17), suggesting a lack of gene transcripts available for sufficient preferential translation to induce measureable protein expression. Repression of ATF4 and CHOP appears to be an important feature of the cytoprotective function of the ISR during UVB stress, as forced ATF4 and CHOP expression during UVB by pretreatment with Sal increased UVB-induced apoptosis (Figures 18-20). Finally, we show that repression of general protein synthesis contributes to protection of keratinocytes from UVB-induced apoptosis. Blocking eIF2α-P dependent translational repression increased cell death in response to UVB (Figure 21), and treatment with the protein synthesis inhibitor CHX substantially alleviated the harmful effects of ISR deficiency and protected against UVB-induced cell death (Fig. 20f).

These results suggest that the ISR attenuation of global translation provides important advantages to keratinocytes exposed to UVB. Reduced protein synthesis would decrease energy and nutrient expenditure, allowing UVB-stressed cells to focus on quality control of existing proteins that can provide protection to UVB damage, such as those related to DNA repair and cell cycle control. Repression of translation may also contribute to lowered levels of key proteins that are short-lived and that function to enhance apoptosis. Furthermore, part of the deleterious functions of ATF4 and CHOP expression during UVB may involve their transcriptional activation of GADD34, which facilitates feedback dephosphorylation of eIF2α-P. ATF4 and CHOP can also promote expression of genes involved in protein synthesis, which can lead to premature resumption of high levels translation that can facilitate cell death during stresses that afflict the ER (Han *et al.*, 2013; Marciniak and Ron, 2006; Marciniak *et al.*, 2004). Therefore, premature resumption of translation accompanying lowered eIF2α-P may render UVB-stressed cells susceptible to complications of folding of existing damaged proteins and an enhanced influx of nascent polypeptides.

6.3 ISR regulation of cell fate and implication in carcinogenesis

Our studies in Chapter 5 delineate a mechanism for ISR cytoprotection following UVB (Figure 28). Induction of eIF2α-P by UVB results in preferential translation of human *CDKN1A* splice variant 4, which is required for a G1 cell cycle arrest. Loss of eIF2α-P shifts cell fate away from senescence and towards

apoptosis, likely due to decreased DNA repair as a result of cell cycle deregulation (Figure 22). We also show that translational control of human *CDKN1A* splice variant 4 is mediated through its 5'-leader (Figure 26). These results highlight a previously unrecognized mechanism for eIF2α-P and translational control in response to UVB, and point towards its potential involvement in diseases initiated by UVB damage such as NMSC. Since UVB can perturb barrier function in intact skin, these results also point to a link between keratinocyte differentiation, UVB, and the ISR.

One of the main drivers of cellular transformation is loss of cell cycle control (Nakanishi *et al.*, 2006). Here we describe a mechanism by which the cell cycle is regulated at the level of translation in response to stress. Our data demonstrate that perturbation of translational control has significant consequences on the fate of the stressed cell, and give credence to the possibility that eIF2α-P could be important in the initiation of cancer. Depending on cellular context and conditions, p21 protein has been suggested act as both a tumor suppressor or as an oncogene (Abbas and Dutta, 2009). *CDKN1A* induction has also been shown to be required for cellular senescence, which is considered an anti-cancer response as it permanently halts proliferation of DNA damaged cells (Roninson, 2002). On the other hand, senescent cells have been shown to actually contribute to carcinogenesis through paracrine signaling to transformed cells (Krtolica *et al.*, 2001). Therefore p21 protein expression must be under tight control as up or downregulation of the protein can contribute to cancer-promoting effects. According to our results, eIF2α-P can regulate

CDKN1A translation in response to both UVB and ER stress (Figure 26). Therefore one could hypothesize that perturbation resulting in either increased or decreased eIF2α-P could play a role in cancer initiation and/or progression.

Induction of eIF2α-P has been shown to contribute to tumor growth under hypoxic stress, and mechanisms of survival and proliferation in part through the PI3K-Akt pathway have implicated both PERK and eIF2α-P in oncogenesis (Bobrovnikova-Marjon *et al.*, 2010; Ye and Koumenis, 2009). Since a myriad of environmental insults can activate eIF2α-P, it is plausible to assume that a variety of carcinogenic stressors could be acting through eIF2α-P during the initiation of cancer. For example, ER stress and oxidative stress, both of which have been implicated in tumorigenesis, induce eIF2α-P through PERK. Alternatively, UVB irradiation (a major cancer risk factor) and nutrient limitation (a hallmark of tumors) elicit eIF2α-P through GCN2. In this case, UVB (which acts through GCN2) and TG (which acts through PERK) both lead to translational control of *CDKN1A* (Figure 26), pointing to eIF2α-P as a universal *CDKN1A* regulator independent of the activation signal.

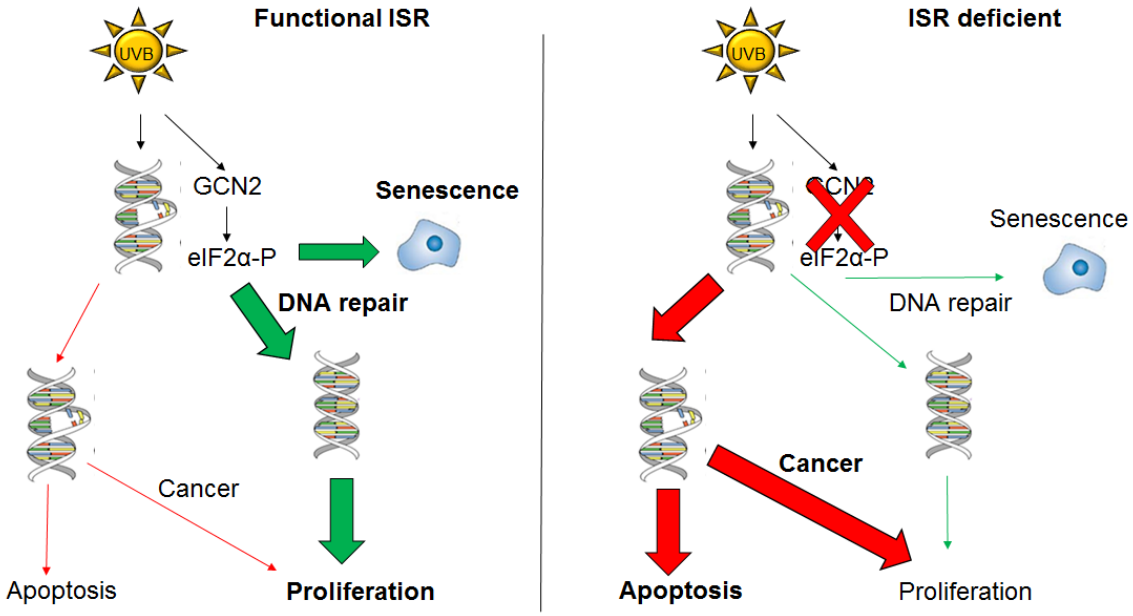

Figure 28. Model: Loss of eIF2α-P switches cell fate following UVB exposure. As described in Figure 2, UVB causes DNA damage in human keratinocytes. As illustrated in Chapters 4 and 5, UVB also elicits translational control through the ISR. When keratinocytes are deficient in ISR activation, cell fate switches away from DNA repair and senescence towards apoptosis. Our results in Chapter 5 suggest that this is due to a decreased G1 arrest mediated by *CDKN1A* expression, allowing less time for DNA repair or to induce senescence. Loss of DNA repair and senescence can also lead to DNA damage containing proliferative cells, a hallmark of human cancers.

6.4 Translational control of human *CDKN1A*

This thesis outlines a previously unknown mechanism for 5'-leader mediated translational control of human *CDKN1A* transcript variant 4. In response to UVB, *CDKN1A* induction is pro-survival in that it halts proliferation to

allow for DNA repair. *CDKN1A* regulation has previously been characterized at the level of transcription, with p53 being the most prominent regulator (Macleod *et al.*, 1995). A recent study delineated a GCN2-dependent mechanism for 5'-leader mediated translation of a mouse *CDKN1A* transcript variant in response to amino acid starvation (Lehman *et al.*, 2015). Interestingly, the transcript described in the previous study bears no resemblance to human *CDKN1A* V4, indicating major differences between the evolution of mouse and human *CDKN1A* alternative splicing. The mouse epidermis is significantly dissimilar to humans in terms of thickness, layers, and hair growth, which could point to a difference in need for regulation of gene expression in response to environmental stressors such as sunlight (Pasparakis *et al.*, 2014). Alternative splicing of human *CDKN1A* also appears to ensure that the protein is induced even in cases where eIF2α-P does not occur, by allowing for transcriptional upregulation of *CDKN1A* variants without significant 5'-leaders. These data suggest a role of splicing in providing new 5'-leader sequences for selective preferential translation of key proteins regulating cell cycle and appropriate adaptation to stress.

6.5 Rationale for targeting the ISR in skin disease therapy

In addition to the importance of the ISR in normal keratinocyte differentiation, our results also point toward potential ISR involvement in skin diseases in which differentiation is dysregulated. Previous reports have shown differential expression of translation-related proteins in psoriasis and squamous cell carcinoma (SCC) tissue, and there are suggestions that SCC-derived cell

lines fail to regulate translation in response to calcium (Gibson *et al.*, 1996; Sugiura *et al.*, 2009; Swindell *et al.*, 2015). Combined with studies herein suggesting specific expression of the ISR in differentiated skin layers, we propose that ISR markers such as eIF2α-P, along with ATF4, CHOP, or GADD34 could serve as valuable markers of skin disease. Previous studies have also shown that the action of the cyclosporin A in psoriasis treatment depends on CHOP, indicating that activation of the ISR could alleviate certain skin lesions (Hibino *et al.*, 2011). Multiple pharmacological agents can alter the ISR, and targeting eIF2α in disease has become an increasingly promising option as the importance of translational control continues to be elucidated (Fullwood *et al.*, 2012). Among drugs that activate the ISR is salubrinal, a GADD34 inhibitor, which has been shown to be effective in cell culture and mouse models of neurodegenerative disease and osteoporosis (Sato *et al.*, 2015; Saxena *et al.*, 2009). Another GADD34 inhibitor, guanabenz, is a clinically approved α2-adrenergic agonist used to treat hypertension (Holmes *et al.*, 1983). Alternatively, ISRIB is an ISR inhibitor that can improve memory function in mice (Sidrauski *et al.*, 2013). Altogether, this work has underscored a previously unrecognized importance for translational control through the ISR in keratinocyte differentiation, and we can now begin to explore the application of well-studied pharmacological agents in the context of skin disease.

This thesis also provides a rationale for exploring the utility of ISR-directed drugs in UVB-induced skin cancers. Chapters 4 and 5 focus specifically on the human keratinocyte response to UVB, which is the major risk factor in the

formation NMSCs. These studies provide for a mechanism of translational control in human keratinocytes that could be implicated in UVB-mediated carcinogenesis, providing new targets for skin disease therapy. High expression of p21 protein in head/neck, esophageal, and oral squamous cell carcinomas has been correlated with poor prognosis, indicating that loss of *CDKN1A* regulation could promote cancer progression in epithelial cells (Choi *et al.*, 2003; Ng *et al.*, 1999; Rigberg *et al.*, 1998). Although p21 protein expression is often dysregulated in a variety of cancers, its expression has been shown to be either increased or decreased depending on the cancer and cell type (Abbas and Dutta, 2009). Therefore, therapies targeting *CDKN1A* have proven to be complex and risky (Eastman, 2004), and targeting factors upstream may serve to circumvent this issue. This thesis provides a rationale for targeting translational control through eIF2α-P to prevent the initiation or halt the progression of NMSCs by modulating aberrant *CDKN1A* expression. The aforementioned ISR-directed pharmacological agents could also prove effective in preventing or eliminating NMSCs.

REFERENCES

Abbas T, Dutta A (2009) p21 in cancer: intricate networks and multiple activities. *Nature reviews Cancer* 9:400-14.

Abhishek S, Palamadai Krishnan S (2016) Epidermal Differentiation Complex: A Review on Its Epigenetic Regulation and Potential Drug Targets. *Cell journal* 18:1-6.

Adhikary G, Crish JF, Bone F*, et al.* (2005) An involucrin promoter AP1 transcription factor binding site is required for expression of involucrin in the corneal epithelium in vivo. *Investigative ophthalmology & visual science* 46:1219-27.

Anthony TG, McDaniel BJ, Byerley RL*, et al.* (2004) Preservation of liver protein synthesis during dietary leucine deprivation occurs at the expense of skeletal muscle mass in mice deleted for eIF2 kinase GCN2. *The Journal of biological chemistry* 279:36553-61.

Averous J, Gabillard JC, Seiliez I*, et al.* (2012) Leucine limitation regulates myf5 and myoD expression and inhibits myoblast differentiation. *Experimental cell research* 318:217-27.

Baird TD, Palam LR, Fusakio ME*, et al.* (2014) Selective mRNA translation during eIF2 phosphorylation induces expression of IBTKalpha. *Molecular biology of the cell* 25:1686-97.

Baird TD, Wek RC (2012) Eukaryotic initiation factor 2 phosphorylation and translational control in metabolism. *Advances in nutrition* 3:307-21.

Banks EB, Crish JF, Welter JF*, et al.* (1998) Characterization of human involucrin promoter distal regulatory region transcriptional activator elements-a role for Sp1 and AP1 binding sites. *The Biochemical journal* 331 (Pt 1):61-8.

Bertolotti A, Zhang Y, Hendershot LM*, et al.* (2000) Dynamic interaction of BiP and ER stress transducers in the unfolded-protein response. *Nature cell biology* 2:326-32.

Bikle DD, Xie Z, Tu CL (2012) Calcium regulation of keratinocyte differentiation. *Expert review of endocrinology & metabolism* 7:461-72.

Bittencourt S, Pereira CM, Avedissian M*, et al.* (2008) Distribution of the protein IMPACT, an inhibitor of GCN2, in the mouse, rat, and marmoset brain. *The Journal of comparative neurology* 507:1811-30.

Bobrovnikova-Marjon E, Grigoriadou C, Pytel D*, et al.* (2010) PERK promotes cancer cell proliferation and tumor growth by limiting oxidative DNA damage. *Oncogene* 29:3881-95.

Borowiec AS, Delcourt P, Dewailly E*, et al.* (2013) Optimal differentiation of in vitro keratinocytes requires multifactorial external control. *PloS one* 8:e77507.

Bouwstra JA, Ponec M (2006) The skin barrier in healthy and diseased state. *Biochimica et biophysica acta* 1758:2080-95.

Brugarolas J, Chandrasekaran C, Gordon JI*, et al.* (1995) Radiation-induced cell cycle arrest compromised by p21 deficiency. *Nature* 377:552-7.

Cadet J, Mouret S, Ravanat JL*, et al.* (2012) Photoinduced damage to cellular DNA: direct and photosensitized reactions. *Photochemistry and photobiology* 88:1048-65.

Cai Q, Brooks HL (2011) Phosphorylation of eIF2alpha via the general control kinase, GCN2, modulates the ability of renal medullary cells to survive high urea stress. *American journal of physiology Renal physiology* 301:F1202-7.

Calkhoven CF, Muller C, Leutz A (2000) Translational control of C/EBPalpha and C/EBPbeta isoform expression. *Genes & development* 14:1920-32.

Campisi J (2005) Suppressing cancer: the importance of being senescent. *Science (New York, NY)* 309:886-7.

Castilho BA, Shanmugam R, Silva RC*, et al.* (2014) Keeping the eIF2 alpha kinase Gcn2 in check. *Biochimica et biophysica acta* 1843:1948-68.

Choi HR, Tucker SA, Huang Z*, et al.* (2003) Differential expressions of cyclin-dependent kinase inhibitors (p27 and p21) and their relation to p53 and Ki-67 in oral squamous tumorigenesis. *International journal of oncology* 22:409-14.

Connor JH, Weiser DC, Li S*, et al.* (2001) Growth arrest and DNA damage-inducible protein GADD34 assembles a novel signaling complex containing protein phosphatase 1 and inhibitor 1. *Molecular and cellular biology* 21:6841-50.

Crish JF, Gopalakrishnan R, Bone F*, et al.* (2006) The distal and proximal regulatory regions of the involucrin gene promoter have distinct functions and are required for in vivo involucrin expression. *The Journal of investigative dermatology* 126:305-14.

D'Errico M, Teson M, Calcagnile A*, et al.* (2003) Apoptosis and efficient repair of DNA damage protect human keratinocytes against UVB. *Cell death and differentiation* 10:754-6.

de Laat A, van Tilburg M, van der Leun JC*, et al.* (1996) Cell cycle kinetics following UVA irradiation in comparison to UVB and UVC irradiation. *Photochemistry and photobiology* 63:492-7.

Delepine M, Nicolino M, Barrett T*, et al.* (2000) EIF2AK3, encoding translation initiation factor 2-alpha kinase 3, is mutated in patients with Wolcott-Rallison syndrome. *Nature genetics* 25:406-9.

Deng C, Zhang P, Harper JW*, et al.* (1995) Mice lacking p21CIP1/WAF1 undergo normal development, but are defective in G1 checkpoint control. *Cell* 82:675-84.

Deng J, Harding HP, Raught B*, et al.* (2002) Activation of GCN2 in UV-irradiated cells inhibits translation. *Current biology : CB* 12:1279-86.

Deng J, Lu PD, Zhang Y*, et al.* (2004) Translational repression mediates activation of nuclear factor kappa B by phosphorylated translation initiation factor 2. *Molecular and cellular biology* 24:10161-8.

Dey M, Cao C, Dar AC*, et al.* (2005) Mechanistic link between PKR dimerization, autophosphorylation, and eIF2alpha substrate recognition. *Cell* 122:901-13.

Dey S, Baird TD, Zhou D*, et al.* (2010) Both transcriptional regulation and translational control of ATF4 are central to the integrated stress response. *The Journal of biological chemistry* 285:33165-74.

Dey S, Savant S, Teske BF*, et al.* (2012) Transcriptional repression of ATF4 gene by CCAAT/enhancer-binding protein beta (C/EBPbeta) differentially regulates integrated stress response. *The Journal of biological chemistry* 287:21936-49.

Dickson MA, Hahn WC, Ino Y*, et al.* (2000) Human keratinocytes that express hTERT and also bypass a p16(INK4a)-enforced mechanism that limits life span become immortal yet retain normal growth and differentiation characteristics. *Molecular and cellular biology* 20:1436-47.

Dong J, Qiu H, Garcia-Barrio M*, et al.* (2000) Uncharged tRNA activates GCN2 by displacing the protein kinase moiety from a bipartite tRNA-binding domain. *Molecular cell* 6:269-79.

Durocher F, Faure R, Labrie Y*, et al.* (2006) A novel mutation in the EIF2AK3 gene with variable expressivity in two patients with Wolcott-Rallison syndrome. *Clinical genetics* 70:34-8.

Eastman A (2004) Cell cycle checkpoints and their impact on anticancer therapeutic strategies. *Journal of cellular biochemistry* 91:223-31.

Eckert RL, Crish JF, Efimova T*, et al.* (2004) Regulation of involucrin gene expression. *The Journal of investigative dermatology* 123:13-22.

Eferl R, Ricci R, Kenner L*, et al.* (2003) Liver tumor development. c-Jun antagonizes the proapoptotic activity of p53. *Cell* 112:181-92.

El-Abaseri TB, Putta S, Hansen LA (2006) Ultraviolet irradiation induces keratinocyte proliferation and epidermal hyperplasia through the activation of the epidermal growth factor receptor. *Carcinogenesis* 27:225-31.

Eleftheriadis T, Pissas G, Antoniadi G*, et al.* (2015) Indoleamine 2,3-dioxygenase depletes tryptophan, activates general control non-derepressible 2 kinase and down-regulates key enzymes involved in fatty acid synthesis in primary human CD4+ T cells. *Immunology* 146:292-300.

Eyries M, Montani D, Girerd B*, et al.* (2014) EIF2AK4 mutations cause pulmonary veno-occlusive disease, a recessive form of pulmonary hypertension. *Nature genetics* 46:65-9.

Fawcett TW, Martindale JL, Guyton KZ*, et al.* (1999) Complexes containing activating transcription factor (ATF)/cAMP-responsive-element-binding protein (CREB) interact with the CCAAT/enhancer-binding protein (C/EBP)-ATF composite site to regulate Gadd153 expression during the stress response. *The Biochemical journal* 339 (Pt 1):135-41.

Fornace AJ, Alamo I, Hollandar MC (1988) DNA damage-inducible transcripts in human cells. *Proceedings of the NAtional Academy of Sciences* 85:8800-8804.

Fuchs E (1990) Epidermal differentiation: the bare essentials. *The Journal of cell biology* 111:2807-14.

Fuchs E (2007) Scratching the surface of skin development. *Nature* 445:834-42.

Fullwood MJ, Zhou W, Shenolikar S (2012) Targeting phosphorylation of eukaryotic initiation factor-2alpha to treat human disease. *Progress in molecular biology and translational science* 106:75-106.

Fusakio ME, Willy JA, Wang Y*, et al.* (2016) Transcription factor ATF4 directs basal and stress-induced gene expression in the unfolded protein response and cholesterol metabolism in the liver. *Molecular biology of the cell* 27:1536-51.

Gao X, Wan J, Liu B*, et al.* (2015) Quantitative profiling of initiating ribosomes in vivo. 12:147-53.

Garcia MA, Meurs EF, Esteban M (2007) The dsRNA protein kinase PKR: virus and cell control. *Biochimie* 89:799-811.

Gartel AL, Tyner AL (1999) Transcriptional regulation of the p21((WAF1/CIP1)) gene. *Experimental cell research* 246:280-9.

Gibson DF, Ratnam AV, Bikle DD (1996) Evidence for separate control mechanisms at the message, protein, and enzyme activation levels for transglutaminase during calcium-induced differentiation of normal and transformed human keratinocytes. *The Journal of investigative dermatology* 106:154-61.

Gyenis A, Umlauf D, Ujfaludi Z*, et al.* (2014) UVB induces a genome-wide acting negative regulatory mechanism that operates at the level of transcription initiation in human cells. *PLoS genetics* 10:e1004483.

Han AP, Yu C, Lu L*, et al.* (2001) Heme-regulated eIF2alpha kinase (HRI) is required for translational regulation and survival of erythroid precursors in iron deficiency. *The EMBO journal* 20:6909-18.

Han J, Back SH, Hur J*, et al.* (2013) ER-stress-induced transcriptional regulation increases protein synthesis leading to cell death. *Nature cell biology* 15:481-90.

Harding HP, Novoa I, Zhang Y*, et al.* (2000) Regulated translation initiation controls stress-induced gene expression in mammalian cells. *Molecular cell* 6:1099-108.

Harding HP, Zhang Y, Ron D (1999) Protein translation and folding are coupled by an endoplasmic-reticulum-resident kinase. *Nature* 397:271-4.

Harding HP, Zhang Y, Zeng H*, et al.* (2003) An integrated stress response regulates amino acid metabolism and resistance to oxidative stress. *Molecular cell* 11:619-33.

Hibino M, Sugiura K, Muro Y*, et al.* (2011) Cyclosporin A induces the unfolded protein response in keratinocytes. *Archives of dermatological research* 303:481-9.

Hill R, Bodzak E, Blough MD*, et al.* (2008) p53 Binding to the p21 promoter is dependent on the nature of DNA damage. *Cell cycle (Georgetown, Tex)* 7:2535-43.

Hinnebusch AG (2005) Translational regulation of GCN4 and the general amino acid control of yeast. *Annual review of microbiology* 59:407-50.

Hinnebusch AG, Ivanov IP, Sonenberg N (2016) Translational control by 5'-untranslated regions of eukaryotic mRNAs. *Science (New York, NY)* 352:1413-6.

Holmes B, Brogden RN, Heel RC*, et al.* (1983) Guanabenz. A review of its pharmacodynamic properties and therapeutic efficacy in hypertension. *Drugs* 26:212-29.

Jackson RJ, Hellen CU, Pestova TV (2010) The mechanism of eukaryotic translation initiation and principles of its regulation. *Nature reviews Molecular cell biology* 11:113-27.

Jascur T, Brickner H, Salles-Passador I*, et al.* (2005) Regulation of p21(WAF1/CIP1) stability by WISp39, a Hsp90 binding TPR protein. *Molecular cell* 17:237-49.

Jiang HY, Wek RC (2005) GCN2 phosphorylation of eIF2alpha activates NF-kappaB in response to UV irradiation. *The Biochemical journal* 385:371-80.

Jiang HY, Wek SA, McGrath BC*, et al.* (2004) Activating transcription factor 3 is integral to the eukaryotic initiation factor 2 kinase stress response. *Molecular and cellular biology* 24:1365-77.

Jiang HY, Wek SA, McGrath BC*, et al.* (2003) Phosphorylation of the alpha subunit of eukaryotic initiation factor 2 is required for activation of NF-kappaB in response to diverse cellular stresses. *Molecular and cellular biology* 23:5651-63.

Kilberg MS, Shan J, Su N (2009) ATF4-dependent transcription mediates signaling of amino acid limitation. *Trends in endocrinology and metabolism: TEM* 20:436-43.

Kozak M (1989a) Context effects and inefficient initiation at non-AUG codons in eucaryotic cell-free translation systems. *Molecular and cellular biology* 9:5073-80.

Kozak M (1989b) The scanning model for translation: an update. *J Cell Biol* 108:229-41.

Krtolica A, Parrinello S, Lockett S*, et al.* (2001) Senescent fibroblasts promote epithelial cell growth and tumorigenesis: a link between cancer and aging. *Proceedings of the National Academy of Sciences of the United States of America* 98:12072-7.

Kuhn C, Hurwitz SA, Kumar MG*, et al.* (1999) Activation of the insulin-like growth factor-1 receptor promotes the survival of human keratinocytes following ultraviolet B irradiation. *International journal of cancer Journal international du cancer* 80:431-8.

Lee S, Liu B, Lee S*, et al.* (2012) Global mapping of translation initiation sites in mammalian cells at single-nucleotide resolution. *Proc Natl Acad Sci U S A* 109:E2424-32.

Lehman SL, Cerniglia GJ, Johannes GJ*, et al.* (2015) Translational Upregulation of an Individual p21Cip1 Transcript Variant by GCN2 Regulates Cell Proliferation and Survival under Nutrient Stress. *PLoS genetics* 11:e1005212.

Lewis DA, Travers JB, Somani AK*, et al.* (2010) The IGF-1/IGF-1R signaling axis in the skin: a new role for the dermis in aging-associated skin cancer. *Oncogene* 29:1475-85.

Lewis DA, Yi Q, Travers JB*, et al.* (2008) UVB-induced senescence in human keratinocytes requires a functional insulin-like growth factor-1 receptor and p53. *Molecular biology of the cell* 19:1346-53.

Loesch MM, Collier AE, Southern DH*, et al.* (2016) Insulin-like growth factor-1 receptor regulates repair of ultraviolet B-induced DNA damage in human keratinocytes in vivo. *Molecular oncology*.

Ma K, Vattem KM, Wek RC (2002) Dimerization and release of molecular chaperone inhibition facilitate activation of eukaryotic initiation factor-2 kinase in response to endoplasmic reticulum stress. *The Journal of biological chemistry* 277:18728-35.

Ma Y, Hendershot LM (2003) Delineation of a negative feedback regulatory loop that controls protein translation during endoplasmic reticulum stress. *The Journal of biological chemistry* 278:34864-73.

Macleod KF, Sherry N, Hannon G*, et al.* (1995) p53-dependent and independent expression of p21 during cell growth, differentiation, and DNA damage. *Genes & development* 9:935-44.

Malhi H, Kaufman RJ (2011) Endoplasmic reticulum stress in liver disease. *Journal of hepatology* 54:795-809.

Mandal M, Bandyopadhyay D, Goepfert TM*, et al.* (1998) Interferon-induces expression of cyclin-dependent kinase-inhibitors p21WAF1 and p27Kip1 that

prevent activation of cyclin-dependent kinase by CDK-activating kinase (CAK). *Oncogene* 16:217-25.

Marciniak SJ, Ron D (2006) Endoplasmic reticulum stress signaling in disease. *Physiological reviews* 86:1133-49.

Marciniak SJ, Yun CY, Oyadomari S*, et al.* (2004) CHOP induces death by promoting protein synthesis and oxidation in the stressed endoplasmic reticulum. *Genes & development* 18:3066-77.

McCullough KD, Martindale JL, Klotz LO*, et al.* (2001) Gadd153 sensitizes cells to endoplasmic reticulum stress by down-regulating Bcl2 and perturbing the cellular redox state. *Molecular and cellular biology* 21:1249-59.

Melnikova VO, Ananthaswamy HN (2005) Cellular and molecular events leading to the development of skin cancer. *Mutation research* 571:91-106.

Menon GK, Elias PM, Feingold KR (1994) Integrity of the permeability barrier is crucial for maintenance of the epidermal calcium gradient. *The British journal of dermatology* 130:139-47.

Micallef L, Belaubre F, Pinon A*, et al.* (2009) Effects of extracellular calcium on the growth-differentiation switch in immortalized keratinocyte HaCaT cells

compared with normal human keratinocytes. *Experimental dermatology* 18:143-51.

Moll R, Franke WW, Schiller DL*, et al.* (1982) The catalog of human cytokeratins: patterns of expression in normal epithelia, tumors and cultured cells. *Cell* 31:11-24.

Munn DH, Sharma MD, Baban B*, et al.* (2005) GCN2 kinase in T cells mediates proliferative arrest and anergy induction in response to indoleamine 2,3-dioxygenase. *Immunity* 22:633-42.

Nakanishi M, Shimada M, Niida H (2006) Genetic instability in cancer cells by impaired cell cycle checkpoints. *Cancer science* 97:984-9.

Ng IO, Lam KY, Ng M*, et al.* (1999) Expression of p21/waf1 in oral squamous cell carcinomas--correlation with p53 and mdm2 and cellular proliferation index. *Oral oncology* 35:63-9.

Novoa I, Zeng H, Harding HP*, et al.* (2001) Feedback inhibition of the unfolded protein response by GADD34-mediated dephosphorylation of eIF2alpha. *The Journal of cell biology* 153:1011-22.

Novoa I, Zhang Y, Zeng H*, et al.* (2003) Stress-induced gene expression requires programmed recovery from translational repression. *The EMBO journal* 22:1180-7.

Ortolan TG, Menck CF (2013) UVB-induced cell death signaling is associated with G1-S progression and transcription inhibition in primary human fibroblasts. *PloS one* 8:e76936.

Oslowski CM, Urano F (2011) The binary switch that controls the life and death decisions of ER stressed beta cells. *Current opinion in cell biology* 23:207-15.

Padyana AK, Qiu H, Roll-Mecak A*, et al.* (2005) Structural basis for autoinhibition and mutational activation of eukaryotic initiation factor 2alpha protein kinase GCN2. *The Journal of biological chemistry* 280:29289-99.

Palam LR, Baird TD, Wek RC (2011) Phosphorylation of eIF2 facilitates ribosomal bypass of an inhibitory upstream ORF to enhance CHOP translation. *The Journal of biological chemistry* 286:10939-49.

Pasparakis M, Haase I, Nestle FO (2014) Mechanisms regulating skin immunity and inflammation. *Nature reviews Immunology* 14:289-301.

Pereira CM, Sattlegger E, Jiang HY*, et al.* (2005) IMPACT, a protein preferentially expressed in the mouse brain, binds GCN1 and inhibits GCN2 activation. *The Journal of biological chemistry* 280:28316-23.

Pillai S, Bikle DD, Mancianti ML*, et al.* (1990) Calcium regulation of growth and differentiation of normal human keratinocytes: modulation of differentiation competence by stages of growth and extracellular calcium. *Journal of cellular physiology* 143:294-302.

Poumay Y, Pittelkow MR (1995) Cell density and culture factors regulate keratinocyte commitment to differentiation and expression of suprabasal K1/K10 keratins. *The Journal of investigative dermatology* 104:271-6.

Rigberg DA, Kim FS, Blinman TA*, et al.* (1998) p21 expression is increased by irradiation in esophageal squamous cell carcinoma. *J Surg Res* 76:137-42.

Roffe M, Hajj GN, Azevedo HF*, et al.* (2013) IMPACT is a developmentally regulated protein in neurons that opposes the eukaryotic initiation factor 2alpha kinase GCN2 in the modulation of neurite outgrowth. *The Journal of biological chemistry* 288:10860-9.

Roninson IB (2002) Oncogenic functions of tumour suppressor p21(Waf1/Cip1/Sdi1): association with cell senescence and tumour-promoting activities of stromal fibroblasts. *Cancer letters* 179:1-14.

Sato AY, Tu X, McAndrews KA*, et al.* (2015) Prevention of glucocorticoid induced-apoptosis of osteoblasts and osteocytes by protecting against endoplasmic reticulum (ER) stress in vitro and in vivo in female mice. *Bone* 73:60-8.

Sattlegger E, Swanson MJ, Ashcraft EA*, et al.* (2004) YIH1 is an actin-binding protein that inhibits protein kinase GCN2 and impairs general amino acid control when overexpressed. *The Journal of biological chemistry* 279:29952-62.

Saxena S, Cabuy E, Caroni P (2009) A role for motoneuron subtype-selective ER stress in disease manifestations of FALS mice. *Nature neuroscience* 12:627-36.

Scheuner D, Kaufman RJ (2008) The unfolded protein response: a pathway that links insulin demand with beta-cell failure and diabetes. *Endocrine reviews* 29:317-33.

Scholpa NE, Zhang X, Kolli RT*, et al.* (2014) Epigenetic changes in p21 expression in renal cells after exposure to bromate. *Toxicological sciences : an official journal of the Society of Toxicology* 141:432-40.

Schroder M, Kaufman RJ (2005) The mammalian unfolded protein response. *Annual review of biochemistry* 74:739-89.

Schwanhausser B, Busse D, Li N*, et al.* (2011) Global quantification of mammalian gene expression control. *Nature* 473:337-42.

Shi Y, Vattem KM, Sood R*, et al.* (1998) Identification and characterization of pancreatic eukaryotic initiation factor 2 alpha-subunit kinase, PEK, involved in translational control. *Molecular and cellular biology* 18:7499-509.

Shuck SC, Short EA, Turchi JJ (2008) Eukaryotic nucleotide excision repair: from understanding mechanisms to influencing biology. *Cell research* 18:64-72.

Sidrauski C, Acosta-Alvear D, Khoutorsky A*, et al.* (2013) Pharmacological brake-release of mRNA translation enhances cognitive memory. *eLife* 2:e00498.

Simpson CL, Kojima S, Getsios S (2010) RNA interference in keratinocytes and an organotypic model of human epidermis. *Methods in molecular biology (Clifton, NJ)* 585:127-46.

Steven AC, Bisher ME, Roop DR*, et al.* (1990) Biosynthetic pathways of filaggrin and loricrin--two major proteins expressed by terminally differentiated epidermal keratinocytes. *Journal of structural biology* 104:150-62.

Sugiura K, Muro Y, Futamura K*, et al.* (2009) The unfolded protein response is activated in differentiating epidermal keratinocytes. *The Journal of investigative dermatology* 129:2126-35.

Swindell WR, Remmer HA, Sarkar MK*, et al.* (2015) Proteogenomic analysis of psoriasis reveals discordant and concordant changes in mRNA and protein abundance. *Genome medicine* 7:86.

Tabas I, Ron D (2011) Integrating the mechanisms of apoptosis induced by endoplasmic reticulum stress. *Nature cell biology* 13:184-90.

Teske BF, Baird TD, Wek RC (2011a) Methods for analyzing eIF2 kinases and translational control in the unfolded protein response. *Methods in enzymology* 490:333-56.

Teske BF, Fusakio ME, Zhou D*, et al.* (2013) CHOP induces activating transcription factor 5 (ATF5) to trigger apoptosis in response to perturbations in protein homeostasis. *Molecular biology of the cell* 24:2477-90.

Teske BF, Wek SA, Bunpo P*, et al.* (2011b) The eIF2 kinase PERK and the integrated stress response facilitate activation of ATF6 during endoplasmic reticulum stress. *Molecular biology of the cell* 22:4390-405.

Vattem KM, Wek RC (2004) Reinitiation involving upstream ORFs regulates ATF4 mRNA translation in mammalian cells. *Proceedings of the National Academy of Sciences of the United States of America* 101:11269-74.

Vogt PK (2002) Fortuitous convergences: the beginnings of JUN. *Nature reviews Cancer* 2:465-9.

Walter P, Ron D (2011) The unfolded protein response: from stress pathway to homeostatic regulation. *Science (New York, NY)* 334:1081-6.

Wang XZ, Lawson B, et al. (1998) Signals from the Stressed Endoplasmic Reticulum Induce C/EBP-Homologous Protein (CHOP/GADD153). *Molecular and Cellular Biology* 16:4273-4280.

Warhol MJ, Roth J, Lucocq JM*, et al.* (1985) Immuno-ultrastructural localization of involucrin in squamous epithelium and cultured keratinocytes. *The journal of histochemistry and cytochemistry : official journal of the Histochemistry Society* 33:141-9.

Wek RC, Anthony TG (2009) Beta testing the antioxidant function of eIF2alpha phosphorylation in diabetes prevention. *Cell metabolism* 10:1-2.

Wek RC, Jackson BM, Hinnebusch AG (1989) Juxtaposition of domains homologous to protein kinases and histidyl-tRNA synthetases in GCN2 protein suggests a mechanism for coupling GCN4 expression to amino acid availability. *Proceedings of the National Academy of Sciences of the United States of America* 86:4579-83.

Wek RC, Jiang HY, Anthony TG (2006) Coping with stress: eIF2 kinases and translational control. *Biochemical Society transactions* 34:7-11.

Wek SA, Zhu S, Wek RC (1995) The histidyl-tRNA synthetase-related sequence in the eIF-2 alpha protein kinase GCN2 interacts with tRNA and is required for activation in response to starvation for different amino acids. *Molecular and cellular biology* 15:4497-506.

Williamson L, Saponaro M, Boeing S*, et al.* (2017) UV Irradiation Induces a Non-coding RNA that Functionally Opposes the Protein Encoded by the Same Gene. *Cell* 168:843-55.e13.

Willy JA, Young SK, Stevens JL*, et al.* (2015) CHOP links endoplasmic reticulum stress to NF-kappaB activation in the pathogenesis of nonalcoholic steatohepatitis. *Molecular biology of the cell* 26:2190-204.

Wisdom R, Johnson RS, Moore C (1999) c-Jun regulates cell cycle progression and apoptosis by distinct mechanisms. *The EMBO journal* 18:188-97.

Yang R, Wek SA, Wek RC (2000) Glucose limitation induces GCN4 translation by activation of Gcn2 protein kinase. *Molecular and cellular biology* 20:2706-17.

Ye J, Koumenis C (2009) ATF4, an ER stress and hypoxia-inducible transcription factor and its potential role in hypoxia tolerance and tumorigenesis. *Current molecular medicine* 9:411-6.

Ye J, Palm W, Peng M*, et al.* (2015) GCN2 sustains mTORC1 suppression upon amino acid deprivation by inducing Sestrin2. *Genes & development* 29:2331-6.

Young SK, Baird TD, Wek RC (2016a) Translation Regulation of the Glutamyl-prolyl-tRNA Synthetase Gene EPRS through Bypass of Upstream Open Reading Frames with Noncanonical Initiation Codons. *The Journal of biological chemistry* 291:10824-35.

Young SK, Palam LR, Wu C*, et al.* (2016b) Ribosome Elongation Stall Directs Gene-specific Translation in the Integrated Stress Response. *The Journal of biological chemistry* 291:6546-58.

Young SK, Wek RC (2016) Upstream Open Reading Frames Differentially Regulate Gene-specific Translation in the Integrated Stress Response. *The Journal of biological chemistry* 291:16927-35.

Young SK, Willy JA, Wu C*, et al.* (2015) Ribosome Reinitiation Directs Gene-specific Translation and Regulates the Integrated Stress Response. *The Journal of biological chemistry* 290:28257-71.

Zaborske JM, Narasimhan J, Jiang L*, et al.* (2009) Genome-wide analysis of tRNA charging and activation of the eIF2 kinase Gcn2p. *The Journal of biological chemistry* 284:25254-67.

Zhao KN, Gu W, Fang NX*, et al.* (2005) Gene codon composition determines differentiation-dependent expression of a viral capsid gene in keratinocytes in vitro and in vivo. *Molecular and cellular biology* 25:8643-55.

Zhou D, Palam LR, Jiang L*, et al.* (2008) Phosphorylation of eIF2 directs ATF5 translational control in response to diverse stress conditions. *The Journal of biological chemistry* 283:7064-73.

CURRICULUM VITAE

Ann E. Collier

Education

Indiana University, Ph.D., Biochemistry & Molecular Biology, 2017

DePauw University, B.A., Biochemistry, 2012

Honors, Awards, and Fellowships

2015-17	NIH F31 Ruth L. Kirschstein National Research Service Award Individual Pre-doctoral Fellowship (NIH 1F31ES026517-01 to AEC)
2016	Second place, Sigma Xi Research Competition (IUSM)
2015	IUSM Student Travel Award
2015	Erica Daniel Kepner Award for Scientific Achievement
2015	Selection for Society for Investigative Dermatology (SID) PhD Retreat for Future Investigators
2015	SID Student Travel Award
2014	IUSM Student Travel Award
2012	Chi Alpha Sigma National College Athlete Honor Society
2012	Phi Lambda Upsilon National Chemistry Honor Society
2011	Jane Williams/Jane Baxter Akins Award, DePauw University
2008-12	Science Research Fellow (SRF) Honors Program, DePauw University

2008 Faculty Distinguished Scholarship, DePauw University

Research and Training Experience

2012-17 Graduate Fellow, Indiana University School of Medicine, Indianapolis, IN

2010-11 Wells Center for Pediatric Research Intern, Indianapolis, IN

2011-12 Science Research Fellow, Department of Biochemistry, DePauw University, Greencastle, IN

2009 Science Research Fellow, Department of Immunology, DePauw University, Greencastle, IN

2008 Science Research Fellow, Department of Psychology, DePauw University, Greencastle, IN

Publications

Collier, A., Wek, R., Spandau, D (2017). Differentiation of human keratinocytes requires translational control by the eIF2α kinase GCN2. *Journal of Investigative Dermatology* accepted article preview, June 1, 2017; doi pending.

Collier, A., Wek, R., Spandau D (2015). Translational repression protects human keratinocytes from UVB-induced apoptosis through a discordant eIF2 kinase stress response. *Journal of Investigative Dermatology* 135(10):2502-11.

Loesch, M., **Collier, A.,** Southern, D., Ward, R., Tholpady, S., Travers, J., Spandau, D. (2016). IGF-1 receptor regulates repair of UVB-induced DNA damage in human keratinocytes. *Molecular Oncology* 10(8):1245-54.

Conferences Attended

2017 Midwest DNA Repair Symposium, Dayton, OH. "Translational control of UVB-induced cell cycle arrest in human keratinocytes (**oral presentation**)."

2017 Experimental Biology Meeting, Chicago, IL. "Differentiation of human keratinocytes requires translational control by the eIF2α kinase GCN2 (**poster**)."

2016 Cold Spring Harbor Meeting on Translational Control, Cold Spring Harbor, NY. "Translational control in the human keratinocyte adaptation to stress (**poster**)."

2016 SID Annual Meeting, Scottsdale, AZ. "Translational control through eIF2α is required for cell cycle arrest following UVB irradiation (**poster**)" and "Preferential translation is required for proper keratinocyte differentiation (**oral presentation**)."

2015 SID Annual Meeting, Atlanta, GA. "Regulation of protein synthesis during keratinocyte differentiation (**oral presentation**)."

2014 SID Annual Meeting, Albuquerque, NM. "UVB irradiation of human keratinocytes causes a discordant eIF2 kinase response (**poster**)."

Teaching Experience

2016 Project SEED/STEM High School Student Research Mentor

2014 Graduate Teaching Assistant, G716 Molecular Biology and Genetics, IUSM